Turun yliopisto
University of Turku

TRANSLATIONAL MODELS OF CORONARY ARTERY DISEASE, MYOCARDIAL INFARCTION AND HEART FAILURE

Development, Validation and *in vivo* Imaging Studies Using Positron Emission Tomography

Miikka Tarkia

TURUN YLIOPISTON JULKAISUJA – ANNALES UNIVERSITATIS TURKUENSIS
Sarja - ser. D osa - tom. 1175 | Medica - Odontologica | Turku 2015

University of Turku

Faculty of Medicine

Institute of Clinical Medicine

Department of Clinical Physiology and Nuclear Medicine and Turku PET Centre

Drug Research Doctoral Programme at University of Turku

Supervised by

Professor Anne Roivainen, PhD
Turku PET Centre and Turku Centre for Disease Modelling
University of Turku
Turku, Finland

Associate Professor Antti Saraste, MD, PhD
Turku PET Centre and Heart Center
University of Turku and Turku University Hospital
Turku, Finland

Reviewed by

Adjunct Professor Esko Kankuri, MD, PhD
Department of Pharmacology
University of Helsinki
Helsinki, Finland

Adjunct Professor Kirsi Timonen, MD, PhD
Department of Clinical Physiology and Nuclear Medicine
Central Hospital of Central Finland and University of Eastern Finland
Kuopio, Finland

Opponent

Professor Johanna Kuusisto, MD, PhD
Department of Medicine
University of Eastern Finland
Kuopio, Finland

The originality of this thesis has been checked in accordance with the University of Turku quality assurance system using the Turnitin OriginalityCheck service.

ISBN 978-951-29-6129-0 (PRINT)
ISBN 978-951-29-6130-6 (PDF)
ISSN 0355-9483
Painosalama Oy - Turku, Finland 2015

To Anna and Maria

ABSTRACT

Miikka Tarkia

TRANSLATIONAL MODELS OF CORONARY ARTERY DISEASE, MYOCARDIAL INFARCTION AND HEART FAILURE

Development, validation and *in vivo* imaging studies using positron emission tomography

Department of Clinical Physiology and Nuclear Medicine and Turku PET Centre, University of Turku, Turku, Finland

Coronary artery disease is an atherosclerotic disease, which leads to narrowing of coronary arteries, deteriorated myocardial blood flow and myocardial ischaemia. In acute myocardial infarction, a prolonged period of myocardial ischaemia leads to myocardial necrosis. Necrotic myocardium is replaced with scar tissue. Myocardial infarction results in various changes in cardiac structure and function over time that results in "adverse remodelling". This remodelling may result in a progressive worsening of cardiac function and development of chronic heart failure.

In this thesis, we developed and validated three different large animal models of coronary artery disease, myocardial ischaemia and infarction for translational studies. In the first study the coronary artery disease model had both induced diabetes and hypercholesterolemia. In the second study myocardial ischaemia and infarction were caused by a surgical method and in the third study by catheterisation. For model characterisation, we used non-invasive positron emission tomography (PET) methods for measurement of myocardial perfusion, oxidative metabolism and glucose utilisation. Additionally, cardiac function was measured by echocardiography and computed tomography. To study the metabolic changes that occur during atherosclerosis, a hypercholesterolemic and diabetic model was used with [^{18}F] fluorodeoxyglucose ([^{18}F]FDG) PET-imaging technology. Coronary occlusion models were used to evaluate metabolic and structural changes in the heart and the cardioprotective effects of levosimendan during post-infarction cardiac remodelling. Large animal models were used in testing of novel radiopharmaceuticals for myocardial perfusion imaging.

In the coronary artery disease model, we observed atherosclerotic lesions that were associated with focally increased [^{18}F]FDG uptake. In heart failure models, chronic myocardial infarction led to the worsening of systolic function, cardiac remodelling and decreased efficiency of cardiac pumping function. Levosimendan therapy reduced post-infarction myocardial infarct size and improved cardiac function. The novel ^{68}Ga-labeled radiopharmaceuticals tested in this study were not successful for the determination of myocardial blood flow.

In conclusion, diabetes and hypercholesterolemia lead to the development of early phase atherosclerotic lesions. Coronary artery occlusion produced considerable myocardial ischaemia and later infarction following myocardial remodelling. The experimental models evaluated in these studies will enable further studies concerning disease mechanisms, new radiopharmaceuticals and interventions in coronary artery disease and heart failure.

Keywords: coronary artery disease, myocardial ischaemia, myocardial infarction, heart failure, positron emission tomography (PET)

TIIVISTELMÄ

Miikka Tarkia

SEPELVALTIMOTAUDIN, SYDÄNINFARKTIN JA SYDÄMEN VAJAATOIMINNAN TRANSLATIONAALISET MALLIT

Kehitys, validointi ja *in vivo* kuvantaminen positroniemissiotomografialla

Kliininen fysiologia ja isotooppilääketiede ja Valtakunnallinen PET-keskus, Turun yliopisto, Turku, Suomi

Sepelvaltimotaudissa sepelvaltimot ahtautuvat ateroskleroosin vuoksi, mikä johtaa sydänlihaksen verenvirtauksen heikkenemiseen ja sydänlihasiskemiaan. Akuutissa sydäninfarktissa pitkittynyt iskemia johtaa sydänlihaskuolioon eli nekroosiin, joka korvautuu arpikudoksella. Sydäninfarktin seurauksena sydämen rakenteessa ja toiminnassa tapahtuu muutoksia, mikä johtaa niin kutsuttuun haitalliseen sydänlihaksen uudelleenmuovautumiseen ja lopulta sydämen toiminnan heikkenemiseen ja kroonisen vajaatoiminnan kehittymiseen.

Tässä väitöskirjatyössä kehitettiin ja validoitiin kolme erilaista sepelvaltimotaudin, sydänlihasiskemian ja infarktin suureläinmallia translationaalisia tutkimuksia varten. Ensimmäisessä osatyössä sepelvaltimotaudin mallissa oli yhdistetty diabetes ja hyperkolesterolemia. Toisessa osatyössä sydänlihasiskemia ja infarkti oli aiheutettu kirurgisesti ja kolmannessa osatyössä katetrisaatiolla. Mallien karakterisoinnissa käytettiin kajoamattomia positroniemissiotomografiaan (PET) perustuvia kuvantamismenetelmiä, joilla mitattiin sydänlihaksen verenvirtausta, hapenkulutusta ja glukoosinkäyttöä. Lisäksi sydämen pumppausominaisuuksia mitattiin ultraäänikardiografialla ja tietokonetomografialla. Hyperkolesterolemia ja diabetesmallilla tutkittiin ateroskleroottisten tautimuutosten kuvantamista [^{18}F]fluorodeoksiglukoosi ([^{18}F]FDG) PET-merkkiaineella. Sepelvaltimon ahtauman malleilla tutkittiin sydämen metabolisia ja rakenteellisia muutoksia ja levosimendaanin sydäntä suojaavaa vaikutusta. Tutkimme myös uusia radiolääkeaineita sydänlihaksen verenvirtauksen määrittämiseen.

Sepelvaltimotaudin mallissa havaitsimme ateroskleroottisia muutoksia, jotka olivat yhteydessä lisääntyneeseen [^{18}F]FDG kertymään. Sydämen vajaatoiminnan malleissa krooninen sydäninfarkti johti systolisen funktion huononemiseen, haitalliseen sydänlihaksen uudelleenmuovautumiseen ja alentuneeseen sydänlihaksen hyötysuhteeseen. Infarktinjälkeinen hoito levosimendaanilla johti infarktialueen rajoittumiseen ja sydämen pumppausominaisuuksien parantumiseen. Uudet testatut ^{68}Ga-leimatut radiolääkeaineet eivät tässä tutkimuksessa soveltuneet sydänlihaksen verenvirtauksen määrittämiseen.

Johtopäätöksenä, diabetes ja hyperkolesterolemia johtavat varhaisen vaiheen ateroskleroottisiin muutoksiin. Sepelvaltimon tukkeuma kehitti merkittävän sydänlihasiskemian ja myöhemmän infarktin johtaen sydänlihaksen uudelleenmuovautumiseen. Testattujen koemallien myötä meillä on mahdollisuus tutkia lisää sepelvaltimotaudin ja sydämen vajaatoiminnan tautimekanismeja, uusia radiolääkeaineita ja hoitomuotoja.

Avainsanat: sepelvaltimotauti, sydänlihasiskemia, sydäninfarkti, sydämen vajaatoiminta, positroniemissiotomografia (PET)

TABLE OF CONTENTS

ABBREVIATIONS

AC	Adenylyl cyclase
ADP	Adenosine diphosphate
$\alpha_v\beta_3$	*Alpha*-V *beta*-3 integrin
AHA	American Heart Association
Akt	Protein kinase B
AMP	Adenosine monophosphate
ATP	Adenosine triphosphate
[^{18}F]FDG	2-[^{18}F]-Fluoro-2-deoxy-*D*-glucose
BAPEN	N,N′-bis(3-aminopropyl)ethylenediamine
BAPDMEN	N,N′-bis(3-aminopropyl)-dimethylenediamine
CFR	Coronary flow reserve
COX-2	Cyclooxygenase-2
CT	Computed tomography
CVR	Coronary vascular resistance
DOTATATE	1,4,7,10-tetraazacyclododecane-1,4,7,10-tetraacetic acid octreotate
ECG	Electrocardiography
EDV	End-diastolic volume
EF5	2-(2-Nitro-1H-imidazol-1-yl)-N-(2,2,3,3,3-pentafluoropropyl) acetamide
EF	Ejection fraction
ESV	End-systolic volume
FFA	Free fatty acids
FDA	United States Food and Drug Administration
FMISO	Fluoromisonidazole
FR	Folate receptor
G_s	Stimulatory G-protein
GSK-3β	Glycogen synthase kinase-3β
HF	Heart failure
HO-1	Heme oxygenase-1
IL	Interleukin
iNOS	Inducible Nitric-Oxide Synthase
IVUS	Intravascular ultrasound
JAK	Janus kinase
K_{ATP}	Adenosine triphosphate-sensitive potassium channel
LAD	Left anterior descending coronary artery
LCX	Left circumflex artery
LDL	Low density lipoprotein
LV	Left ventricle

MAPK	Mitogen-activated protein kinase
MBF	Myocardial blood flow
MCP-1	Monocyte chemotactic protein 1
M-CSF	Macrophage-colony stimulating factor
MFR	Myocardial flow reserve
MI	Myocardial infarction
MMP	Matrix metalloproteinase
MnSOD	Manganese superoxide dismutase
MPI	Myocardial perfusion imaging
MR	Mannose receptor
MRI	Magnetic resonance imaging
NF-κB	Nuclear factor kappa-B
NO	Nitric oxide
OCT	Optical coherence tomography
PCSK9	Proprotein convertase subtilisin/kexin type 9
PET	Positron emission tomography
PI3K	Phosphatidylinositol-3-kinase
PK11195	N-butan-2-yl-1-(2-chlorophenyl)-N-methylisoquinoline-3-carboxamide
PKA	Protein kinase A
PKC	Protein kinase C
PTI	Perfusable tissue index
PTF	Perfusable tissue fraction
RCA	Right coronary artery
RGD	Tripeptide arginylglycylaspartic acid
ROI	Region of interest
RPP	Rate-pressure product
SR	Scavenger receptor
SPECT	Single-photon emission computed tomography
STAT	Signal transducers and activators of transcription
SUV	Standardised uptake value
TGF-β1	Transforming growth factor-β1
TK	Tyrosine kinase
TLR	Toll-like receptor
TNFα	Tumour necrosis factor alpha
TSPO	Translocator protein
TTC	2,3,5-triphenyl-tetrazolium chloride
VCAM-1	Vascular cell adhesion molecule 1
VOI	Volume of interest
WMI	Work-metabolic index

LIST OF ORIGINAL PUBLICATIONS

This thesis is based on the following original publications

I. Tarkia M, Saraste A, Stark C, Vähäsilta T, Savunen T, Strandberg M, Saunavaara V, Tolvanen T, Teuho J, Teräs M, Metsälä O, Rinne P, Heinonen I, Savisto N, Pietilä M, Saukko P, Roivainen A, Knuuti J. [^{18}F]FDG accumulation in early coronary atherosclerotic lesions in pigs. Manuscript submitted for publication.

II. Tarkia M, Stark C, Haavisto M, Kentala R, Vähäsilta T, Savunen T, Strandberg M, Hynninen V-V, Saunavaara V, Tolvanen T, Teräs M, Rokka J, Pietilä M, Saukko P, Roivainen A, Saraste A, Knuuti J. Cardiac remodeling in a new pig model of chronic heart failure: assessment of left ventricular functional, metabolic and structural changes using PET, CT and echocardiography. Journal of Nuclear Cardiology, published online 20 February 2015.

III. Rissanen TT, Nurro J, Halonen PJ, Tarkia M, Saraste A, Rannankari M, Honkonen K, Pietilä M, Leppänen O, Kuivanen A, Knuuti J, Ylä-Herttuala S. The bottleneck stent model for chronic myocardial ischemia and heart failure in pigs. American Journal of Physiology - Heart and Circulatory Physiology. 2013;305(9):H1297-H1308.

IV. Tarkia M, Saraste A, Saanijoki T, Oikonen V, Vähäsilta T, Strandberg M, Stark C, Tolvanen T, Teräs M, Savunen T, Green MA, Knuuti J, Roivainen A. Evaluation of ^{68}Ga-labeled tracers for PET imaging of myocardial perfusion in pigs. Nuclear Medicine and Biology. 2012;39(5):715-723.

V. Tarkia M, Stark C, Haavisto M, Kentala R, Vähäsilta T, Savunen T, Strandberg M, Saunavaara V, Tolvanen T, Teräs M, Pietilä M, Nyman L, Duvall E, Saukko P, Levijoki J, Roivainen A, Saraste A, Knuuti J. Effect of levosimendan therapy on myocardial infarct size and left ventricle function after acute coronary occlusion. A study with experimental pig model of post-infarction heart failure. Manuscript submitted for publication.

1. INTRODUCTION

Ischaemic heart disease is the leading cause of death worldwide. It is caused by coronary artery disease (CAD), which is a slowly progressing disease in which inflammatory processes together with cholesterol accumulation lead to the narrowing of the coronary artery. Narrowing of a coronary artery causes insufficient myocardial blood flow that leads to myocardial ischaemia, which is defined as reduced myocardial oxygen supply and metabolic changes due to decreased blood flow. Severely disturbed coronary blood flow or rupture of an atherosclerotic plaque resulting in intraluminal thrombosis can cause prolonged periods of ischaemia resulting in myocardial necrosis, i.e., acute myocardial infarction (MI). MI is followed by adverse cardiac remodelling including changes in size, shape, structure and physiology of the heart after myocardial injury. Chronic heart failure (HF) occurs when the heart is unable to pump enough blood to supply the blood flow needed to maintain the circulation of the body. It is an increasing health problem that is associated with high morbidity and mortality together with poor prognosis. (Finegold et al. 2013 and Sanz et al. 2013)

Finding an effective animal model of atherosclerosis and myocardial ischaemia as well as MI involving reduced left ventricle (LV) function and remodelling with long survival is difficult to achieve. Several porcine models of CAD and MI exist and are used in research (Hughes et al. 2003 and Lukács et al. 2012). Still, better models for translational research are desired.

Positron emission tomography (PET) imaging of myocardial perfusion has shown high performance for diagnosis of CAD (Schelbert et al. 1982 and reviewed in Danad et al. 2014). For example oxygen-15 labelled water ([^{15}O]water) can be used in quantification of myocardial perfusion (Bergmann et al. 1984) and assessment of CAD (Reviewed in Saraste et al. 2012). Myocardial perfusion and oxidative metabolism can be measured simultaneously in a single PET study by using a carbon-11 labelled acetate ([^{11}C] acetate) tracer. Further, calculation together with cardiac function measurements gives an estimation of cardiac efficiency (Wolpers et al. 1994 and reviewed in Knaapen et al. 2007). A fluorine-18 labelled glucose analogue 2-[^{18}F]-Fluoro-2-deoxy-*D*-glucose ([^{18}F] FDG) can be used to determine myocardial viability (Tillisch et al. 1986 and reviewed in Knuuti et al. 2002). Viable myocardium is defined as myocardium, which does not contract normally due to ischaemia, but has the potential to recover its function.

New radiopharmaceuticals for cardiac PET perfusion imaging are demanded. Nitrogen-13 labelled ammonia ([^{13}N]ammonia), rubidium-82 chloride ([^{82}Rb]Cl) and [^{15}O]water are the currently used PET tracers for myocardial blood flow quantification. These tracers have short physical half-lives and the production requires an expensive on-site cyclotron. A longer half-life enables centred production of the tracer and delivery for longer distances. Gallium-68 (^{68}Ga) labelled radiopharmaceuticals have certain advantages in preclinical research including production with relatively inexpensive

germanium (^{68}Ge)/^{68}Ga generator and easy labelling of different molecules (Maecke et al. 2007). Recently, promising ^{68}Ga-labelled tracers for myocardial perfusion imaging (MPI) have been introduced (Hsiao et al. 2009).

Because of a high mortality and poor prognosis, new treatments for HF are needed. Positive inotropic therapy improves the cardiac performance including contractility leading to increased pump function. A calcium sensitiser agent levosimendan has also shown to restrict the size of MI via activation of adenosine triphosphate-sensitive potassium (K_{ATP}) channels (Kersten et al. 2000).

In these studies we aimed to develop large animal models of CAD, myocardial ischaemia and MI. Multimodality imaging methods were used in validation of these experimental models together with histopathological evaluation. Also, new radiopharmaceuticals for MPI with PET were tested. Additionally, the effect of levosimendan therapy on myocardial infarct size and LV function were tested in a model of chronic HF.

2. REVIEW OF THE LITERATURE

2.1 Coronary artery disease

Atherosclerosis is a progressive inflammatory disease. Signs of atherosclerosis have been reported already in children and even in fetuses (Stary 2000 and Napoli et al. 1997). Several risk factors like hypertension, high cholesterol levels, diabetes, obesity and smoking are all related to increased risk of atherosclerosis (Dahlöf 2010). Coronary artery disease (CAD) is caused by atherosclerotic plaque formation in the coronary artery vessel wall. Formation of an atherosclerotic plaque is a complex process including inflammation, accumulation of lipids, cell death and fibrosis (Hansson et al. 2006). Narrowing of coronary arteries caused by atherosclerosis can finally lead to reduced blood flow and myocardial ischaemia. Myocardial infarction (MI) is usually caused by advanced CAD and atherosclerotic plaque rupture. Atherosclerosis usually develops slowly over years and is often diagnosed after the onset of symptoms or an acute cardiac event. Ischaemic heart disease, originating from coronary atherosclerosis, is the leading cause of death worldwide (Finegold et al. 2013).

2.1.1 Atherosclerotic inflammation and plaque formation

Atherosclerotic plaques develop in the arterial wall in response to local endothelial cell dysfunction and local inflammation (Libby 2012). Cardiovascular risk factors like hypertension, hypercholesterolemia, diabetes and smoking can cause endothelial cell dysfunction, which leads to the upregulation of adhesion molecules and inflammatory cell recruitment (Libby et al. 2005). Atherosclerosis is initiated by the accumulation of low-density lipoprotein (LDL) particles into the vessel wall (Skålén et al. 2002). Oxidation of LDL leads to the expression of leukocyte adhesion molecules like vascular cell adhesion molecule-1 (VCAM-1), which lead to the infiltration of monocytes and T lymphocytes and, in combination with leukocytes, causes the secretion of chemokines such as tumour-necrosis factor alpha (TNFα), interleukins (ILs), monocyte chemoattractant protein-1 (MCP-1) and matrix metalloproteinases (MMPs) (Libby 2002). Monocyte differentiation into macrophages is induced by macrophage-colony stimulating factor (M-CSF). Subsequently, scavenger receptors (SRs) and Toll-like receptors (TLRs) are upregulated. Formation of foam cells is mediated by SR, whereas TLR initiated signal cascades lead to the activation of inflammation (Figure 1) (Yan et al. 2007). Inflammatory processes and accumulation of lipid droplets lead to initial atherosclerotic changes called fatty streaks and later formation of advanced plaques and atheromas (Hansson et al. 2006).

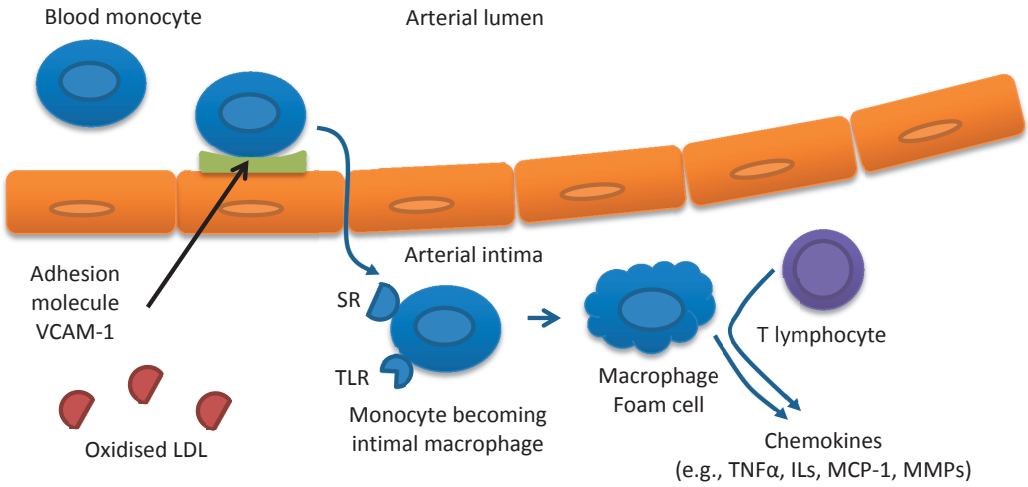

Figure 1. Inflammatory processes related to atherosclerosis.

2.1.2 Coronary artery stenosis and plaque rupture

The earliest stage of progressive atherosclerosis is intimal thickening, which is defined as an increased number of intimal smooth muscle cells. This continuous inflammatory process leads to the formation of a fibroatheroma, a lesion with a necrotic core and an overlying fibrous cap. Progressive atherosclerosis leads to more advanced plaques and narrowing of vessel lumen. Over time, atherosclerosis can cause myocardial ischaemia by the narrowing of the vessel lumen or plaque rupture. Rupture often develops a luminal thrombus, which is a common cause of acute MI and sudden death (Virmani et al. 2000).

2.2 Ischaemic cardiomyopathy

2.2.1 Myocardial ischaemia

Myocardial ischaemia occurs when the supply of oxygen no longer meets the requirement of myocardial demand. Myocardial ischaemia is caused by the limited amount of blood supply into myocardial tissue. The blood supply of heart is organised through coronary circulation and CAD is the most common cause of chronic myocardial ischaemia or infarction (Sanz et al. 2013). Insufficient blood flow can lead to regional myocardial dysfunction and later on to cardiac remodelling and HF.

Under normal aerobic conditions, fatty acids supply 60% to 90% of the energy for adenosine triphosphate (ATP) synthesis. Approximately 10% to 40% of the energy comes from oxidation of pyruvate and only small amount (3%) is derived by glycolysis (Stanley 2004). Partial reduction in coronary blood flow shifts cardiomyocytes to utilise

more glucose. Glucose metabolism needs 10% less oxygen than the oxidation of fatty acids. Still, the most of the energy (50-70%) is derived from the oxidation of fatty acids (Figure 2) (Stanley 2001). Critical myocardial ischaemia results in increase of anaerobic glycolysis leading to production of lactate. The myocyte swells due to imbalance of intracellular homeostasis, which can lead to ischaemic cell death and a decrease in contractile work.

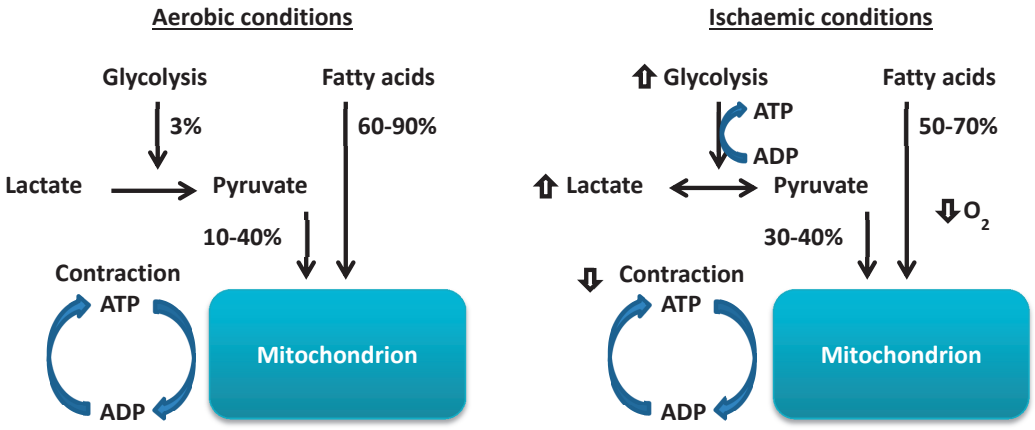

Figure 2. Myocyte energy metabolism under normal aerobic and ischaemic conditions.

2.2.2 Ischaemic preconditioning

Ischaemic preconditioning refers to the myocardial protection occurring after brief periods of sublethal ischaemia. It has been linked to reduced MI size and increased survival. Protective effects start immediately after coronary occlusion following reperfusion (first window) (Murry et al. 1986). The first window of protection is activated through opioid, adenosine, bradykinin or *alpha*1-adrenergic receptors lasting 4 to 6 hours (Figure 3) (Rodrigo et al. 2008). Activation of protein kinase C (PKC) leads to activation of mitochondrial K_{ATP} channel. The second window of protection has been demonstrated 24 hours after the preconditioning lasting up to 72 hours (Buja 2005 and Das et al. 2008). The second window is activated through nuclear factor kappa-B (NF-κB) (Figure 3). Preconditioning reduces the energy demand of the myocardium leading to preserved myocardial function and reduction of arrhythmias (Hagar et al. 1991). The exact mechanisms of this preconditioning effect remain unclear.

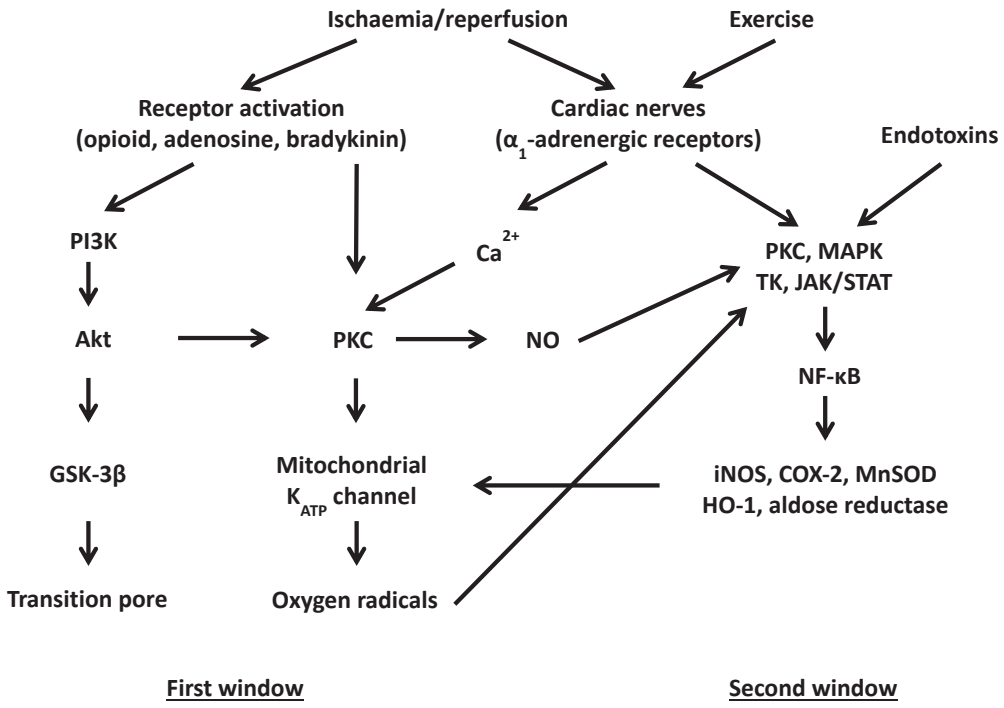

Figure 3. Mechanisms of the first and second window of ischaemic preconditioning.

2.2.3 Myocardial infarction

Myocardial infarction (MI) is caused by severe and prolonged ischaemia. The existence of coronary collateral flow is one determinant of infarct size. Necrosis occurs first in the subendocardial region. The necrotic area expands progressively transmurally, i.e., affecting the entire thickness of the wall within time (Reimer et al. 1979). The major cause of acute MI is coronary atherosclerosis with luminal thrombus. MI without atherosclerosis is rare. A prolonged period of insufficient blood flow leads to MI. Wound-healing involves fibrosis formation and MI scarring. Inflammatory cells, mainly macrophages, initially infiltrate into the necrotic myocardium. Interstitial fibroblasts are transformed into myofibroblasts by transforming growth factor-β1 (TGF-β1). Myofibroblasts express *alpha*-type smooth muscle actin and contain angiotensin-converting enzyme and matrix metalloproteinases. TGF-β1 and angiotensin II are responsible for accumulation of collagen. Changes in the myocardial extracellular matrix are very rapid and formation of collagen in the infarcted area is visible two to three days after MI. Infarcted myocardium thins and is replaced with non-functioning collagen-rich scar tissue (Swynghedauw 1999 and Bujak et al. 2007).

2.2.4 Cardiac remodelling

Myocardial remodelling includes all those changes that occur after MI to compensate for the loss of a functional myocardium. Remodelling is initiated by increased mechanical

stretch due to MI scarring. A major determinant for infarct expansion and remodelling is the transmural extent of necrosis. Complex neurohumoral remodelling processes usually lead to viable cardiac tissue hypertrophy, fibrosis and cell death. After MI, systolic function will be impaired due to the loss of contractile myocardium. This leads to increased end-systolic volume, increased heart size and increased diastolic filling pressure (Swynghedauw 1999). Elevated myocardial wall stress will be normalised by hypertrophy according to Laplace's law. The wound healing and remodelling processes after MI involves both the infarcted and non-infarcted myocardium. Fibrosis is more related to scar formation when it is replacing necrotic tissue but also to remodelling occurring interstitially in non-infarcted remote tissue. Fibrosis in the remote myocardium can be induced by vasoactive peptides and hormones like angiotensin II and by mechanical pressure overload (Heusch et al. 2014).

2.2.5 Heart failure

HF occurs when the heart is unable to pump enough blood to maintain normal circulation. It is a consequence of an abnormality in cardiac structure, function, rhythm or conduction. The most common causes of heart failure are myocardial infarction and hypertension (McMurray et al. 2005). HF can appear acutely especially in the case of MI. Most clinical signs are non-specific. Electrocardiography (ECG) can be used to measure pathological changes in the electrical conduction system of the heart. Echocardiography is widely used to demonstrate cardiac dysfunction. Other imaging modalities, such as computed tomography (CT), PET and magnetic resonance imaging (MRI) are used increasingly in the evaluation of HF. Despite recent advances in pharmacological and device therapies, prognosis of HF is often poor: 30 to 40 percent of patients die within a year and 60 to 70% die within 5 years of diagnosis (McMurray et al. 2005).

Energy metabolism is disturbed in HF. Contractile performance is decreased together with reduction of ATP, phosphocreatine and creatine kinase concentration (Liao et al. 1996). Oxygen deprivation results in impaired relaxation and contraction. Stunning can be present after prolonged ischaemia as decreased contraction persisting for hours after the return of blood flow. During hibernation, blood flow is chronically limited and the myocardium contraction fails. Inadequate blood flow leads to MI, LV remodelling and further HF (Vanoverschelde et al. 1993).

The oxygen requirement of the heart can be increased in HF due to increased cardiac work, myocardial mass, increased myocardial wall stress and wasted contractile energy. After MI, neurohumoral activation and myocardial load and stretch are increased. It leads to myocardial growth response inducing myocardial hypertrophy and myocardial remodelling. The final outcome is an increased cardiac energy expenditure and myocardial cell death through apoptosis and necrosis leading to HF (Figure 4) (Heusch et al. 2014).

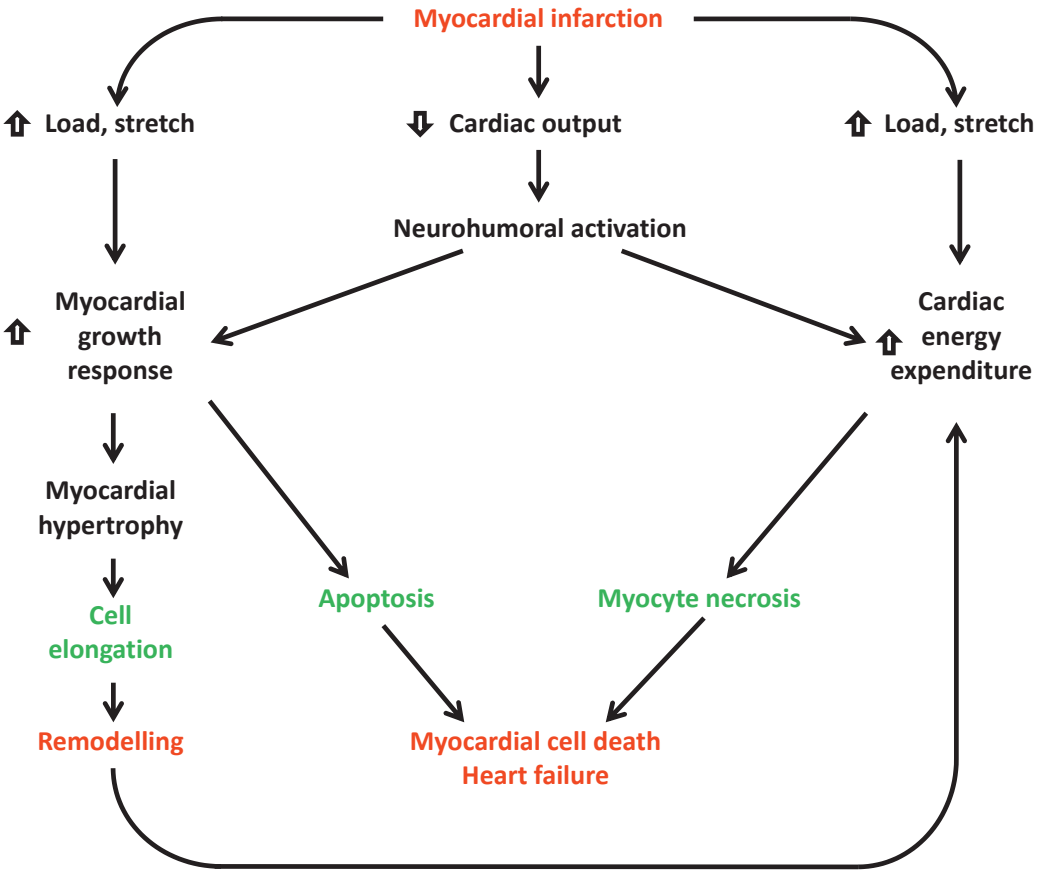

Figure 4. Mechanisms leading to myocardial remodelling and HF.

2.3 Experimental models of coronary artery disease

Atherosclerosis research using human samples is difficult because of the slow and unnoticeable development of the disease. Tissue samples are also difficult or impossible to obtain from humans. Therefore, animal models are needed. Several small animal atherosclerosis models have been developed by genetic engineering, e.g., modifying genes coding the LDL receptor or apolipoproteins (Heinonen et al. 2007). Despite several benefits, small animals have some restrictions like small size and differences in anatomy and physiology compared to humans. Large animal models are better suitable for studying coronary arteries, which are difficult or even impossible to study by using small animals. Also, achieving a more human-like size, anatomy and physiology is critical in translational research where basic research advances can be easily transferred onto a clinical stage.

Rabbit models have been widely used in cardiovascular research. Watanabe rabbits have a high serum level of LDL-cholesterol and are prone to produce atherosclerosis within a reasonable time when fed with an atherogenic diet (Aliev et al. 1998). A pig model

is considered very appropriate because the anatomy and physiology of the heart and coronary vasculature are very similar to that of humans (Bertho et al. 1964, Kamimura et al. 1996, Kassab et al. 1997 and Swindle et al. 2012). The anatomy of the pig heart is nearly similar than that of the human heart. The LV wall is thicker than in human heart. Only two pulmonary veins drain into the left atrium. The left azygous vein drains into the coronary sinus, but otherwise the coronary circulation is identical with humans (Weaver et al. 1986, Crick et al. 1998 and Swindle et al. 2012).

Pig models are used for characterising the role of monocytes during early atherosclerosis as well as smooth muscle and endothelial cell proliferation in plaque development (Gerrity 1981a, Gerrity 1981b and Gerrity et al. 1985). Atherosclerotic lesions are mainly located similarly as in humans in the proximal part of coronary arteries (Gerrity et al. 2001 and Thim et al. 2010). The morphology and progression of plaques in pig are similar to that seen in humans. Also, blood glucose, cholesterol and lipoprotein levels and metabolism are similar to those of humans.

2.3.1 Large animal models of atherosclerosis

A large animal model mimicking human-like coronary atherosclerosis is lacking, but highly needed for translational research approaches. Farm pigs with familial hypercholesterolemia develop atherosclerosis in two to three years (Thim et al. 2010). In that case, animals are usually weighing more than 200 kg and the extensive housing costs of pigs are expensive. Atherosclerosis can be induced by different techniques. The most relevant techniques with characteristics are presented in Table 1.

Normally farm pigs are naturally very resistant to develop inherent atherosclerosis. Early atherosclerotic lesions, mainly fatty streaks, are possible to achieve by hypercholesterolemia that is induced by an atherogenic diet containing high amounts of saturated fatty acids and cholesterol. Blood total cholesterol level increases from a normal level of 2 mmol/L to 5 mmol/L with a diet containing 2 percent cholesterol and 17 percent to 20 percent fat (Artinger et al. 2009 and Pueyo Palazón et al. 1998). With additional sodium cholate in the diet (1.5%), it is possible to achieve more advanced atherosclerotic plaques including fibroatheroma and cholesterol crystals with 24 to 41 percent coronary artery stenosis (Thorpe et al. 1996).

The formation of atherosclerosis can be accelerated by inducing diabetes by using streptozotocin to destroy insulin-secreting beta cells in pancreatic tissue and feeding pigs an atherogenic diet containing a high amount of cholesterol (1.5%) and lard (15%) (Gerrity et al. 2001). In that model both plasma glucose and cholesterol levels are possible to maintain near 20 mmol/L leading to more advanced atherosclerotic plaque formation including a well-developed fibrous cap overlying necrotic lipid core and coronary artery stenosis as high as 98 percent (Gerrity et al. 2001). Plaque development can also be controlled in these models using statin or angiotensin converting enzyme inhibitor therapy (Chatzizisis et al. 2009).

Genetic models have also been demonstrated. In a minipig model that has a LDL receptor mutation, atherosclerosis was successfully induced by an atherogenic diet and mechanical injury of vessel wall (Thim et al. 2010).

Pigs having mutant alleles for apolipoprotein B develop spontaneous hypercholesterolemia. Early atherosclerotic changes are visible during the first year. At two years of age, advanced plaques with a necrotic core with fibrous cap and stenotic lesions exist. By three years of age, complicated lesions and rupture are common. (Prescott et al. 1991)

Rapacz familiar hypercholesterolemia pigs develop atherosclerotic lesions mainly in peripheral arteries and are thus more relevant in studies related to peripheral arterial disease (Bahls et al. 2011).

D374Y gain-of-function mutations in the proprotein convertase subtilisin/kexin type 9 (PCSK9) gene lead to autosomal dominant hypercholesterolemia and atherosclerosis in humans. Pigs with DNA transposition of a human PCSK9 gain-of-function mutant represent an atherosclerosis model of familial hypercholesterolemia. (Al-Mashhadi et al. 2013)

Ossabaw swine represents a metabolic disease model representing increased blood glucose and impaired insulin sensitivity. Early atherosclerotic changes develop over time. (Dyson et al. 2006)

To accelerate CAD development, an oversized angioplasty balloon can be used to induce mechanical vessel wall injury. Histological changes are usually occur at the very early stage, but also advanced atherosclerotic lesions including neointima expansive remodelling and fibroatheroma have been observed in these models (Thim et al. 2010).

Coronary occlusion can be induced with a mechanical occluder to simulate plaque rupture, a complication of atherosclerosis. An ameroid constrictor has been used in atherogenic diet fed pigs in studies related to mechanisms after the rupture, e.g., collateral formation (Matyal et al. 2012).

The limitations of pig models of CAD include the lack of spontaneous development of atherosclerosis and that formed plaques remain at the initiation state without stenosis and rupture leading to MI. Also, atherosclerosis can only be induced over prolonged periods of time, which leads to increased costs and difficulties when handling heavy animals.

Table 1. Characteristics of pig models of atherosclerosis.

Technique	Characteristics	Reference
Hypercholesterolemia	Early atherosclerotic lesions, fatty streaks, intimal thickening, low-grade stenosis	Artinger et al. 2009, Turk et al. 2005, Pueyo Palazón et al. 1998, Thorpe et al. 1996, Kim et al. 1993 and Shimokawa et al. 1988
Hypercholesterolemia + hyperglycemia	Advanced atherosclerotic lesions, necrotic lipid core, well-developed fibrous cap, high-grade stenosis	Gerrity et al. 2001, Wilensky et al. 2008, LiFeng Zhang et al. 2003, Hamamdzic et al. 2010, Mohler et al. 2008, Artinger et al. 2009, McDonald et al. 2007, Dixon et al. 1999 and Chatzizisis et al. 2009
Genetic modifications	Spontaneous hypercholesterolemia, fatty streaks, advanced plaques containing necrotic core, calcification, neovascularization, hemorrhage and rupture.	Prescott et al. 1991, Hasler-Rapacz et al. 1998, Hasler-Rapacz et al. 1995, Prescott et al. 1995, Tellez et al. 2010, Bahls et al. 2011, Granada et al. 2011, Thim et al. 2010, Al-Mashhadi et al. 2013 and Thim, Hagensen, Wallace-Bradley, et al. 2010
Metabolic disease	Increased blood glucose, insulin resistance, early atherosclerotic changes	Dyson et al. 2006, Neeb et al. 2010 and Kreutz et al. 2011
Vessel wall injury	Early atherosclerotic-like lesions, eccentric fibrocellular plaques, increased intima-media ratio	Tellez et al. 2011, Worthley et al. 2000, Worthley et al. 2000, Mihaylov et al. 2000, Carter et al. 1996, Shimokawa et al. 1985 and Thim et al. 2010
Hypercholesterolemia + mechanical coronary occlusion	Regional ischaemia/infarction	Matyal et al. 2012, Matyal et al. 2013, Lassaletta et al. 2012 and Robich et al. 2011
Intramural injection of cholesteryl linoleate	Lipid-containing inflammatory lesions	Granada et al. 2005

2.4 Experimental models of ischaemic cardiomyopathy

The most used experimental models for ischaemic cardiomyopathy are mouse and rat. Rodents have many advantages like the availability, cost-effectiveness, easy handling and transgenic strains. However, there are significant differences in the anatomy and physiology of the heart and circulatory system between rodents and humans.

Dog models of myocardial ischaemia have been successfully used to study mechanisms behind MI and later myocardial remodelling and HF (Reimer et al. 1977, Reimer et al. 1979, Przyklenk et al. 1986 and Jugdutt et al. 1979). The pre-existing collateral circulation makes it difficult to induce large myocardial ischaemia or infarction in dogs (Jugdutt et al. 1979). The absence of an existing collateral network enables studies related to myocardial adaptation to ischaemia in pigs. The pig heart and circulatory system is very close to that of humans and is therefore suitable as a humanoid model of heart diseases (Swindle et al. 2012).

Several pig models having different cardiomyopathies have been introduced and can be used in studies of mechanisms of heart failure and cardiac remodelling. Pressure

overload induced by aortic stenosis can be used to cause LV hypertrophy through adaptive mechanisms that normalise to increased LV wall stress (Gelsomino et al. 2013). This situation contributes to the preservation of normal LV function and excessive collagen accumulation (Dixon et al. 2009). LV hypertrophy is a significant contributor of HF. Reduced LV relaxation and filling together with increased LV stiffness creates pressure overload models well-suited for the investigation of HF. Volume overload models can be used to mimic the clinical situation of mitral valve regurgitation. A disease model can be induced by chordal rupture of the mitral valve. Volume overload produces cellular level abnormalities causing decreased myocyte contractile function finally leading to HF. (Dixon et al. 2009)

Doxorubicin-induced HF is another model to study global HF. Intravenous injection of cardiotoxic doxorubicin rapidly progresses to systolic and diastolic dysfunction and ECG abnormalities (Torrado et al. 2011).

Dilated cardiomyopathy is defined as LV dilatation resulting in increased LV wall stress. Pacemaker-induced chronic tachycardia has been used to induce dilated cardiomyopathy and HF since 1962 (Dixon et al. 2009). Nowadays modern telemetry systems can be used in these models for chronic monitoring of changes in several hemodynamic parameters simultaneously (Choy et al. 2014).

2.4.1 Large animal models of chronic myocardial ischaemia

Myocardial ischaemia is possible to induce in several ways by causing limited blood flow in coronary artery with stenosis. In surgical open-chest models, coronary artery stenosis is induced by an occluder placed around the coronary artery. An ameroid constrictor placed around the coronary artery induces gradually an increasing reduction in blood flow leading finally to total occlusion of coronary artery. An adjustable occluder or shunt applications can be used to obtain different levels of stenosis. Mechanically working hydraulic, screw type or inflatable occluders can be used to achieve adjusted blood flow. For studies concerning myocardial angiogenesis, energy metabolism and other cellular mechanisms under chronic myocardial ischaemia, a constantly limited blood flow is desired. Fixed-diameter occluders produce constant stenosis and permanently limited blood flow. Delran stenosis, C-shape occluder or ligations are mostly used to produce fixed stenosis.

Myocardial ischaemia is possible to induce percutaneously by using invasive angiographic methods. In closed-chest models, ischaemia can be induced with an angioplasty balloon, intracoronary flow-reducer, stent or by vessel wall injury. An angioplasty balloon can be used to create acute myocardial ischaemia whereas chronic ischaemia is possible to induce by stents or vessel wall injury.

Chronic myocardial ischaemia leads to deteriorated LV function due to decreased contractility. Regional ischaemia is often seen as decreased wall motion, perfusion and

oxygen consumption. Apoptosis, glucose utilisation and lactate accumulation are usually increased. Different techniques with characteristics and selected references are listed in Table 2.

Changes in vessel geometry and intracoronary artificial occluders predispose to thrombosis leading to acute MI. Anticoagulant therapy has been successfully used to prevent premature coronary obstruction.

Table 2. Characteristics of pig models of chronic myocardial ischaemia.

Technique	Characteristics	Reference
Ameroid constrictor	Reduced left ventricular function, reduced blood flow	Caillaud et al. 2010 and Giordano et al. 2013
Carotid coronary shunt	Increased K^+ concentration, decreased pH, ST changes	Watanabe et al. 1987
Fixed-diameter occluder	Regional LV motion abnormality, reduced resting perfusion, hibernating myocardium, reduced ejection fraction (EF), increased apoptosis, reduced flow reserve	Fallavollita et al. 1999, Fallavollita et al. 1997, Fallavollita, Lim, et al. 2001, Fallavollita, Logue, et al. 2001, Fallavollita 2000, Fallavollita 2002, Fallavollita et al. 2002, Fallavollita et al. 2005, Lim et al. 1999, Hardt et al. 2001, McFalls et al. 2006, McFalls et al. 1997, Mills et al. 1994, Bloor et al. 1984, Ishikawa et al. 2011 and Heilmann et al. 2006
Adjustable occluder	Regional LV motion abnormality, decreased wall-thickening, reduced perfusion, impaired Ca^{2+} handling, depletion of contractile material, glycogen accumulation, increased amount of mitochondria, decreased oxygen consumption, increased glucose consumption, lactate production, reduced left ventricular EF, increased apoptosis, decreased flow reserve	Thomas et al. 1999, Kim et al. 2001, St. Louis et al. 2000, Hughes et al. 2001, Chen et al. 1996, Chen et al. 1997, Lai et al. 2000, Liedtke et al. 1995, Chen et al. 1997, Liedtke et al. 1994, Bolukoglu et al. 1992, Cason et al. 1991, Galiuto et al. 2002 and Sassen et al. 1988
Angioplasty balloon	Regional perfusion defect	Bamberg et al. 2012 and Mahnken et al. 2010
Intracoronary flow-reducer	Regional perfusion defect, impaired myocardial function, increased glucose utilisation	Gewirtz et al. 1981, de Groot et al. 2011, von Degenfeld et al. 2003, Johnson et al. 1998, Gewirtz, Brautigan, et al. 1983, Gewirtz, Williams, et al. 1983, Kraitchman et al. 2000 and Kraitchman et al. 2002
Copper stent	Decreased ejection fraction, hibernation, decreased wall-thickening	Wu et al. 2011, Wu et al. 2010, Bito et al. 2004, Szilárd et al. 2000 and Horstick et al. 2009
In-stent neointimal hyperplasia	Over 40% stenosis after 1-month follow-up	Hemetsberger et al. 2008 and Johnson et al. 2000
Coronary artery injury	Neointimal thickening, over 50% stenosis after 1-month follow-up	Grinstead et al. 1994, Schwartz et al. 1990, Schwartz et al. 1992 and Andersen et al. 1996

2.4.2 Large animal models of acute ischaemia-reperfusion injury and infarction

Myocardial injury leading to impaired LV function and HF can be induced by prolonged episodes of myocardial ischaemia followed by reperfusion. Temporal occlusion by angioplasty balloon is the most commonly used method to occlude coronary artery completely but only for a short period of time. Regional ischaemia occurs immediately after inflating the balloon. Deflating the balloon leads to reperfusion. Severity of ischaemia-reperfusion injury depends on the duration of ischaemia following reperfusion. Different techniques and characteristics are presented in Table 3.

A cardiopulmonary bypass model can be used to mimic the situation in open heart surgery or transplantation. An animal is first connected to a heart-lung machine. The heart is arrested with cardioplegia and the remaining body is perfused by using cardiopulmonary bypass. Global myocardial ischaemia-reperfusion injury can be studied after weaning from a heart-lung machine. Despite that the heart is well-protected with cardioplegia, damage of muscular fibres, mitochondrial swelling and intracellular oedema can be observed with transmission electron microscopy (Hong et al. 2013). Hemodilution, volume loading as well as cytokine and catecholamine surge are often induced after cardiopulmonary bypass and reperfusion (Olson et al. 2012).

The clinical situation with coronary artery occlusion following the resolution of clots and reperfusion can be modelled by regional ischaemia-reperfusion injury induced with temporal occlusion of the coronary artery surgically with clamping and ligation or percutaneously with angioplasty balloon. An ischaemic period of 30 to 120 minutes seems to be well-tolerated. Ventricular extrasystoles, non-sustained tachycardia and ventricular fibrillation can occur during ischaemia. Myocardial stunning is related to inadequate contractility of cardiomyocytes after an ischaemic condition following reperfusion and is possible to study with these models. MI is usually observed in these models without protective cardiac arrest.

Cardiac arrest has been caused also by using alternative methods like asphyxia induced by endotracheal tube clamping, electric fibrillation or placement of intracoronary ball.

Table 3. Characteristics of pig models of acute ischaemia-reperfusion injury and infarction.

Technique	Characteristics	Reference
Cardiopulmonary bypass	Decreased LV contractility, function and blood pressure, increased myocyte apoptosis, coronary blood flow and troponin levels, myofibril damage and neutrophil infiltration	Hong et al. 2013, Olson et al. 2012, Shinohara et al. 2011, Salminen et al. 2011, Abdel-Rahman et al. 2009, Banz et al. 2008, Jormalainen et al. 2007, Malmberg et al. 2006, Vähäsilta et al. 2005 and Lim et al. 2005
Coronary clamping	Stunning, decreased LV function and blood pressure, increased heart rate, MI	Díez et al. 2013, Aarsæther et al. 2012 and Sala-Mercado et al. 2010
Coronary ligation	Decreased LV function, increased apoptosis and oxidative stress, MI	Xiang-dong Li et al. 2013, Doganci et al. 2012, Meyer et al. 2013, Skyschally et al. 2013, Chinda et al. 2013, Kanlop et al. 2011, Arslan et al. 2012, Gelsomino et al. 2012, Gelsomino et al. 2011, Oyamada et al. 2010, Sodha et al. 2009, Osipov et al. 2009, Metzsch et al. 2006 and Garcia-Dorado et al. 1987
Balloon occlusion	Decreased LV contractility, function, increased apoptosis, MI	Hashizume et al. 2013, Duran et al. 2012, Ogura et al. 2012, Wheeler et al. 2012, Barallobre-Barreiro et al. 2012, Lu et al. 2013, Wojakowski et al. 2012, Chatziathanasiou et al. 2012, Bhindi et al. 2012, Poulsen et al. 2011, Dash et al. 2011, van der Pals et al. 2010, Wiggers et al. 1997, Silva et al. 2009, Boekstegers et al. 2002 and Hinkel et al. 2013
Asphyxia	Decreased LV contractility and function	Lin et al. 2013
Electric fibrillation	Elevated cardiac enzymes	Bertsch et al. 2001 and Bertsch et al. 2000
Intracoronary ball	Elevated cardiac enzymes, MI	Näslund, Häggmark, Johansson, Marklund, et al. 1992 and Näslund, Häggmark, Johansson, Pennert, et al. 1992

2.4.3 Large animal models of chronic myocardial infarction, remodelling and heart failure

A large animal model of chronic MI and HF is crucial in translational research to study complex mechanisms underlying ischaemic heart diseases. Based on literature searches, the most common way to induce MI is to use an angioplasty balloon to occlude coronary artery totally for a temporal period of time following reperfusion. Coronary artery ligation, ameroid constrictor and embolisation are also widely used methods. Different techniques and characteristics are presented in Table 4.

MI can be induced percutaneuosly by angioplasty balloon. The coronary artery is catheterised under X-ray angiography. An angioplasty balloon is placed into the coronary artery and inflated to occlude the vessel totally. After the desired occlusion time, the balloon is deflated and removed. The severity of MI depends on the occlusion

time and the balloon location. A 60-minute occlusion time produces a large transmural MI. Occlusion of 30 minutes does not produce myocardial necrosis and a 45-minute occlusion produces only a small necrotic area (Garcia-Dorado et al. 1987). Ischaemic preconditioning can be induced with repetitive balloon occlusions (Yang et al. 2011).

Coronary artery ligation and ameroid constrictor placement requires surgery. Usually thoracotomy is enough for accessing coronary arteries. A direct view of the left anterior descending coronary artery (LAD) is possible to achieve by dissecting skin and muscle between the third and fourth ribs. A spreader needs to be used to separate the ribs. After dissecting pericardium, LAD is visible.

Permanent ligation of the coronary artery leads to acute MI following LV remodelling and worsening of LV function (Huang et al. 2010 and J. Zhang et al. 1996). Infarction can also be induced by temporal coronary artery ligation following reperfusion (So et al. 2012).

An ameroid constrictor placed around a coronary artery induces gradual occlusion leading usually to MI. Complete coronary occlusion is necessary in research related to MI and for example, collateral growth.

Induction of MI by inducing embolisation with thrombogenic material like embolisation coils, intracoronary ethanol or a gelatine sponge leads to very similar MI and later changes than coronary ligation (Gálvez-Montón et al. 2014).

The size of MI should be large enough to induce remodelling processes. Distal and midpoint ligation of LAD leads to a MI size of 10 percent and 14.9 percent, respectively (Munz et al. 2011). MI sizes of 12.8 percent and 23.8 percent are reported to be achieved by ligating one-third of the LAD from the apex and below the second diagonal branch, respectively (Huang et al. 2010). Over 25 percent MI of LV is possible to achieve with proximal occlusion of LAD whereas proximal left circumflex artery (LCX) occlusion induces MI covering 20 percent of LV (Teramoto et al. 2011, Munz et al. 2011 and Roth et al. 1987). High mortality rates have been reported if the MI size exceeds 25% of the LV (Kamimura et al. 1996). Sudden cardiac deaths are reported to be in relation to fatal arrhythmias due to intolerance of ischaemia (Fallavollita et al. 2005). The ligation of a distal part of coronary artery demonstrates reasonable survival rates but only small MI. Gradual coronary artery occlusion induced using an ameroid constrictor has interestingly led to very small MI and an aggressive collateral development may be the cause (Roth et al. 1987). Combining the distal coronary ligation and proximal ameroid constrictor demonstrates large MI (>25% of LV) with clear signs of remodelling. End-diastolic and end-systolic volumes were markedly larger and EF lower in MI group when compared to controls. Hypertrophy and fibrotic changes can visualised by histology in MI group. Also, a survival rate at the 4-month time point was reported to be as high as 75 percent (Teramoto et al. 2011). A study configuration with only a proximal ameroid constrictor produced a survival rate of 30 percent. The pig heart is very sensitive to acute ischaemia

and sudden cardiac deaths can occur (Fallavollita et al. 2005). The mechanism of inhibition of sudden cardiac death with distal coronary ligation is not well-known. One hypothesis is that distal ligation provides a preconditioning effect through ischaemia and small MI as demonstrated by several studies (Murry et al. 1986, Kuzuya et al. 1993 and Hagar et al. 1991). Also, gradual occlusion may adapt the myocardium to tolerate ischaemia. A chronic HF model with impaired LV systolic function including LV dilatation, reduced EF and cellular evidence of LV remodelling offers new possibilities in translational research.

Table 4. Characteristics of pig models of chronic MI, remodelling and HF

Technique	Characteristics	Reference
Coronary ligation	Transmural MI, impaired LV function, LV dilatation, increased apoptosis	Garcia-Dorado et al. 1987, Jiang et al. 2014, Zhu et al. 2013, Prescimone et al. 2013, Munz et al. 2011, Kuster et al. 2011, So et al. 2012, Qu et al. 2012, Sahul et al. 2011, Weiss et al. 2010, Huang et al. 2010, Cho et al. 2008 and Shuros et al. 2007
Ameroid constrictor	Transmural MI, impaired LV function, LV dilatation, impaired LV wall motion and increased myocyte hypertrophy and interstitial fibrosis in the non-infarcted remote tissue, rapid collateral development	Giordano et al. 2013, Kawamura et al. 2012, Shudo et al. 2011, Teramoto et al. 2011, Barandon et al. 2010, Schneider et al. 2010, Tuzun et al. 2010, Pätilä et al. 2009, Christian et al. 2008, Ikonen et al. 2007 and Roth et al. 1987
Angioplasty balloon	Transmural MI, impaired LV function, LV dilatation	Xiaorong Li et al. 2014, Tanaka et al. 2014, Sheriff et al. 2014, Vilahur et al. 2014, Varga-Szemes et al. 2014, Pavo et al. 2014, van Hout et al. 2013, Koudstaal et al. 2013, Yan Chen et al. 2013, Duran et al. 2012, Yang et al. 2011, Pleger et al. 2011, Angeli, Amabile, Shapiro, et al. 2010, Angeli, Amabile, Burjonroppa, et al. 2010, Lautamäki et al. 2009, Pérez de Prado et al. 2009, Holz et al. 2009, Brødløs et al. 2009, Krombach et al. 2005, Garcia-Dorado et al. 1987 and Abegunewardene et al. 2009
Embolisation	Transmural MI, impairer LV function and wall motion, LV dilatation	Gálvez-Montón et al. 2014, Gálvez-Montón et al. 2013, Biondi-Zoccai et al. 2013, Fish et al. 2013, Saeed et al. 2013, Song-Yan Liao et al. 2010, Peukert et al. 2009, Dib et al. 2006, Cui et al. 2005, Dogné et al. 2005, Waksman et al. 2004, Reffelmann et al. 2004, Sakaguchi et al. 2003, Crisóstomo et al. 2013, Weon Kim et al. 2011, Joudinaud et al. 2005 and Ohtsuka et al. 2003

2.5 Imaging of coronary artery disease and ischaemic cardiomyopathy

2.5.1 Invasive coronary artery imaging

Coronary artery stenosis, plaques and their progression can be evaluated with invasive angiography combined with intravascular ultrasound (IVUS) and optical coherence tomography (OCT). Calcified plaques, shear stress as well as atheroma volume and fibrous cap thickness can be assessed with OCT (Sanz et al. 2013).

2.5.2 Molecular imaging of atherosclerotic inflammation

Several pathological processes related to atherosclerosis can be assessed with PET imaging. Plaque formation is a response to the inflammatory process. Macrophages are a good imaging target (Rudd et al. 2002). Also, neoangiogenesis, hypoxia and microcalcification are associated with advanced plaque formation and are good targets for imaging purposes (Tarkin et al. 2014).

[^{18}F]FDG is a radiolabelled glucose analogue, which is widely used in PET imaging of metabolic activity. [^{18}F]FDG is taken up by the cells using glucose transporters. Phosphorylated [^{18}F]FDG is trapped inside the cell. Clearance from blood circulation is rapid and trapped tracer accumulation can be visualised even with a low background if PET imaging is performed for some time after the tracer injection. Because of high glucose metabolism of myocardium, the analysis of the [^{18}F]FDG uptake in coronary arteries can be difficult due to high background activity. A low-carbohydrate, high-fat meal prior to scanning has been introduced to suppress myocardial uptake (Wykrzykowska et al. 2009). Increased vascular [^{18}F]FDG accumulation indicates increased macrophage activity in atherosclerotic inflammation (Figure 5) (Tarkin et al. 2014).

Mannose receptors (MRs) are expressed by macrophages in high-risk plaques and are suggested to serve as more specific targets of imaging tracers (Figure 5). ^{18}F-labelled mannose has successfully been used in the visualisation of atherosclerotic lesions (Tahara et al. 2014).

Overexpression of somatostatin receptors in activated macrophages can be visualised with the [^{68}Ga]DOTATATE (1,4,7,10-tetraazacyclododecane-1,4,7,10-tetraacetic acid octreotate) tracer (Figure 5) (Rominger et al. 2010).

The translocator protein (TSPO) ligand [^{11}C]PK11195 (N-butan-2-yl-1-(2-chlorophenyl)-N-methylisoquinoline-3-carboxamide) accumulates during vascular inflammation through increased TSPO expression in activated macrophages (Figure 5) (Laitinen et al. 2009).

Folate receptors (FRs) are expressed by activated macrophages (Figure 5). Increased uptake of folate receptor targeting tracers in atherosclerotic plaques has been shown in recent studies (Ayala-López et al. 2010 and Jager et al. 2014).

Scavenger receptors (SRs) are related to the macrophage differentiation into foam cells. Radiotracers targeting scavenger receptor may help to visualise foam cells in active atherosclerotic lesions (Bigalke et al. 2014).

Increased expression of different adhesion molecules are related to atherosclerotic inflammation and, for example, P-selectin and VCAM-1 are possible targets for imaging tracers (Figure 5) (Nakamura et al. 2013 and Nahrendorf et al. 2009).

Choline takes part in cell membrane formation. Choline is believed to be accumulated in activated macrophages and incorporated into cell membranes after phosphorylation by choline kinase (Figure 5). Increased uptake of [^{11}C]choline and [^{18}F]choline in atherosclerotic plaques has been demonstrated (Laitinen et al. 2010 and Matter et al. 2006).

Hypoxia plays an important role in atherosclerotic plaque formation (Figure 5). [^{18}F] fluoromisonidazole ([^{18}F]FMISO) is used to successfully visualise hypoxia. FMISO is a cell permeable compound, which is rapidly reoxidised and moved out from the cell under normal oxygenation conditions. In hypoxic cells, FMISO is covalently bound to intracellular macromolecules and remains in the cells (Mateo et al. 2014). [^{18}F]EF5 (2-(2-Nitro-1H-imidazol-1-yl)-N-(2,2,3,3,3-pentafluoropropyl) acetamide) is a lipophilic compound and has better pharmacokinetic properties than FMISO. Atherosclerotic lesions containing hypoxia have been successfully visualised with [^{18}F] EF5 in atherosclerotic mouse models (Silvola et al. 2011).

Formation of atherosclerotic plaques leads to local hypoxia. Hypoxia is able to induce increased expression of integrin $\alpha_v\beta_3$, which is related to angiogenesis (Figure 5). Elevated integrin $\alpha_v\beta_3$ expression is linked to macrophages involved in atherosclerotic inflammation (Antonov et al. 2004). Experiments with radiolabelled tri-peptide sequence arginine-glycine-asparagine based tracers such as [^{68}Ga]NOTA-RGD and [^{18}F]galacto-RGD have increased tracer accumulation in atherosclerotic plaques (Paeng et al. 2013, Laitinen et al. 2009, Beer et al. 2014 and Haukkala et al. 2009). Also, apoptosis plays a central role in atherosclerotic inflammation and has shown to be a possible target for molecular imaging. For instance, apoptosis-specific Annexin 5 is used to visualise vascular inflammation (Laufer et al. 2008).

Microcalcification is related to atherosclerotic plaque development. [^{18}F]Sodium fluoride ([^{18}F]NaF) is an option for identifying plaques (Figure 5) (Joshi et al. 2014).

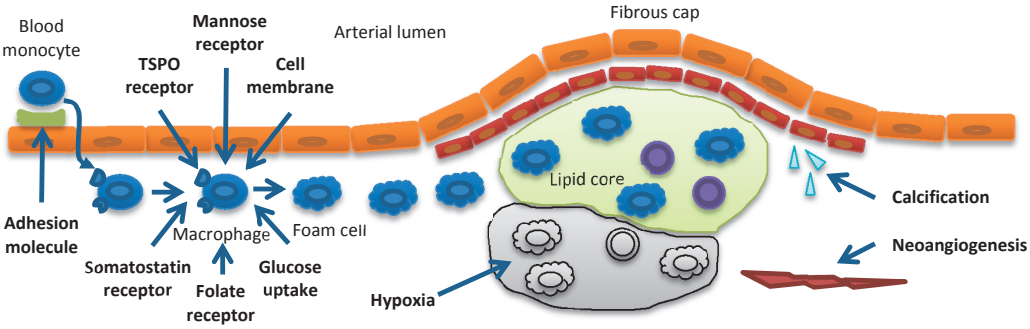

Figure 5. Possible PET imaging targets related to atherosclerosis are macrophage infiltration, hypoxia, neoangiogenesis and microcalcification.

2.5.3 Left ventricular function and structure

Echocardiography is one of the most important techniques for the detection and assessment of myocardial ischaemia and infarction. Cardiac ultrasound is used in the detection of the effects of myocardial ischaemia or infarction on LV function. LV size, wall thickness and myocardial wall motion can be examined by conventional 2D imaging. Diastolic and systolic volumes and EF of LV can be calculated using well-established methods. Echocardiography is a valuable tool for diagnosing MI with assessment of wall motion. MI is, in most cases, associated with regional LV motion abnormality (Greupner et al. 2012).

CT is a technique that allows for the evaluation of cardiac structure and function. When combined with ECG gating and a contrast agent, high quality images can be obtained. Diastolic and systolic volumes and EF of LV can be calculated using semi-automated analysis software. LV size, wall thickness and myocardial wall motion can also be examined easily. The advances of CT imaging include high spatial resolution (Greupner et al. 2012).

Cardiovascular magnetic resonance imaging (CMR) is the gold standard for the assessment of LV function (Pennell et al. 2004). The assessment of cardiac function can be implemented using CineMRI, which is accurate in the measurement of diastolic and systolic volumes and EF as well as cardiac mass (Scholtz et al. 2014).

2.5.4 Myocardial perfusion

Myocardial perfusion imaging (MPI) can be performed with several techniques. Nuclear cardiology has been growing in the diagnosis and risk assessment of patients with suspected heart disease. Single-photon emission computed tomography (SPECT) was used in MPI since the early 1980s with thallium-201 (^{201}Tl) and Technetium-99m hexakis(2-methoxy-2-methylpropylisonitrile) ([^{99m}Tc]sestamibi) after approval by the United States Food and Drug Administration (FDA) in 1990. In addition to ^{201}Tl and [^{99m}Tc]sestamibi, a newer widely used SPECT tracer [^{99m}Tc]tetrofosmin allows evaluation of myocardial perfusion (Kelly et al. 1993).

PET is increasingly used in MPI. Kinetic properties of PET tracers enable more accurate quantification of myocardial blood flow. For example, [^{15}O]water is ideal for the blood flow quantitation (Knuuti et al. 2009).

Cardiac MRI is becoming more commonly used in MPI with a gadolinium-based contrast agent. First-pass perfusion can be detected. The gradient echo pulse sequence is most commonly used to visualise perfusion. Stress perfusion MRI has a high diagnostic accuracy in detecting coronary artery disease (Scholtz et al. 2014).

CT imaging allows also MPI with dynamic acquisition. Iodinated contrast bolus behaves similar to gadolinium-based contrast agents used in MRI. The most recent techniques

with 320-row CT enable MPI covering whole heart with relatively high temporal resolution (George et al. 2012).

Myocardial perfusion can be assessed with echocardiography using gas-filled microbubbles, nano- or microparticles as a contrast media (Seol et al. 2014).

Resting myocardial perfusion remains normal until occlusion of a coronary artery exceeds 90% (Gould et al. 1974). Stress imaging can be used to confirm perfusion defect in unclear case. Pharmacologic stress testing is used with coronary vasodilators, e.g., adenosine or regadenoson. Coronary blood flow will be increased three- to five-fold. Combining rest- and stress-imaging enables calculation of myocardial flow reserve (MFR). Resting myocardial blood flow (MBF) values can be corrected with rate-pressure product (RPP).

Changes in hemodynamics during vasodilatator infusion are possible at least with a high dose of vasodilators used in experimental study settings. To maintain blood pressure, the α1-adrenoceptor agonist phenylephrine can be used to oppose the systemic effects of adenosine, while leaving adenosine-induced coronary vasodilation unperturbed (Sorop et al. 2008).

MPI results are usually presented using 17-segmental standardised myocardial segmentation and nomenclature for the tomographic imaging of the heart as proposed by the American Heart Association (Cerqueira et al. 2002).

2.5.5 Myocardial infarction and viability

[^{99m}Tc]Sestamibi is the most used SPECT tracer for assessment of myocardial viability. Retention in myocardium is dependent on the intensity of the Na^+/K^+ pump in the cell membrane and reflects the intracellular level of potassium. [^{99m}Tc]Sestamibi is taken up by mitochondria (Allman 2013).

[^{18}F]FDG is a widely used PET tracer for assessing myocardial viability. PET has higher spatial resolution than SPECT. Metabolic clamping can be used for standardising myocardial glucose utilisation. The myocardium usually uses free fatty acids (FFAs) for energy production. Glucose and insulin administration before tracer injection switches energy metabolism to use more glucose than FFAs. [^{18}F]FDG is trapped inside the viable myocyte through phosphorylation by hexokinase. The clearance from blood circulation is fast allowing high myocardium-to-blood ratios. [^{18}F]FDG viability imaging is often combined with MPI using [^{13}N]ammonia, [^{82}Rb]Cl or [^{15}O]water.

Previous approaches can be replaced by a dynamic imaging with carbon-11 labelled acetate ([^{11}C]acetate). Quantification of regional MBF and oxidative metabolism are possible with a single study (Wolpers et al. 1997).

[^{15}O]Water enables calculation of perfusable tissue fraction (PTF) and perfusable tissue index (PTI). Assessment of viability has also demonstrated to be possible by using PTF calculated by a [^{15}O]water study (Iida et al. 2012).

Cardiac MRI enables viability assessment by using a gadolinium-based late enhancement method to define the existence of the MI scar. The transmural extent of the MI scar is possible to visualise very accurately from MRI images with high spatial resolution (Kim et al. 2000).

Viable myocardium can be estimated by measuring the contractile reserve during stress. Based on this, echocardiography can be used for the evaluation of viable myocardium (Bisplinghoff et al. 2014).

2.5.6 PET imaging of myocardial metabolism

Myocardial energy expenditure can be measured with PET. FFAs are a major myocardial energy substrate under normal conditions. Energy metabolism in failing myocytes is altered and shifted to use more glucose. Myocardial glucose utilisation can be assessed with [^{18}F]FDG or [^{11}C]glucose and fatty acid utilisation with [^{18}F]FTHA (14(*R,S*)-[^{18}F] fluoro-6-thia-heptadecanoic acid) or [^{11}C]palmitate (Tuunanen et al. 2011).

Oxidative metabolism is affected rapidly after MI. Myocardial oxygen consumption can be estimated with [^{11}C]acetate imaging. Myocardial efficiency, which is defined as the ratio between cardiac work and myocardial oxygen consumption, is often decreased in HF and can be measured non-invasively by combining measurement of myocardial oxygen consumption and LV work (Bengel et al. 2000).

New specific radioligands make it possible to evaluate cellular changes related to post-MI remodelling. For example the development of new blood vessels can be assessed with RGD–based tracers targeting $\alpha_v\beta_3$ integrin in relation with neoangiogenesis (Kiugel et al. 2014).

2.6 Positive inotropic therapy in heart failure

The calcium ion (Ca^{2+}) has a central role in myocyte contraction. The calcium ion makes the contraction possible by binding to troponin C, which leads to conformational changes in troponin I. During relaxation, Ca^{2+} will be released from troponin C and will be transported to sarcoplasmic reticulum or outside the cell (Figure 6). Phospholamban regulates the storing of calcium ions into the sarcoplasmic reticulum. The Na^+/Ca^{2+} exchanger delivers calcium ions out of the cell, which is also regulated by Na^+/K^+-ATPase. Cyclic AMP increases the activity of protein kinase A (PKA), which leads to phosphorylation of the Ca^{2+} channel and increased calcium ion influx into the cell. Intracellular concentration of Ca^{2+} increases leading to contraction. Activation of β-receptor leads to increased cyclic AMP and the activation of PKA. (Francis et al. 2014)

The PKA-dependent contractility of myocardium can be increased with β-receptor agonists like dobutamine and dopamine or phosphodiesterase inhibitor, e.g., milrinone.

The Na^+/Ca^{2+} exchanger can be regulated with cardiac glycosides (digoxin). Calcium sensitisers act by binding to troponins.

Levosimendan is a calcium sensitiser used for inotropic support in acutely decompensated congestive HF. Levosimendan binds to cardiac troponin C and with the presence of calcium ions stabilises the troponin conformation. Levosimendan has also a vasodilatory effect by opening ATP sensitive potassium channels leading to vascular smooth muscle relaxation. Unlike inotropic agents in general, levosimendan has neutral effects on myocardial efficiency (Ukkonen et al. 2000). Inotropic and vasodilatory effects result in an increased contractility and decreased preload and afterload. Also, the mitochondrial ATP sensitive K^+-channel-mediated cardioprotective effect is linked to levosimendan (Papp et al. 2012).

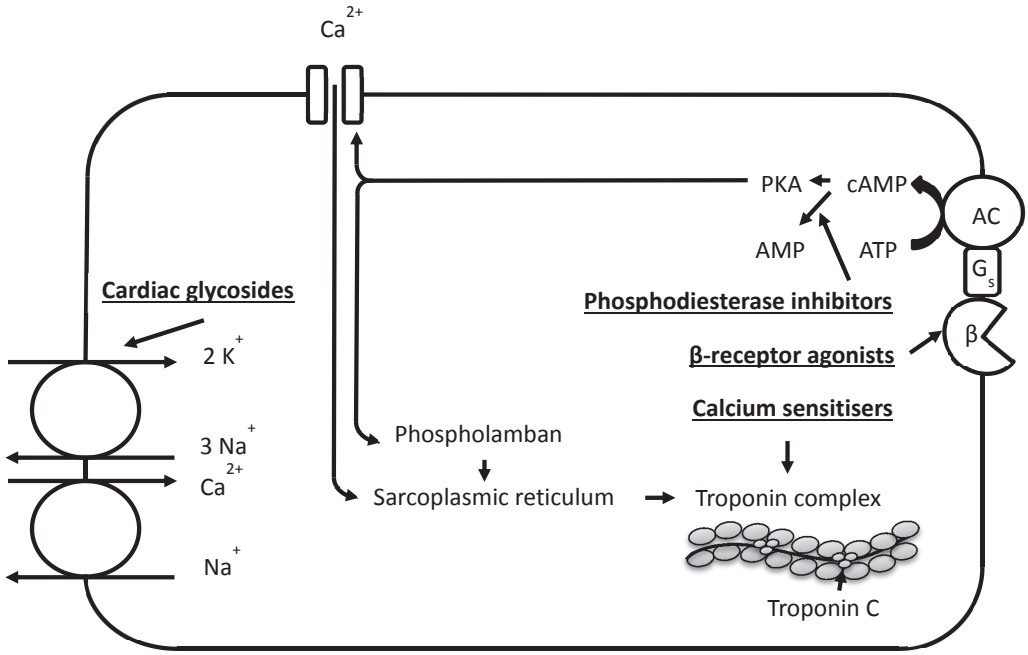

Figure 6. Mechanisms of cardiomyocyte calcium metabolism and contraction. Levosimendan is a calcium sensitiser acting through binding to cardiac troponin C and with the presence of calcium ions stabilises troponin conformation.

3. AIMS OF THE STUDY

The purpose of this study was to develop and validate experimental large animal models for the use in studying coronary artery disease, MI and HF using multimodality imaging approaches. Additionally, potential radiopharmaceuticals and therapies were tested.

The specific aims of the study were:

1. To investigate the feasibility of [^{18}F]FDG PET imaging of inflammation in early coronary atherosclerotic lesions in a pig model of diabetes and hypercholesterolemia
2. To characterise cardiac remodelling in a new pig model of chronic heart failure by assessment of left ventricular functional, metabolic and structural changes using PET, CT and echocardiography
3. To characterise a bottleneck stent model for chronic myocardial ischaemia and infarction in pigs using PET imaging of myocardial perfusion
4. To test new ^{68}Ga-labeled tracers for PET imaging of myocardial perfusion in pigs
5. To study the effects of long-term levosimendan therapy on myocardial infarct size and left ventricle function after acute coronary occlusion in a pig model of post-infarction heart failure

4. MATERIALS AND METHODS

Finnish landrace pigs were used in the experiments. All animal experiments were conducted in accordance with the European Union Directive for the use of experimental animals and approved by the national Animal Experiment Board of Finland (ELLA) and the Regional State Administrative Agency for Southern Finland (ESAVI).

4.1 Coronary artery disease model (I)

4.1.1 Experimental protocol

The formation of atherosclerotic plaques was accelerated by inducing diabetes. Diabetes was induced by destroying beta cells using streptozotocin injections. Pigs were sedated with ketamine (30 mg/kg intramuscularly (*i.m.*), Ketalar, Amgen Technology Ireland, Dublin, Ireland) and streptozotocin 50 mg/kg (Zanosar, Pharmacia & Upjohn, Kalamazoo, MI, USA) was injected via ear vein once a day for 3 days. In order to offset insulin release from pancreas, glucose was given 25 g *per os* twice daily for 2 days. An atherogenic diet containing either 1.5% cholesterol and 15% lard (HF, n=6) or 4% cholesterol, 20% lard and 1.5% sodium cholate (HF+c, n=4) (Special Diet Services, Witham, UK) was started five days after the last streptozotocin injection and was continued for 6 months. Blood glucose and cholesterol levels were monitored regularly.

4.1.2 In vivo PET imaging of atherosclerotic inflammation

After six months of diet intervention, [^{18}F]FDG uptake of coronary arteries was studied by PET. Myocardial glucose uptake was suppressed with an overnight fasting and by giving a carbohydrate free diet for two days before the PET study. PET studies were performed by a PET and a 64 slice CT hybrid scanner (Discovery VCT, General Electric Medical Systems, Milwaukee, WI, USA) operated in 3-dimensional mode. List-mode acquisition for 30 minutes started 120 minutes after intravenous (*i.v.*) [^{18}F]FDG injection. The acquired list-mode data was divided into cardiac and respiratory gates and were combined as dual gates compensating for both respiratory and cardiac motion. Results were presented as target-to-background ratios (TBR) calculated by dividing maximum standardised uptake value (SUV) of each coronary segment by mean SUV value of the blood.

4.1.3 Ex vivo studies

After the PET study, animals were sacrificed by *i.v.* injection of potassium chloride (B. Braun Medical Oy, Helsinki, Finland). Coronary arteries were prepared and proximal samples were collected. Samples were weighed and [^{18}F]FDG uptake was measured with a gamma counter (1480 Wizard 3″; PerkinElmer/Wallac, Turku, Finland). SUVs and further vessel-to-blood ratios were calculated.

The coronary artery samples were mounted, frozen in isopentane mixed with dry ice and cut into longitudinally sections. An autoradiography study with a phosphor imaging plate (BAS-TR2025, Fuji Photo Film Co. Ltd., Tokyo, Japan) was performed. Radioactivity distribution of the 40 μm cryosections was analysed using Fluorescent Image Analyser (Fujifilm FLA-5100, Fuji Photo Film Co. Ltd., Tokyo, Japan).

Cryosections of 8 μm were stained with hematoxylin & eosin (HE) and Movat's pentachrome staining. Movat's pentachrome stained samples were graded using a light microscope with the following scores: 1=healthy normal vessel wall, 2=intimal thickening, and 3=atheroma.

Tissue sections stained with HE were digitally photographed using a light microscope. Autoradiographs and HE images were co-registered and [^{18}F]FDG accumulation of atherosclerotic lesions and non-atherosclerotic vessel wall as photostimulated luminescence per square millimetre (PSL/mm^2). Lesion-to-normal vessel wall ratios were calculated for each segment.

4.2 Surgical and percutaneous myocardial infarction model (II, III)

4.2.1 Experimental protocol

Before operations or imaging studies, animals were anaesthetised by *i.m.* administration of midazolam 1 mg/kg (Midazolam Hameln, Hameln Pharmaceuticals GmbH, Hameln, Germany) and xylazine 4 mg/kg (Rompun vet, Bayer Animal Health GmbH, Leverkusen, Germany) (II) or with atropine (0.05 mg/kg; Leiras, Helsinki, Finland) and azaperone (Stresnil, 8 mg/kg; Janssen, Titusville, NJ, USA) (III). Animals were intubated and ventilated mechanically. Anaesthesia was maintained with *i.v.* infusion of propofol 10−50 mg/kg/h (Propofol Lipuro, B. Braun Melsungen AG, Melsungen, Germany) combined with fentanyl 4−10 μg/kg/h (Fentanyl-Hameln, Hameln Pharmaceuticals GmbH, Hameln, Germany).

In order to induce myocardial ischaemia and infarction surgically (II), a short left anterior thoracotomy was performed. The pericardium was opened and a complete ligation of the distal LAD was made immediately after the second diagonal branch using a 5-0 monofilament polypropylene suture (Prolene, Ethicon, Norderstedt, Germany). After 15 minutes, the proximal LAD was prepared free and an ameroid constrictor (2.50 mm or 2.75 mm, model MRI-2.50-TI and MRI-2.75-TI; Research Instruments SW, Escondido, CA, USA) was placed around the LAD. Arrhythmias were prevented by administration of amiodarone (Cordarone, Sanofi-Synthelabo Ltd, Newcastle upon Tyne, UK) 8 mg/kg perorally (p.o.) daily for 1 week before and for 2 weeks after the operation. Amiodarone 6 mg/kg *i.v.*, metoprolol 0.2 mg/kg *i.v.* (Seloken, Genexi, Fontenay sous Bois, France) and magnesium sulphate ($MgSO_4$) 25 mg/kg *i.v.* (Addex-magnesium sulfate, Fresenius Kabi AB, Uppsala, Sweden) were administered intraoperatively. Clopidogrel 3 mg/kg p.o. (Plavix, Sanofi Winthrop Industrie S.A., Ambarès et Lagrave, France) was administered

daily 1 day before and daily for 2 weeks after the surgery to prevent premature thrombosis of the LAD.

A percutaneously placed intracoronary bottleneck stent was used to induce myocardial ischaemia and infarction (III). Catheterisation was done using a GE Innova 3100^{IQ} three-dimensional (3-D) angiography device (GE Healthcare, Waukesha, WI, USA). The bottleneck stent consisted of a bare metal stent and polytetrafluoroethylene heat shrink tube. The other end of the tube was shaped into a bottleneck to restrict coronary blood flow. The construct was placed into LAD with 6-F AR-2 guiding catheter. In order to prevent arrhythmias, per oral amiodarone (Cordarone, 200 mg/day, Sanofi-Aventis, Paris, France) and bisoprolol (Bisoprolol-ratiopharm, 2.5 mg/day, Ratiopharm, Ulm, Germany) was started 1 week before stenting. Prior to stenting, 100 mg intravenous lidocaine (10 mg/ml, Orion Pharma, Espoo, Finland) and 2.5 ml $MgSO_4$ (Addex-magnesium sulfate, 246 mg/ml, Fresenius Kabi, Uppsala, Sweden) was administered. One day before stenting, per oral acetylsalicylic acid (ASA-ratiopharm, 300 mg, Lannacher Heilmittel GmbH, Lannach, Austria) and clopidogrel (Clopidogrel Mylan, 300 mg, Mylan, Saint Priest, France) was given. ASA (100 mg/day p.o.), clopidogrel (75 mg/day p.o.) and enoxaparin (30 mg/day *s.c.*) were continued for one week to keep the stent open.

4.2.2 PET imaging of myocardial perfusion and viability

Myocardial perfusion was measured at 3 months after the ameroid constrictor placement (II) and one week and five weeks after the bottleneck stenting (III) with [^{15}O]water PET. MPI was done at rest and under pharmacological stress with adenosine 200 µg/kg/min (Adenosin Life Medical, Life Medical Sweden AB, Stocksund, Sweden). The acquisition protocol consisted of following frames: 14 × 5 s, 3 × 10 s, 3 × 20 s, 4 × 30 s (total duration 4 min 40 s). The segmental LV myocardial blood flow was quantified using a single-compartment model (Iida et al. 1992).

Infarcted and ischaemic myocardial regions were defined using 70% of maximum as a threshold in [^{15}O]water PET flow quantitation at rest and during stress, respectively (III).

Myocardial viability was assessed at five weeks after the bottleneck stenting with [^{18}F]FDG PET (III). Myocardial glucose utilisation was normalised with an intravenous injection of 1 g/kg glucose and 10 IU of insulin prior tracer injection. A static 15-min PET scan was performed 40 minutes after the injection. Viability was determined as viable, partially viable or nonviable (relative [^{18}F]FDG uptake 85, 67–85 and 67%, respectively).

4.2.3 Left ventricular size and function (II)

Transthoracic echocardiography was performed for measurement of cardiac output by pulsed-wave Doppler from the LV outflow tract (LVOT) and calculated as velocity time integral × heart rate.

End-diastolic and end-systolic volumes (EDV, ESV) and EF as well as LV mass were evaluated by contrast-enhanced CT.

4.2.4 Myocardial oxidative metabolism and efficiency (II)

Myocardial perfusion and oxidative metabolism was assessed by [^{11}C]acetate PET imaging. The scanning frames were as follows: 10 × 10 s, 1 × 60 s, 5 × 100 s, 5 × 120 s, 5 × 240 s (total duration 41 min). Myocardial blood flow was determined by the initial uptake rate (k_1) of [^{11}C]acetate (van den Hoff et al. 2001). The clearance rate constant of [^{11}C]acetate (K_{mono}) was assessed reflecting myocardial oxygen consumption (Armbrecht et al. 1990).

Myocardial infarct size was determined using a reduction of 40% as a cut-off for the k_1 of [^{11}C]acetate PET.

Global myocardial efficiency was estimated by a work-metabolic index (WMI) with the following equation: WMI = (cardiac output) × (systolic blood pressure) / K_{mono} × LV mass (Ukkonen et al. 2009). Regional efficiency of the remote non-infarcted myocardium, K_{mono}, was studied in relation to the systolic wall stress using the following equation: Efficiency = wall stress / regional K_{mono}.

4.2.5 Tissue samples and histology

Immediately after the imaging studies, the animals were sacrificed and heart was prepared and sliced horizontally to four slices. After 15-min incubation in 1% 2,3,5-triphenyltetrazolium chloride (TTC) (Sigma-Aldrich, Saint Louis, MO, USA), samples were photographed and the size of infarcted region was visually estimated.

Samples for histology were collected from the infarcted, non-infarcted remote (inferolateral wall). Samples were mounted and frozen in isopentane mixed with dry ice. Cryosections of 7 μm were stained with Masson's trichrome staining. The content of fibrosis was quantified from remote sections with the colour deconvulation method using ImageJ software (Ruifrok et al. 2001).

4.3 New myocardial perfusion tracers (IV)

4.3.1 Study design

The suitability of four previously discovered ^{68}Ga-labelled ligands for MPI was tested. Results obtained with ^{68}Ga-tracers were compared with [^{15}O]water PET flow quantitation. Hexadentate bis(salicylaldimine) ligands, tris(3-methoxysalicylaldimine) (Tracer-1) and tris(3-ethoxysalicylaldimine) (Tracer-2) of bis(2,2-dimethyl-3-aminopropyl)-ethylenediamine (BAPEN) and the bis(salicylaldimine) (Tracer-3) and

bis(3-methoxysalicylaldimine) (Tracer-4) of bis(3-aminopropyl)-dimethylenediamine (BAPDMEN) were tested in healthy pigs.

4.3.2 PET imaging and kinetic modelling of [^{68}Ga] ligands

Myocardial blood flow (MBF) was measured first with [^{15}O]water. Then ^{68}Ga-tracer was injected following 92-min scanning with following frames: 18 × 10 s, 4 × 30 s, 2 × 120 s, 1 × 180 s, 4 × 300 s, 6 × 600 s. For analysis of MBF with ^{68}Ga-chelates, single-compartment model and multiple-time graphical analyses for irreversible tracer uptake (Patlak plot) and reversible tissue uptake (Logan plot) were applied. Linear correlation between MBF measured with [^{15}O]water and modelling results of ^{68}Ga-ligands was calculated as using Pearson correlation.

4.3.3 Organ distribution

Organ samples were collected immediately after the PET imaging. Samples of whole blood, plasma, urine, heart, lung, liver, spleen, kidney, muscle, brain, bone, bone marrow, salivary gland and abdominal fat were prepared, weighed and measured for radioactivity using a gamma counter (Wizard). Additionally, myocardium-to-liver, myocardium-to-lung and myocardium-to-blood ratios were calculated.

4.3.4 In vitro binding to serum proteins

Binding of ^{68}Ga-ligands to serum proteins was determined using serum obtained from human, pig or rat. The assay was performed with the ultrafiltration method as described earlier by Basken et al. (Basken et al. 2008) and results were expressed as an unbound fraction (%).

4.4 Chronic levosimendan therapy for heart failure (V)

4.4.1 Study design

The pigs had a two-step occlusion of the LAD with distal ligation and proximal ameroid constrictor. Three weeks after the surgical operation, transthoracic echocardiography was done to visualise LV wall motion (Figure 7). Clear signs of large motion abnormality in the LAD region was defined to be inclusion criteria. Animals with LV wall motion defect were allocated into control group (n=18) or levosimendan group (n=7). Levosimendan was given per orally 5 mg/kg once a day (Orion Pharma Ltd, Espoo, Finland). Intervention was continued 8 weeks and was stopped one week before terminal imaging studies. Imaging studies consisted of echocardiography, PET and CT. After imaging studies, animals were sacrificed and cardiac tissue samples were collected.

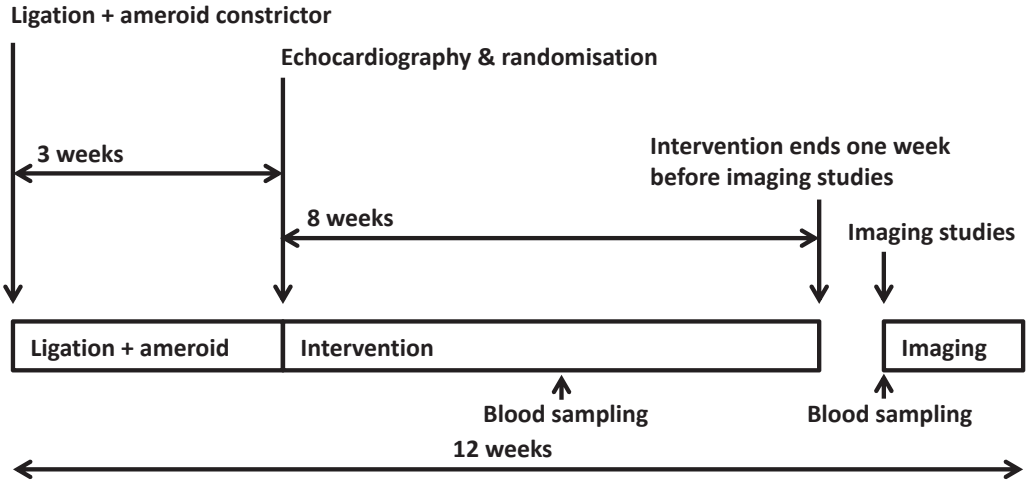

Figure 7. Study outline of the 8-week levosimendan intervention study where distal left anterior descending coronary artery (LAD) was ligated and ameroid constrictor was placed in the proximal part of LAD.

4.4.2 Effects of chronic levosimendan therapy on MI size, LV function and remodelling

Myocardial infarct size was determined by TTC-stained tissue samples and using a reduction of 40% as a cut-off in the initial uptake rate (k_1) of [^{11}C]acetate PET.

Left ventricular function was evaluated by measurement of end-diastolic and end-systolic volumes and ejection fraction from CT images.

Cardiac remodelling was evaluated by calculation of work-metabolic index reflecting myocardial efficiency. Myocyte hypertrophy and amount of fibrosis was estimated by histology.

4.5 Statistical analyses

Results were expressed as means ± standard deviation. A Shapiro-Wilk test was applied to determine whether the data were normally distributed. Correlation between study characteristics was analysed using either Pearson or Spearman correlation. Statistical significances between two study groups were evaluated by Mann-Whitney U test or two-tailed t-test. Statistical significances between more than two study groups were evaluated with one-way ANOVA and Bonferroni *post hoc* tests. P-values <0.05 were considered significant.

5. RESULTS

5.1 Atherosclerotic plaque inflammation (I)

The principal study consisted of 10 pigs with a 6-month diet intervention. Pigs were hyperglycemic and hypercholesterlomic. Prior to imaging studies, the blood glucose level was 12.3±4.7 mmol/L and plasma total cholesterol level was 12.7±5.1 mmol/L.

5.1.1 Ex vivo studies

In total, 33 coronary artery segments were prepared and studied. As histological grading based on Movat pentachrome staining, seven segments were defined as a healthy vessel wall, 16 as intimal thickening and 10 as an atheroma. Intimal thickening and atheroma lesions contained a high density of inflammatory cells.

Increased [^{18}F]FDG uptake was seen by autoradiography in coronary segments with intimal thickening and atheroma. Lesion-to-normal vessel wall ratio was 1.7±0.7 times higher in the areas of intimal thickening and 4.1±2.3 in the atheroma plaques.

The *ex vivo* biodistribution study showed increased [^{18}F]FDG accumulation in atheroma lesions compared to healthy coronary segments. Vessel-to-blood ratios of [^{18}F]FDG accumulation were 1.3±0.7, 2.0±1.0 and 2.6±1.2 in the segments with no plaque, intimal thickening or atheroma lesions, respectively.

5.1.2 In vivo PET imaging

Coronary [^{18}F]FDG accumulation was visualised by dual-gated cardiac PET images co-registered with CTA image (Figure 8). [^{18}F]FDG uptake in the myocardium was low. Average TBR was 1.1±0.5, 1.2±0.4 and 1.6±0.6 in the segments with no plaque, intimal thickening and fibroatheroma, respectively. In dual-gated PET, the highest TBR was 2.7 whereas it was only 2.0 in non-gated PET.

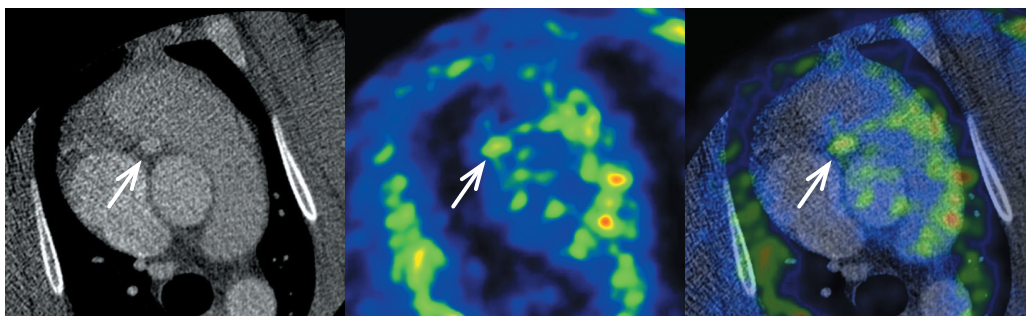

Figure 8. Fused axial coronary CTA and dual-gated [^{18}F]FDG PET images showing cross-section of the proximal right coronary artery (arrow) in an animal with atheroma.

5.2 Myocardial infarction and remodelling (II, III)

5.2.1 Myocardial perfusion and viability

Average MBF measured in the remote non-infarcted myocardium with [^{15}O]water PET was comparable between pigs with distal LAD ligation and proximal ameroid constrictor and sham-operated control pigs (rest MBF: 0.97±0.32 *vs.* 1.24±0.40 mL/g/min, *P*=0.12; stress MBF: 1.61±0.75 *vs.* 1.94±1.00 mL/g/min, *P*=0.43). Also, further calculations of coronary flow reserve (CFR) and coronary vascular resistance (CVR) in the remote tissue showed no statistical differences between study groups (CFR 1.68±0.63 in ameroid pigs, 1.60±0.65 in control group, *P*=0.80; CVR 107.1±31.5 in ameroid pigs, 93.0±29.2 mm Hg/(mL/g/min) in control group, *P*=0.33) (II).

In the bottleneck stented pigs, a smaller perfusion defect (24±12% of the LV) was seen at rest and larger during stress (53±10% of the LV). Four weeks after discontinuation of antiplatelet medication, large perfusion defect areas were seen in both at rest and during stress (42±13% and 54±10% of the LV, respectively) (Figure 9) (III).

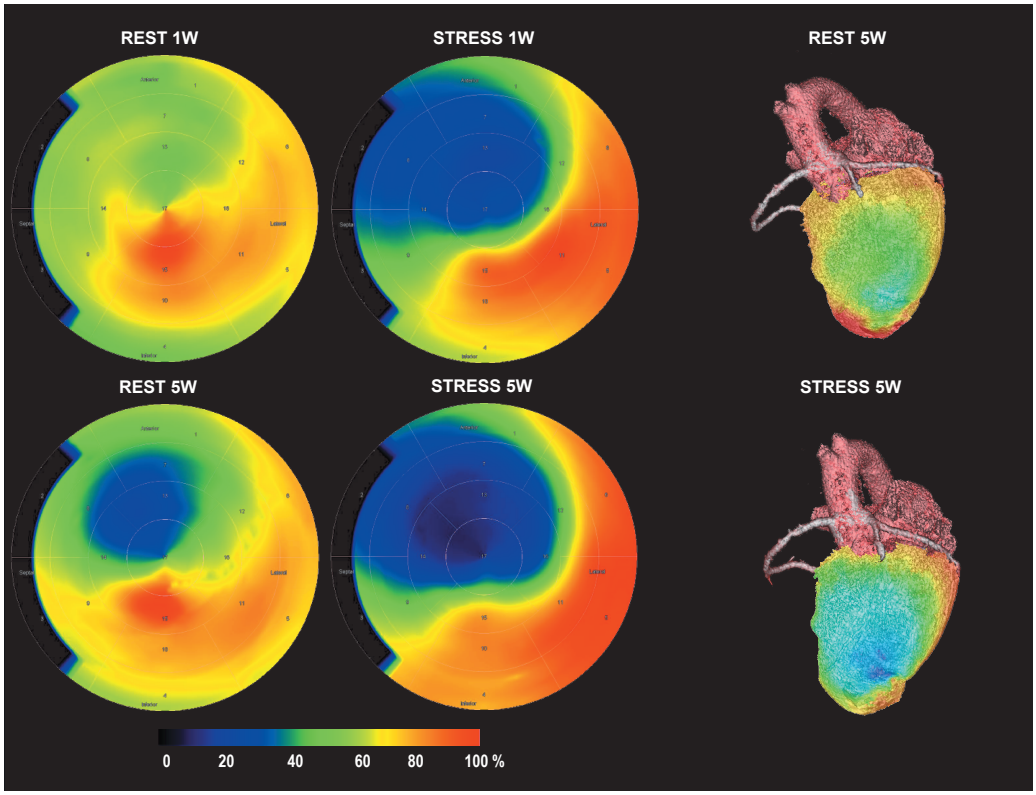

Figure 9. Inducible ischaemia seen in perfusion maps obtained with [^{15}O]water PET at 1 week after placing a bottleneck stent into the left anterior descending coronary artery (LAD). After stopping the antiplatelet medication, the stent has occluded and caused myocardial infarction as seen at the 5-week time point.

Analysis of the [^{18}F]FDG viability study performed in bottleneck stented pigs at four weeks after discontinuation of antiplatelet medication showed that 36±3% of the LV myocardium was non-viable and 36±18% viable whereas 28±15% was defined as partially viable (III).

5.2.2 Left ventricular function (II)

CT imaging showed increased LV end-diastolic and end-systolic volumes in pigs having distal ligation of the LAD and proximal ameroid constrictor compared to controls (EDV 252±84 *vs*. 145±17 mL, P=0.003; ESV 154±68 *vs*. 53±7 mL, P<0.001) (Figure 12). Ejection fraction was reduced in ameroid pigs (40±8% *vs*. 63±4%, P<0.001). LV mass normalised for body weight showed a higher LV mass to body weight index in ameroid pigs (1.90±0.39 *vs*. 1.37±0.61 g/kg, P=0.02).

5.2.3 Myocardial oxidative metabolism and efficiency (II)

Analysis of the clearance rate (K_{mono}) of [^{11}C]acetate showed that oxygen consumption was reduced in the infarcted regions, but was comparable in the non-infarcted remote myocardium of the ameroid pigs and sham-operated controls (remote K_{mono} 0.104±0.020 *vs*. 0.119±0.028 min^{-1}, P=0.16). Global myocardial efficiency was lower in the ameroid than sham-operated pigs (33.2±11.1 *vs*. 52.7±16.6 mmHg × mL × min × g^{-1} × 10^3, P=0.005). Regional efficiency in the remote tissue was increased in ameroid pigs (995±287 *vs*. 647±99 mmHg × min, P=0.004).

5.2.4 Tissue samples and histology (II)

TTC staining revealed that there was mostly a transmural infarct scar in the LV region vascularised by the LAD. Based on analysis of [^{11}C]acetate data, the size of MI was 29±14% (range 14%-57%) of the LV. MI size defined by [^{11}C]acetate perfusion and TTC staining corresponded well.

Measurement of cardiomyocyte diameter in samples from the remote non-infarcted myocardium indicated increased myocyte hypertrophy in ameroid pigs (23.5±2.6 *vs*. 21.4±1.6 µm, P=0.04). The amount of fibrosis was comparable between the study groups (5.5±1.9% in ameroid pigs; 4.9±1.1% in control group, P=0.39).

5.3 Evaluation of new perfusion tracers (IV)

5.3.1 PET imaging and kinetic modelling of [^{68}Ga] ligands

PET imaging of four ^{68}Ga labelled hexadentate bis(salicylaldimine) ligands showed the highest and fastest uptake into myocardium on Tracer-3 (Figure 10).

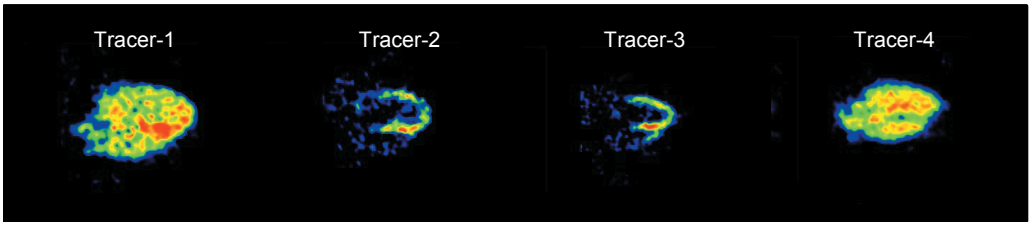

Figure 10. Representative horizontal long-axis view of heart showing the myocardial uptake of the ^{68}Ga tracers at 52-92 min after the tracer injection.

Patlak plots (K_i) and one-tissue compartmental model (K_1) were calculated. Modelling results were plotted against MBF results obtained with [^{15}O]water. There was no correlation between K_i and MBF measured with [^{15}O]water. There tended to be a weak correlation between K_1 and MBF for Tracer-1 (r=0.81, P=0.20), but not for any other tracer.

5.3.2 Organ distribution

Uptake of ^{68}Ga labelled hexadentate bis(salicylaldimine) ligands was slightly higher in the myocardium than in other examined organs. Accumulation in kidney and bile were high indicating elimination and excretion routes. Tracer-3 showed good myocardium-to-blood (7.63±1.89), myocardium-to-lung (3.03±0.33) and myocardium-to-liver (1.80±0.82) ratios.

5.3.3 In vitro binding to serum proteins

A high difference in tracer binding to serum proteins was seen between human, pig and rat serum. The unbound tracer fraction was similarly low between human serum (9.4±5.7%) and pig serum (5.5±2.1%), whereas it was markedly higher in rat serum (45.4±20.9%).

5.4 Evaluation of chronic levosimendan intervention for heart failure (V)

5.4.1 Effects of chronic levosimendan therapy on MI size, LV function and remodelling

As measured after the 8-week intervention period following one week washout, myocardial infarct size was smaller in the levosimendan group when compared with control animals (12±13% *vs*. 27±15%, P=0.03).

CT imaging showed smaller LV EDV and ESV in the levosimendan group (EDV 161±29 mL *vs*. 245±84 mL, P = 0.06; ESV 81±18 mL *vs*. 149±67 mL, P=0.03). The ejection fraction tended to be higher in the levosimendan group (50±6% *vs*. 41±8%, P=0.06).

Myocardial efficiency remained unchanged after intervention and was comparable between study groups (44±11 in the levosimendan group and 33±11 mmHg × mL × min × g^{-1} × 10^3 in the control group, P=0.15).

Histological analysis of non-infarcted remote sections indicated that the average diameter of cardiomyocytes (levosimendan group 23.2±2.0 μm *vs.* control group 23.5±2.6 μm, P=0.83) and the amount of fibrosis (4.8±1.9% in the levosimendan group; 5.5±1.9% in the control group, P=0.37) were comparable between study groups.

6. DISCUSSION

Non-invasive assessment of atherosclerotic inflammation can be beneficial to recognise patients having a high risk for cardiac events. Early detection of highly inflamed atherosclerotic lesions could give us an opportunity to identify unstable plaques, improve the care of CAD patients and reduce the risk of sudden cardiac death.

Myocardial infarction often leads to adverse cardiac remodelling and finally heart failure. Oxidative metabolism and perfusion of myocardial tissue can be evaluated by [^{11}C] acetate PET. Additionally, efficiency of cardiac work can be calculated. In this study we wanted to validate the HF model of distal LAD ligation and proximal ameroid constrictor with the evaluation of perfusion, oxidative metabolism and cardiac efficiency.

As the prognosis of heart failure is poor, new therapies for the management of progression of post-MI adverse cardiac remodelling and heart failure are warranted. As earlier studies have already shown levosimendan could have multiple positive effects to prevent adverse cardiac remodelling. This study proved the beneficial effects of levosimendan as well as that the developed model of HF can be used for the evaluation of new interventions.

6.1 PET imaging of early atherosclerotic lesions

Imaging of atherosclerotic inflammation by [^{18}F]FDG PET could be valuable for identifying high-risk patients. Increased [^{18}F]FDG accumulation exists in culprit lesions by *in vivo* imaging studies (Rogers et al. 2010). In this study we evaluated [^{18}F]FDG uptake in early atherosclerotic lesions by *in vivo* imaging and *ex vivo* studies. The main finding of this study was that [^{18}F]FDG accumulation was increased in coronary arteries with intimal thickening and atheroma as confirmed by autoradiography and histological evaluation.

PET imaging of coronary arteries may be an effective method to differentiate atherosclerosis patients having highly inflamed vulnerable plaques or stable plaques with low inflammatory activity. The dual-gated method for minimising the cardiac and respiratory movement artefact increased TBR as the highest TBR in dual-gated PET was 2.7 and 2.0 in non-gated PET that is consistent with previous studies (Tarkin et al. 2014). Still, it was not statistically possible to differentiate [^{18}F]FDG uptake between a healthy vessel wall or one with intimal thickening or an atheroma. The sensitivity of *in vivo* PET is probably not sensitive enough for detecting small objects with a low accumulation of imaging tracer.

Advanced atherosclerotic lesions with coronary stenosis was reported in a previous study with a similar study setting that combined hyperglycemia and hypercholesterolemia (Gerrity et al. 2001 and Chatzizisis et al. 2008). However, very early atherosclerotic

changes were noticed in the current study. Coronary stenosis was not identified as confirmed with CTA and histology.

Further studies are warranted to clarify if more advanced atherosclerotic lesions can be induced within a reasonable follow-up time. PET imaging of atherosclerotic lesions showed to be effective and the dual-gating method improved the signal-to-noise ratio. Clinically relevant CAD model could be beneficial in developing further clinical diagnostics and treatments.

6.2 Validation of a surgically induced model of myocardial infarction

A translational research model to study chronic changes after MI is needed. In this study, cardiac remodelling was followed 3 months after MI. Two-step occlusion of LAD with distal ligation and proximal ameroid constrictor led to MI covering 24 percent of the LV as confirmed with [^{11}C]acetate perfusion imaging and TTC staining of myocardial organ samples.

LV size was increased over 70 percent whereas EF was decreased 37 percent. Global myocardial efficiency was decreased 37 percent, which is connected to HF. Increased LV size led to increased myocardial wall stress. Histologically-detectable myocyte hypertrophy is linked to cardiac remodelling and is a compensatory mechanism for increased wall stress. Interestingly, interstitial fibrosis was not seen as described previously in a similar study (Teramoto et al. 2011).

As high as a 75 percent survival rate was reported by the authors of the original model description (Teramoto et al. 2011). In this study, the overall survival was only 26%. Still, most of unexpected sudden deaths occurred during the first week of the surgery and chronic phase survival was 44%. Sudden cardiac deaths are common in other pig studies and are probably linked to large MI size (Fallavollita et al. 2005, Huang et al. 2010 and Ishikawa et al. 2011).

In this study, we confirmed the feasibility of a chronic post-MI heart failure model utilising two-step occlusion of the LAD with distal ligation followed by implantation of an ameroid constrictor in the proximal part. Left ventricular hypertrophy, impaired systolic function and LV remodelling were confirmed by imaging studies and histological evaluation. Measurements of myocardial oxidative metabolism demonstrated reduced cardiac efficiency. We conclude that this model may be used for the evaluation of new interventions.

As the mortality observed in this study was very high, further development of the model of chronic HF is needed. This study furthered the understanding behind the mechanisms of cardiac remodelling. Further studies relating to ischaemic preconditioning and preventing adverse cardiac remodelling post-MI are needed.

6.3 Validation of percutaneously-induced model of myocardial ischaemia and infarction

Bottleneck stenting of LAD induced large ischaemic region as measured with [^{15}O]water (24% of LV at rest and 53% of LV during stress). Discontinuing of antiplatelet medication led to an increased defect area (42% of LV at rest and 54% of LV during stress).

As measured by [^{18}F]FDG, the non-viable portion of LV was 36 percent at four weeks after discontinuing of antiplatelet medication. Infarct size was large referring to the clinical situation and this measurement makes it possible to evaluate processes after MI.

An advantage of this model compared to ameroid model is that chronic myocardial ischaemia can be studied by continuing antiplatelet medication. Also, a lack of adhesion and inflammation induced by wound healing occurring after thoracic surgery noticed in surgical MI model can be beneficial in studies based on surgical interventions. Inflammation induced by wound healing can influence negatively also imaging studies of inflammation.

6.4 PET imaging and kinetic modelling of [^{68}Ga] ligands

Studied ^{68}Ga-labelled hexadentate bis(salicylaldimine) ligands were retained in the myocardium as shown in previous study with rats (Hsiao et al. 2009). Uptake into the myocardium was slow as well as clearance from blood pool. Kinetic modelling showed that myocardial perfusion cannot be determined with these four [^{68}Ga] ligands as compared to MBF results obtained with [^{15}O]water.

There was no significant correlation between results obtained with [^{15}O]water and the net uptake rate K_i (Patlak plot) and K_1 (one-compartmental model). One possible explanation for slow kinetics could be that tracers are very slowly moved across the cell membranes. A slow transport rate is a limiting factor for K_i and K_1. An unknown factor other than perfusion may be limiting the accumulation into the myocardium. Another explanation could be a high tracer binding to serum proteins (91%-96% in pig *vs*. 29%-73% in rat) because the protein-bound fraction tracers are not expected to freely diffuse into tissues, which is one requirement for an effective perfusion tracer.

A slow transport rate and high protein binding together could be the explanation for the lack of correlation between MBF measured with [^{15}O]water and [^{68}Ga] ligands as tested in healthy pigs.

Despite the lack of correlation between tested [^{68}Ga] tracers and [^{15}O]water in this study with pigs, further studies are needed to clarify the mechanisms of the [^{68}Ga] ligands, which showed to be promising for MPI in a previous rat study.

6.5 Chronic levosimendan intervention for heart failure

In this study, the effects of 8-week levosimendan intervention, started three weeks after distal ligation of the LAD and placement of proximal ameroid constrictor, were studied. A significant reduction in MI size was seen in animals that received levosimendan 5 mg/kg for 8 weeks. Previously this kind of cardioprotection and reduced MI sizes were reported in a study where levosimendan therapy was initiated before inducing myocardial ischaemia and infarction (Kersten et al. 2000). In this study, a LV wall motion defect was confirmed by echocardiography before allocating animals into study groups and beginning the therapy.

Animals in the levosimendan group have also smaller EDV and ESV and higher EF than animals in the control group. That is probably explained by a smaller MI size. These results are consistent with the results of previous small animal studies.

Beneficial effects of levosimendan in this study are possibly explained by mitochondrial K_{ATP} channel-mediated preconditioning, which protects myocytes against ischaemia (Gross et al. 1992). Also, increased collateral blood flow has been noticed after levosimendan administration (Kersten et al. 2000).

Levosimendan intervention restricted the size of MI and further cardiac remodelling, but more studies are needed to explain the exact mechanisms. Levosimendan is used for the management of acutely decompensated heart failure. Based on our results, levosimendan could have benefits also in the early treatment of acute myocardial infarction. Large animal models and clinical imaging methods used in this study enable quantitative analysis of myocardial perfusion and efficiency. This study that experimental pig model for CAD, MI, and HF could be used for further intervention studies.

6.6 Critical evaluation of the results

Large animal models of atherosclerosis enable the evaluation of coronary arteries by using *in vivo* imaging methods. In this study we were able to induce early atherosclerotic changes including intimal thickening and atheroma-type lesions in relation to clinical coronary artery disease. This study showed how *ex vivo* methods can be used in a validation of *in vivo* results obtained by clinical imaging device. Despite the relatively long follow-up time we did not noticed any narrowing of coronary arteries with anatomical imaging methods. Also, highly inflamed coronary lesions clinically related to increased risk for cardiac events were lacking. Long follow-up led to high expenses due to costly animal housing and special high-fat diet. Also, a significant increase in body mass in short periods of time led to difficulties in animal handling.

Surgical protocol consisted of distal ligation of the LAD and proximal ameroid constrictor led to large myocardial infarction following LV adverse cardiac remodelling in relation to clinical picture of myocardial infarction and heart failure. Even though we used distal

ligation of the LAD to induce ischaemic preconditioning, a high amount of sudden deaths were noticed in this study. Intolerance of myocardial ischaemia leading to high mortality was one important limitation in this study. Mortality in this study was higher than in HF patients and is probably not reflecting well the clinical picture. Additionally, in the clinic, HF is mainly a problem in older adults. Fairly young animals need to be used in experiments. Physiologic increases in heart mass during follow-up can be avoided by using models involving adult minipigs (Schuleri et al. 2008).

A bottleneck stent placed into the LAD led to the situation mimicking clinically relevant myocardial ischaemia and infarction. Premature occlusion of coronary artery was prevented by antiplatelet medication, which can lead to bleeding complications. Also, a high quality coronary angiography device and good operator skills are needed to perform this percutaneous method.

The evaluation of myocardial perfusion with ^{68}Ga-labelled hexadentate bis(salicylaldimine) ligands was positive in rat studies. In this study with healthy pigs, these ligands were retained into myocardium, but the kinetics were very slow. We noticed that tracers were binding highly to serum proteins. Binding properties to serum proteins were very similar between pig and human (91%-96% in pig *vs.* 83%-96% in human), whereas it was remarkable different in rat (29%-73%). This large animal model was better for translational studies because it is more close to human metabolism than rodent models in this case.

Chronic levosimendan therapy tested in chronic MI model showed to have beneficial properties to restrict the size of MI and cardiac remodelling post-MI. Limitations in this study are related to high variability in the size of MI and imbalance of study population between control and intervention group.

6.7 Future aspects

Experimental pig models of atherosclerosis having myocardial ischaemia and infarction offer a versatile platform for translational research. In the future, more novel radiopharmaceuticals and interventions can be studied. Novel therapeutics can be focused on prevention of atherosclerotic plaque formation and rupture. New interventions concerning heart failure could consist of an innovative batch materials replacing infarcted myocardium. Also, gene and stem cell therapies are promising to improve cardiac function after MI. Large animal models with a human-like clinical picture are effective and valuable tools for biomedical research.

Large animal models are needed because it is not possible to study complex mechanisms of atherosclerosis and HF with alternative methods like cell cultures. The size of pig enables the imaging studies of coronary arteries. In small animal models, we need to use another vessel like the aorta for modelling of atherosclerosis. In large animal studies, we can use already existing methods and devices dedicated to clinical studies and thus

new innovations are more easily translated into clinical use. Despite many advantages of large animal models, there are also some disadvantages, which might be taken into account in study planning like difficulties in handling of heavy animals. Large animal studies need special facilities for animal housing and operations and can lead to high expenses. The use of large animal models remains restricted to research of new concepts close to clinical application.

More advanced mechanisms behind atherosclerosis and heart failure can be evaluated with multimodality imaging methods. We and others have evaluated the imaging of different stages of atherosclerotic changes with [^{18}F]FDG PET, but it is still unsolved how to use this information in clinical imaging of atherosclerotic patients in the future. Myocardial oxidative metabolism and further assessment of cardiac efficiency is possible with [^{11}C]acetate PET. Still, these methods are relatively rarely used in clinical imaging and thus have a huge potential in monitoring of efficacy of treatment in HF patients. Large animals enable the use of clinical imaging methods and thus new interventions can be studied in translational models before entering clinical trials.

7. SUMMARY AND CONCLUSIONS

On the basis of our experimental studies on atherosclerosis and heart failure, we make these conclusions:

1. Model of diabetes and hypercholesterolemia was feasible and we found an increased uptake of [^{18}F]FDG in early coronary atherosclerotic lesions in a pig model of diabetes and hypercholesterolemia.

2. Two-step occlusion of the LAD with distal ligation and proximal ameroid constrictor resulted in a large MI and LV remodelling together with decreased myocardial efficiency during a 3-month follow-up.

3. The bottleneck stent placed in the LAD resulted in a large ischaemic region of myocardium followed by large MI after discontinuing of antiplatelet medication.

4. Evaluation of four ^{68}Ga-labelled hexadentate bis(salicylaldimine) ligands showed no correlation between myocardial perfusion measured with [^{15}O]water.

5. Eight-week levosimendan therapy started after recent occlusion of the LAD resulted in decreased MI size followed by attenuation of myocardial remodelling and improved systolic function.

Large animal models mimicking clinical conditions and multimodality imaging can be used as valuable tools in translational research of atherosclerosis and HF. Large animals enable the use of clinical imaging methods and thus new interventions can be studied in translational models before entering clinical trials.

9. REFERENCES

Aarsæther, E., Straumbotn, E., Rösner, A. and Busund, R. 2012. "Oral B-Glucan Reduces Infarction Size and Improves Regional Contractile Function in a Porcine Ischaemia/reperfusion Model." *European Journal of Cardio-Thoracic Surgery : Official Journal of the European Association for Cardio-Thoracic Surgery* 41 (4): 919–25.

Abdel-Rahman, U., Risteski, P., Tizi, K., Kerscher, S., Behjati, S., Bejati, S., Zwicker, K., Scholz, M., Brandt, U. and Moritz, A. 2009. "Hypoxic Reoxygenation during Initial Reperfusion Attenuates Cardiac Dysfunction and Limits Ischemia-Reperfusion Injury after Cardioplegic Arrest in a Porcine Model." *The Journal of Thoracic and Cardiovascular Surgery* 137 (4): 978–82.

Abegunewardene, N., Vosseler, M., Gori, T., Hoffmann, N., Schmidt, K.-H., Becker, D., Kreitner, K.-F. et al. 2009. "Usefulness of MRI to Differentiate between Temporary and Long-Term Coronary Artery Occlusion in a Minimally Invasive Model of Experimental Myocardial Infarction." *Cardiovascular and Interventional Radiology* 32 (5): 1033–41.

Aliev, G. and Burnstock, G. 1998. "Watanabe Rabbits with Heritable Hypercholesterolaemia: A Model of Atherosclerosis." *Histology and Histopathology* 13 (3): 797–817.

Allman, K.C. 2013. "Noninvasive Assessment Myocardial Viability: Current Status and Future Directions." *Journal of Nuclear Cardiology : Official Publication of the American Society of Nuclear Cardiology* 20 (4): 618–37; quiz 638–39.

Al-Mashhadi, R.H., Sørensen, C.B., Kragh, P.M., Christoffersen, C., Mortensen, M.B., Tolbod, L.P., Thim, T. et al. 2013. "Familial Hypercholesterolemia and Atherosclerosis in Cloned Minipigs Created by DNA Transposition of a Human PCSK9 Gain-of-Function Mutant." *Science Translational Medicine* 5 (166): 166ra1.

Angeli, F.S., Amabile, N., Burjonroppa, S., Shapiro, M., Bartlett, L., Zhang, Y., Virmani, R. et al. 2010. "Prolonged Therapy with Erythropoietin Is Safe and Prevents Deterioration of Left Ventricular Systolic Function in a Porcine Model of Myocardial Infarction." *Journal of Cardiac Failure* 16 (7): 579–89.

Angeli, F.S., Amabile, N., Shapiro, M., Mirsky, R., Bartlett, L., Zhang, Y., Virmani, R. et al. 2010. "Cytokine Combination Therapy with Erythropoietin and Granulocyte Colony Stimulating Factor in a Porcine Model of Acute Myocardial Infarction." *Cardiovascular Drugs and Therapy / Sponsored by the International Society of Cardiovascular Pharmacotherapy* 24 (5-6): 409–20.

Antonov, A.S., Kolodgie, F.D., Munn, D.H. and Gerrity, R.G. 2004. "Regulation of Macrophage Foam Cell Formation by alphaVbeta3 Integrin: Potential Role in Human Atherosclerosis." *The American Journal of Pathology* 165 (1): 247–58.

Armbrecht, J.J., Buxton, D.B. and Schelbert, H.R. 1990. "Validation of [1-11C]acetate as a Tracer for Noninvasive Assessment of Oxidative Metabolism with Positron Emission Tomography in Normal, Ischemic, Postischemic, and Hyperemic Canine Myocardium." *Circulation* 81: 1594–1605.

Arslan, F., Houtgraaf, J.H., Keogh, B., Kazemi, K., de Jong, R., McCormack, W.J., O'Neill, L.A.J. et al. 2012. "Treatment with OPN-305, a Humanized Anti-Toll-Like Receptor-2 Antibody, Reduces Myocardial Ischemia/reperfusion Injury in Pigs." *Circulation. Cardiovascular Interventions* 5 (2): 279–87.

Artinger, S., Deiner, C., Loddenkemper, C., Schwimmbeck, P.L., Schultheiss, H.-P. and Pels, K. 2009. "Complex Porcine Model of Atherosclerosis: Induction of Early Coronary Lesions after Long-Term Hyperlipidemia without Sustained Hyperglycemia." *The Canadian Journal of Cardiology* 25 (4): e109–14.

Ayala-López, W., Xia, W., Varghese, B. and Low, P.S. 2010. "Imaging of Atherosclerosis in Apoliprotein E Knockout Mice: Targeting of a Folate-Conjugated Radiopharmaceutical to Activated Macrophages." *Journal of Nuclear Medicine : Official Publication, Society of Nuclear Medicine* 51 (5): 768–74.

Bahls, M., Bidwell, C.A., Hu, J., Krueger, C.G., Reed, J.D., Tellez, A., Kaluza, G.L., Granada, J.F., Van Alstine, W.G. and Newcomer, S.C. 2011. "Gene Expression Differences in Healthy Brachial and Femoral Arteries of Rapacz Familial Hypercholesterolemic Swine." *Physiological Genomics* 43 (12): 781–88.

Bamberg, F., Hinkel, R., Schwarz, F., Sandner, T.A., Baloch, E., Marcus, R., Becker, A. et al. 2012. "Accuracy of Dynamic Computed Tomography Adenosine Stress Myocardial Perfusion Imaging in Estimating Myocardial Blood Flow at Various Degrees of Coronary Artery Stenosis Using a Porcine Animal Model." *Investigative Radiology* 47 (1): 71–77.

Banz, Y., Rieben, R., Zobrist, C., Meier, P., Shaw, S., Lanz, J., Carrel, T. and Berdat, P. 2008. "Addition of Dextran Sulfate to Blood Cardioplegia Attenuates Reperfusion Injury in a Porcine Model of Cardiopulmonary Bypass." *European Journal of Cardio-Thoracic Surgery : Official Journal of the European Association for Cardio-Thoracic Surgery* 34 (3): 653–60.

Barallobre-Barreiro, J., Didangelos, A., Schoendube, F.A., Drozdov, I., Yin, X., Fernández-Caggiano, M., Willeit, P. et al. 2012. "Proteomics Analysis of Cardiac Extracellular Matrix Remodeling in a Porcine Model of Ischemia/reperfusion Injury." *Circulation* 125 (6): 789–802.

Barandon, L., Calderon, J., Réant, P., Caillaud, D., Lafitte, S., Roques, X., Couffinhal, T. and Dos Santos, P. 2010. "Adjustment and Characterization of an Original Model of Chronic Ischemic Heart Failure in Pig." *Cardiology Research and Practice* 2010.

Basken, N.E., Mathias, C.J., Lipka, A.E. and Green, M.A. 2008. "Species Dependence of [64Cu]Cu-Bis(thiosemicarbazone) Radiopharmaceutical Binding to Serum Albumins." *Nuclear Medicine and Biology* 35 (3): 281–86.

Beer, A.J., Pelisek, J., Heider, P., Saraste, A., Reeps, C., Metz, S., Seidl, S. et al. 2014. "PET/CT Imaging of Integrin αvβ3 Expression in Human Carotid Atherosclerosis." *JACC. Cardiovascular Imaging* 7 (2): 178–87.

Bengel, F.M., Permanetter, B., Ungerer, M., Nekolla, S. and Schwaiger, M. 2000. "Non-Invasive Estimation of Myocardial Efficiency Using Positron Emission Tomography and Carbon-11 Acetate--Comparison between the Normal and Failing Human Heart." *Eur.J.Nucl.Med.* 27: 319–26.

Bergmann, S.R., Fox, K.A., Rand, A.L., McElvany, K.D., Welch, M.J., Markham, J. and Sobel, B.E. 1984. "Quantification of Regional Myocardial Blood Flow in Vivo with H215O." *Circulation* 70 (4): 724–33.

Bertho, E. and Gagnon, G. 1964. "A Comparative Study in Three Dimension of the Blood Supply of the Normal Interventricular Septum in Human, Canine, Bovine, Procine, Ovine and Equine Heart." *Diseases of the Chest* 46 (September): 251–62.

Bertsch, T., Denz, C., Janke, C., Weiss, M., Fassbender, K., Luiz, T., Ellinger, K. and Krieter, H. 2001. "Hypertonic-Hyperoncotic Solutions Decrease Cardiac Troponin I Concentrations in Peripheral Blood in a Porcine Ischemia-Reperfusion Model." *Experimental and Toxicologic Pathology : Official Journal of the Gesellschaft Für Toxikologische Pathologie* 53 (2-3): 153–56.

Bertsch, T., Janke, C., Denz, C., Weiss, M., Luiz, T., Ellinger, K., Korth, U., Hannak, D., Bartelt, U. and Krieter, H. 2000. "Cardiac Troponin I and Cardiac Troponin T Increases in Pigs during Ischemia-Reperfusion Damage." *Experimental and Toxicologic Pathology : Official Journal of the Gesellschaft Für Toxikologische Pathologie* 52 (2): 157–59.

Bhindi, R., Fahmy, R.G., McMahon, A.C., Khachigian, L.M. and Lowe, H.C. 2012. "Intracoronary Delivery of DNAzymes Targeting Human EGR-1 Reduces Infarct Size Following Myocardial Ischaemia Reperfusion." *The Journal of Pathology* 227 (2): 157–64.

Bigalke, B., Phinikaridou, A., Andia, M.E., Cooper, M.S., Schuster, A., Wurster, T., Onthank, D. et al. 2014. "PET/CT and MR Imaging Biomarker of Lipid-Rich Plaques Using [64Cu]-Labeled Scavenger Receptor (CD68-Fc)." *International Journal of Cardiology* 177 (1): 287–91.

Biondi-Zoccai, G., De Falco, E., Peruzzi, M., Cavarretta, E., Mancone, M., Leoni, O., Caristo, M.E. et al. 2013. "A Novel Closed-Chest Porcine Model of Chronic Ischemic Heart Failure Suitable for Experimental Research in Cardiovascular Disease." *BioMed Research International* 2013 (January): 410631.

Bisplinghoff, S., Hänisch, C., Becker, M., Radermacher, K. and de la Fuente, M. 2014. "Fusion of Coronary Angiography and Stress Echocardiography for Myocardial Viability Evaluation." *International Journal of Computer Assisted Radiology and Surgery*, May.

Bito, V., Heinzel, F.R., Weidemann, F., Dommke, C., van der Velden, J., Verbeken, E., Claus, P. et al. 2004. "Cellular Mechanisms of Contractile Dysfunction in Hibernating Myocardium." *Circulation Research* 94 (6): 794–801.

Bloor, C.M., White, F.C. and Sanders, T.M. 1984. "Effects of Exercise on Collateral Development in Myocardial Ischemia in Pigs." *Journal of Applied Physiology: Respiratory, Environmental and Exercise Physiology* 56 (3): 656–65.

Boekstegers, P., Raake, P., Al Ghobainy, R., Horstkotte, J., Hinkel, R., Sandner, T., Wichels, R. et al. 2002. "Stent-Based Approach for Ventricle-to-Coronary Artery Bypass." *Circulation* 106 (8): 1000–1006.

Bolukoglu, H., Liedtke, A.J., Nellis, S.H., Eggleston, A.M., Subramanian, R. and Renstrom, B. 1992. "An Animal Model of Chronic Coronary Stenosis Resulting in Hibernating Myocardium." *Am J Physiol Heart Circ Physiol* 263 (1): H20–29.

Brødløs, H.K., Bramsen, M.B., Agger, P., Jensen, H., Bjerre, M., Ringgaard, S., Wierup, P., Nielsen, S.L., Hasenkam, J.M. and Smerup, M. 2009. "A Catheter Based Chronic Porcine Model of Post-Infarct Dilated Heart Failure." *Scandinavian Cardiovascular Journal : SCJ* 43 (4): 260–66.

Buja, L.M. 2005. "Myocardial Ischemia and Reperfusion Injury." *Cardiovascular Pathology : The Official Journal of the Society for Cardiovascular Pathology* 14 (4): 170–75.

Bujak, M. and Frangogiannis, N.G. 2007. "The Role of TGF-Beta Signaling in Myocardial Infarction and Cardiac Remodeling." *Cardiovascular Research* 74 (2): 184–95.

Caillaud, D., Calderon, J., Réant, P., Lafitte, S., Dos Santos, P., Couffinhal, T., Roques, X. and Barandon, L. 2010. "Echocardiographic Analysis with a Two-Dimensional Strain of Chronic Myocardial Ischemia Induced with Ameroid Constrictor in the Pig." *Interactive Cardiovascular and Thoracic Surgery* 10 (5): 689–93.

Carter, A.J., Laird, J.R., Kufs, W.M., Bailey, L., Hoopes, T.G., Reeves, T., Farb, A. and Virmani, R. 1996. "Coronary Stenting with a Novel Stainless Steel Balloon-Expandable Stent: Determinants of Neointimal Formation and Changes in Arterial Geometry after Placement in an Atherosclerotic Model." *Journal of the American College of Cardiology* 27 (5): 1270–77.

Cason, B.A., Demas, K.A., Mazer, C.D., Gordon, H.J. and Hickey, R.F. 1991. "Effects of Nitrous Oxide on Coronary Pressure and Regional Contractile Function in Experimental Myocardial Ischemia." *Anesthesia and Analgesia* 72 (5): 604–11.

Cerqueira, M.D., Weissman, N.J., Dilsizian, V., Jacobs, A.K., Kaul, S., Laskey, W.K., Pennell, D.J., Rumberger, J.A., Ryan, T. and Verani, M.S. 2002. "Standardized Myocardial Segmentation and Nomenclature for Tomographic Imaging of the Heart. A Statement for Healthcare Professionals from the Cardiac Imaging Committee of the Council on Clinical Cardiology of the American Heart Association." *Circulation* 105: 539–42.

Chatziathanasiou, G.N., Nikas, D.N., Katsouras, C.S., Kazakos, N.D., Bouba, V., Vougiouklakis, T., Naka, K.K. and Michalis, L.K. 2012. "Combined Intravenous Treatment with Ascorbic Acid and Desferrioxamine to Reduce Myocardial Reperfusion Injury in an Experimental Model Resembling the Clinical Setting of Primary PCI." *Hellenic Journal of Cardiology : HJC = Hellēnikē Kardiologikē Epitheōrēsē* 53 (3): 195–204.

Chatzizisis, Y.S., Jonas, M., Beigel, R., Coskun, A.U., Baker, A.B., Stone, B. V, Maynard, C. et al. 2009. "Attenuation of Inflammation and Expansive Remodeling by Valsartan Alone or in Combination with Simvastatin in High-Risk Coronary Atherosclerotic Plaques." *Atherosclerosis* 203 (2): 387–94.

Chatzizisis, Y.S., Jonas, M., Coskun, A.U., Beigel, R., Stone, B. V, Maynard, C., Gerrity, R.G. et al. 2008. "Prediction of the Localization of High-Risk Coronary Atherosclerotic Plaques on the Basis of Low Endothelial Shear Stress: An Intravascular Ultrasound and Histopathology Natural History Study." *Circulation* 117 (8): 993–1002.

Chen, C., Chen, L., Fallon, J.T., Ma, L., Li, L., Bow, L., Knibbs, D., McKay, R., Gillam, L.D. and Waters, D.D. 1996. "Functional and Structural Alterations With 24-Hour Myocardial Hibernation and Recovery After Reperfusion: A Pig Model of Myocardial Hibernation." *Circulation* 94 (3): 507–16.

Chen, C., Ma, L., Dyckman, W., Santos, F., Lai, T., Gillam, L.D. and Waters, D.D. 1997. "Left Ventricular Remodeling in Myocardial Hibernation." *Circulation* 96 (9 Suppl): II – 46–50.

Chen, C., Ma, L., Linfert, D.R., Lai, T., Fallon, J.T., Gillam, L.D., Waters, D.D. and Tsongalis, G.J. 1997. "Myocardial Cell Death and Apoptosis in Hibernating Myocardium." *Journal of the American College of Cardiology* 30 (5): 1407–12.

Chen, Y., Shao, D.-B., Zhang, F.-X., Zhang, J., Yuan, W., Man, Y.-L., Du, W. et al. 2013. "Establishment and Evaluation of a Swine Model of Acute Myocardial Infarction and Reperfusion-Ventricular Fibrillation-Cardiac Arrest Using the Interventional Technique." *Journal of the Chinese Medical Association : JCMA* 76 (9): 491–96.

Chinda, K., Palee, S., Surinkaew, S., Phornphutkul, M., Chattipakorn, S. and Chattipakorn, N. 2013. "Cardioprotective Effect of Dipeptidyl Peptidase-4 Inhibitor during Ischemia-Reperfusion Injury." *International Journal of Cardiology* 167 (2): 451–57.

Cho, K.R., Choi, J.-S., Hahn, W., Kim, D.S., Park, J.S., Lee, D.S. and Kim, K.-B. 2008. "Therapeutic Angiogenesis Using Naked DNA Expressing Two Isoforms of the Hepatocyte Growth Factor in a Porcine Acute Myocardial Infarction Model." *European Journal of Cardio-Thoracic Surgery : Official Journal of the European Association for Cardio-Thoracic Surgery* 34 (4): 857–63.

Choy, J.S., Zhang, Z.-D., Pitsillides, K., Sosa, M. and Kassab, G.S. 2014. "Longitudinal Hemodynamic Measurements in Swine Heart Failure Using a Fully Implantable Telemetry System." *PloS One* 9 (8): e103331.

Christian, T.F., Peters, K., Keck, B., Allen, J., Owens, T. and Borah, B. 2008. "Gated SPECT Imaging to Detect Changes in Myocardial Blood Flow during Progressive Coronary Occlusion." *The International Journal of Cardiovascular Imaging* 24 (3): 269–76.

Crick, S.J., Sheppard, M.N., Ho, S.Y., Gebstein, L. and Anderson, R.H. 1998. "Anatomy of the Pig Heart: Comparisons with Normal Human Cardiac Structure." *Journal of Anatomy* 193 (Pt 1 (July): 105–19.

Crisóstomo, V., Maestre, J., Maynar, M., Sun, F., Báez-Díaz, C., Usón, J. and Sánchez-Margallo, F.M. 2013. "Development of a Closed Chest Model of Chronic Myocardial Infarction in Swine: Magnetic Resonance Imaging and Pathological Evaluation." *ISRN Cardiology* 2013 (January): 781762.

Cui, J., Li, J., Mathison, M., Tondato, F., Mulkey, S.P., Micko, C., Chronos, N.A.F. and Robinson, K.A. 2005. "A Clinically Relevant Large-Animal Model for Evaluation of Tissue-Engineered Cardiac Surgical Patch Materials." *Cardiovascular Revascularization Medicine : Including Molecular Interventions* 6 (3): 113–20.

Dahlöf, B. 2010. "Cardiovascular Disease Risk Factors: Epidemiology and Risk Assessment." *The American Journal of Cardiology* 105 (1 Suppl): 3A – 9A.

Danad, I., Uusitalo, V., Kero, T., Saraste, A., Raijmakers, P.G., Lammertsma, A.A., Heymans, M.W. et al. 2014. "Quantitative Assessment of Myocardial Perfusion in the Detection of Significant Coronary Artery Disease: Cutoff Values and Diagnostic Accuracy of Quantitative [(15)O]H2O PET Imaging." *Journal of the American College of Cardiology* 64 (14): 1464–75.

Das, M. and Das, D.K. 2008. "Molecular Mechanism of Preconditioning." *IUBMB Life* 60 (4): 199–203.

Dash, R., Chung, J., Ikeno, F., Hahn-Windgassen, A., Matsuura, Y., Bennett, M. V, Lyons, J.K. et al. 2011. "Dual Manganese-Enhanced and Delayed Gadolinium-Enhanced MRI Detects Myocardial Border Zone Injury in a Pig Ischemia-Reperfusion Model." *Circulation. Cardiovascular Imaging* 4 (5): 574–82.

De Groot, D., Grundmann, S., Timmers, L., Pasterkamp, G. and Hoefer, I.E. 2011. "Assessment of Collateral Artery Function and Growth in a Pig Model of Stepwise Coronary Occlusion." *American Journal of Physiology. Heart and Circulatory Physiology* 300 (1): H408–14.

Dib, N., Diethrich, E.B., Campbell, A., Gahremanpour, A., McGarry, M. and Opie, S.R. 2006. "A Percutaneous Swine Model of Myocardial Infarction." *Journal of Pharmacological and Toxicological Methods* 53 (3): 256–63.

Díez, J.L., Hernandiz, A., Cosín-Aguilar, J., Aguilar, A. and Portolés, M. 2013. "Sum of Effects of Myocardial Ischemia Followed by Electrically Induced Tachycardia on Myocardial Function." *Medical Science Monitor Basic Research* 19 (January): 153–62.

Dixon, J.A. and Spinale, F.G. 2009. "Large Animal Models of Heart Failure: A Critical Link in the Translation of Basic Science to Clinical Practice." *Circulation. Heart Failure* 2 (3): 262–71.

Dixon, J.L., Stoops, J.D., Parker, J.L., Laughlin, M.H., Weisman, G.A. and Sturek, M. 1999. "Dyslipidemia and Vascular Dysfunction in Diabetic Pigs Fed an Atherogenic Diet." *Arteriosclerosis, Thrombosis, and Vascular Biology* 19 (12): 2981–92.

Doganci, S., Yildirim, V., Bolcal, C., Korkusuz, P., Gumusel, B., Demirkilic, U. and Aydin, A. 2012. "Sodium Nitrite and Cardioprotective Effect in Pig Regional Myocardial Ischemia-Reperfusion Injury Model." *Advances in Clinical and Experimental Medicine : Official Organ Wroclaw Medical University* 21 (6): 713–26.

Dogné, J.-M., Rolin, S., Pétein, M., Tchana-Sato, V., Ghuysen, A., Lambermont, B., Hanson, J. et al. 2005. "Characterization of an Original Model of Myocardial Infarction Provoked by Coronary Artery Thrombosis Induced by Ferric Chloride in Pig." *Thrombosis Research* 116 (5): 431–42.

Duran, J.M., Taghavi, S., Berretta, R.M., Makarewich, C.A., Sharp Iii, T., Starosta, T., Udeshi, F., George, J.C., Kubo, H. and Houser, S.R. 2012. "A Characterization and Targeting of the Infarct Border Zone in a Swine Model of Myocardial Infarction." *Clinical and Translational Science* 5 (5): 416–21.

Dyson, M.C., Alloosh, M., Vuchetich, J.P., Mokelke, E.A. and Sturek, M. 2006. "Components of Metabolic Syndrome and Coronary Artery Disease in Female Ossabaw Swine Fed Excess Atherogenic Diet." *Comparative Medicine* 56 (1): 35–45.

Fallavollita, J.A. 2000. "Spatial Heterogeneity in Fasting and Insulin-Stimulated 18F-2-Deoxyglucose Uptake in Pigs With Hibernating Myocardium." *Circulation* 102 (8): 908–14.

Fallavollita, J.A. 2002. "Coronary Patency and Its Relation to Contractile Reserve in Hibernating Myocardium." *Cardiovascular Research* 55 (1): 131–40.

Fallavollita, J.A. and Canty, J.M. 2002. "Ischemic Cardiomyopathy in Pigs with Two-Vessel Occlusion and Viable, Chronically Dysfunctional Myocardium." *American Journal of Physiology.*

Heart and Circulatory Physiology 282 (4): H1370–79.

Fallavollita, J.A., Jacob, S., Young, R.F. and Canty, J.M. 1999. "Regional Alterations in SR Ca(2+)-ATPase, Phospholamban, and HSP-70 Expression in Chronic Hibernating Myocardium." *The American Journal of Physiology* 277 (4 Pt 2): H1418–28.

Fallavollita, J.A., Lim, H. and Canty, J.M. 2001. "Myocyte Apoptosis and Reduced SR Gene Expression Precede the Transition from Chronically Stunned to Hibernating Myocardium." *Journal of Molecular and Cellular Cardiology* 33 (11): 1937–44.

Fallavollita, J.A., Logue, M. and Canty, J.M. 2001. "Stability of Hibernating Myocardium in Pigs with a Chronic Left Anterior Descending Coronary Artery Stenosis: Absence of Progressive Fibrosis in the Setting of Stable Reductions in Flow, Function and Coronary Flow Reserve." *Journal of the American College of Cardiology* 37 (7): 1989–95.

Fallavollita, J.A., Perry, B.J. and Canty, J.M. 1997. "18F-2-Deoxyglucose Deposition and Regional Flow in Pigs With Chronically Dysfunctional Myocardium : Evidence for Transmural Variations in Chronic Hibernating Myocardium." *Circulation* 95 (7): 1900–1909.

Fallavollita, J.A., Riegel, B.J., Suzuki, G., Valeti, U. and Canty, J.M. 2005. "Mechanism of Sudden Cardiac Death in Pigs with Viable Chronically Dysfunctional Myocardium and Ischemic Cardiomyopathy." *American Journal of Physiology. Heart and Circulatory Physiology* 289 (6): H2688–96.

Finegold, J.A., Asaria, P. and Francis, D.P. 2013. "Mortality from Ischaemic Heart Disease by Country, Region, and Age: Statistics from World Health Organisation and United Nations." *International Journal of Cardiology* 168 (2): 934–45.

Fish, K.M., Ladage, D., Kawase, Y., Karakikes, I., Jeong, D., Ly, H., Ishikawa, K. et al. 2013. "AAV9.I-1c Delivered via Direct Coronary Infusion in a Porcine Model of Heart Failure Improves Contractility and Mitigates Adverse Remodeling." *Circ.Heart Fail.* 6: 310–17.

Francis, G.S., Bartos, J.A. and Adatya, S. 2014. "Inotropes." *Journal of the American College of Cardiology* 63 (20): 2069–78.

Galiuto, L., May-Newman, K., del Balzo, U., Flaim, S.F., Iliceto, S. and DeMaria, A.N. 2002. "Assessment of Coronary Stenoses of Graded Severity by Myocardial Contrast Echocardiography." *Journal of the American Society of Echocardiography* 15 (3): 197–205.

Gálvez-Montón, C., Prat-Vidal, C., Díaz-Güemes, I., Crisóstomo, V., Soler-Botija, C., Roura, S., Llucià-Valldeperas, A., Perea-Gil, I., Sánchez-Margallo, F.M. and Bayes-Genis, A. 2014. "Comparison of Two Preclinical Myocardial Infarct Models: Coronary Coil Deployment versus Surgical Ligation." *Journal of Translational Medicine* 12: 137.

Gálvez-Montón, C., Prat-Vidal, C., Roura, S., Soler-Botija, C., Llucià-Valldeperas, A., Díaz-Güemes, I., Sánchez-Margallo, F.M. and Bayes-Genis, A. 2013. "Post-Infarction Scar Coverage Using a Pericardial-Derived Vascular Adipose Flap. Pre-Clinical Results." *International Journal of Cardiology* 166 (2): 469–74.

Garcia-Dorado, D., Theroux, P., Elizaga, J., Galinanes, M., Solares, J., Riesgo, M., Gomez, M.J., Garcia-Dorado, A. and Aviles, F.F. 1987. "Myocardial Reperfusion in the Pig Heart Model: Infarct Size and Duration of Coronary Occlusion." *Cardiovascular Research* 21 (7): 537–44.

Gelsomino, S., Lucà, F., Nediani, C., Orlandini, S.Z., Bani, D., Rubino, A.S., Renzulli, A. et al. 2013. "Early Hemodynamic and Biochemical Changes in Overloaded Swine Ventricle." *Texas Heart Institute Journal / from the Texas Heart Institute of St. Luke's Episcopal Hospital, Texas Children's Hospital* 40 (3): 235–45.

Gelsomino, S., Lucà, F., Renzulli, A., Rubino, A.S., Romano, S.M., van der Veen, F.H., Carella, R., Maessen, J.G., Gensini, G.F. and Lorusso, R. 2011. "Increased Coronary Blood Flow and Cardiac Contractile Efficiency with Intraaortic Balloon Counterpulsation in a Porcine Model of Myocardial Ischemia-Reperfusion Injury." *ASAIO Journal (American Society for Artificial Internal Organs : 1992)* 57 (5): 375–81.

Gelsomino, S., Renzulli, A., Rubino, A.S., Romano, S.M., Lucà, F., Valente, S., Gensini, G.F. and Lorusso, R. 2012. "Effects of 1:1, 1:2 or 1:3 Intra-Aortic Balloon Counterpulsation/heart Support on Coronary Haemodynamics and Cardiac Contractile Efficiency in an Animal Model of Myocardial Ischaemia/reperfusion." *European Journal of Cardio-Thoracic Surgery : Official Journal of the European Association for Cardio-Thoracic Surgery* 42 (2): 325–32; discussion 332.

George, R.T., Mehra, V.C., Saraste, A. and Knuuti, J. 2012. "Myocardial Perfusion by CT versus Hybrid Imaging." *Cardiology Clinics* 30 (1): 135–46.

Gerrity, R.G. 1981a. "The Role of the Monocyte in Atherogenesis: I. Transition of Blood-Borne Monocytes into Foam Cells in Fatty Lesions." *The American Journal of Pathology* 103 (2): 181–90.

Gerrity, R.G. 1981b. "The Role of the Monocyte in Atherogenesis: II. Migration of Foam Cells from Atherosclerotic Lesions." *The American Journal of Pathology* 103 (2): 191–200.

Gerrity, R.G., Goss, J.A. and Soby, L. 1985. "Control of Monocyte Recruitment by Chemotactic Factor(s) in Lesion-Prone Areas of Swine Aorta." *Arteriosclerosis* 5 (1): 55–66.

Gerrity, R.G., Natarajan, R., Nadler, J.L. and Kimsey, T. 2001. "Diabetes-Induced Accelerated Atherosclerosis in Swine." *Diabetes* 50 (7): 1654–65.

Gewirtz, H., Brautigan, D.L., Olsson, R.A., Brown, P. and Most, A.S. 1983. "Role of Adenosine in the Maintenance of Coronary Vasodilation Distal to a Severe Coronary Artery Stenosis. Observations in Conscious Domestic Swine." *Circulation Research* 53 (1): 42–51.

Gewirtz, H. and Most, A.S. 1981. "Production of a Critical Coronary Arterial Stenosis in Closed Chest Laboratory Animals." *The American Journal of Cardiology* 47 (3): 589–96.

Gewirtz, H., Williams, D.O. and Most, A.S. 1983. "Quantitative Assessment of the Effects of a Fixed 50% Coronary Artery Stenosis on Regional Myocardial Flow Reserve and Transmural Distribution of Blood Flow." *Journal of the American College of Cardiology* 1 (5): 1273–80.

Giordano, C., Thorn, S.L., Renaud, J.M., Al-Atassi, T., Boodhwani, M., Klein, R., Kuraitis, D. et al. 2013. "Preclinical Evaluation of Biopolymer-Delivered Circulating Angiogenic Cells in a Swine Model of Hibernating Myocardium." *Circulation. Cardiovascular Imaging* 6 (6): 982–91.

Gould, K.L., Lipscomb, K. and Hamilton, G.W. 1974. "Physiologic Basis for Assessing Critical Coronary Stenosis." *The American Journal of Cardiology* 33 (1): 87–94.

Granada, J.F., Milewski, K., Zhao, H., Stankus, J.J., Tellez, A., Aboodi, M.S., Kaluza, G.L. et al. 2011. "Vascular Response to Zotarolimus-Coated Balloons in Injured Superficial Femoral Arteries of the Familial Hypercholesterolemic Swine." *Circulation. Cardiovascular Interventions* 4 (5): 447–55.

Granada, J.F., Moreno, P.R., Burke, A.P., Schulz, D.G., Raizner, A.E. and Kaluza, G.L. 2005. "Endovascular Needle Injection of Cholesteryl Linoleate into the Arterial Wall Produces Complex Vascular Lesions Identifiable by Intravascular Ultrasound: Early Development in a Porcine Model of Vulnerable Plaque." *Coronary Artery Disease* 16 (4): 217–24.

Greupner, J., Zimmermann, E., Grohmann, A., Dübel, H.-P., Althoff, T.F., Althoff, T., Borges, A.C. et al. 2012. "Head-to-Head Comparison of Left Ventricular Function Assessment with 64-Row Computed Tomography, Biplane Left Cineventriculography, and Both 2- and 3-Dimensional Transthoracic Echocardiography: Comparison with Magnetic Resonance Imaging as the Reference S." *Journal of the American College of Cardiology* 59 (21): 1897–1907.

Grinstead, W.C., Rodgers, G.P., Mazur, W., French, B.A., Cromeens, D., Van Pelt, C., West, S.M. and Raizner, A.E. 1994. "Comparison of Three Porcine Restenosis Models: The Relative Importance of Hypercholesterolemia, Endothelial Abrasion, and Stenting." *Coronary Artery Disease* 5 (5): 425–34.

Gross, G.J. and Auchampach, J.A. 1992. "Blockade of ATP-Sensitive Potassium Channels Prevents Myocardial Preconditioning in Dogs." *Circ.Res.* 70: 223–33.

Hagar, J.M., Hale, S.L. and Kloner, R.A. 1991. "Effect of Preconditioning Ischemia on Reperfusion Arrhythmias after Coronary Artery Occlusion and Reperfusion in the Rat." *Circulation Research* 68 (1): 61–68.

Hamamdzic, D., Fenning, R.S., Patel, D., Mohler, E.R., Orlova, K.A., Wright, A.C., Llano, R. et al. 2010. "Akt Pathway Is Hypoactivated by Synergistic Actions of Diabetes Mellitus and Hypercholesterolemia Resulting in Advanced Coronary Artery Disease." *American Journal of Physiology. Heart and Circulatory Physiology* 299 (3): H699–706.

Hansson, G.K. and Libby, P. 2006. "The Immune Response in Atherosclerosis: A Double-Edged Sword." *Nature Reviews. Immunology* 6 (7): 508–19.

Hardt, S.E., Pekrul, I., Hansen, A., Gebhard, M.M., Kuebler, W. and Kuecherer, H.F. 2001. "Differential Value of Adenosine Myocardial Contrast Echocardiography and Dobutamine Stress Echocardiography in Evaluating Functional Significance of Coronary Artery Stenosis in a Porcine Model." *Basic Research in Cardiology* 96 (4): 415–21.

Hashizume, R., Fujimoto, K.L., Hong, Y., Guan, J., Toma, C., Tobita, K. and Wagner, W.R. 2013. "Biodegradable Elastic Patch Plasty Ameliorates Left Ventricular Adverse Remodeling after Ischemia-Reperfusion Injury: A Preclinical Study of a Porous Polyurethane Material in a Porcine Model." *The Journal of Thoracic and Cardiovascular Surgery* 146 (2): 391–99.e1.

Hasler-Rapacz, J., Ellegren, H., Fridolfsson, A.K., Kirkpatrick, B., Kirk, S., Andersson, L. and Rapacz, J. 1998. "Identification of a Mutation in the Low

Density Lipoprotein Receptor Gene Associated with Recessive Familial Hypercholesterolemia in Swine." *American Journal of Medical Genetics* 76 (5): 379–86.

Hasler-Rapacz, J., Prescott, M.F., Von Linden-Reed, J., Rapacz, J.M., Hu, Z. and Rapacz, J. 1995. "Elevated Concentrations of Plasma Lipids and Apolipoproteins B, C-III, and E Are Associated with the Progression of Coronary Artery Disease in Familial Hypercholesterolemic Swine." *Arteriosclerosis, Thrombosis, and Vascular Biology* 15 (5): 583–92.

Heilmann, C., Kostic, C., Giannone, B., Grawitz, A.B., Armbruster, W., Lutter, G., Beyersdorf, F. and Göbel, H. 2006. "Improvement of Contractility Accompanies Angiogenesis rather than Arteriogenesis in Chronic Myocardial Ischemia." *Vascular Pharmacology* 44 (5): 326–32.

Heinonen, S.E., Leppänen, P., Kholová, I., Lumivuori, H., Häkkinen, S.-K., Bosch, F., Laakso, M. and Ylä-Herttuala, S. 2007. "Increased Atherosclerotic Lesion Calcification in a Novel Mouse Model Combining Insulin Resistance, Hyperglycemia, and Hypercholesterolemia." *Circulation Research* 101 (10): 1058–67.

Hemetsberger, R., Farhan, S., Strehblow, C., Sperker, W., Pavo, I., Petrasi, Z., Hemetsberger, H. et al. 2008. "Association between the Efficacy of Dual Antiplatelet Therapy and the Development of in-Stent Neointimal Hyperplasia in Porcine Coronary Arteries." *Coronary Artery Disease* 19 (8): 635–43.

Heusch, G., Libby, P., Gersh, B., Yellon, D., Böhm, M., Lopaschuk, G. and Opie, L. 2014. "Cardiovascular Remodelling in Coronary Artery Disease and Heart Failure." *Lancet* 383 (9932): 1933–43.

Hinkel, R., Penzkofer, D., Zühlke, S., Fischer, A., Husada, W., Xu, Q.-F., Baloch, E. et al. 2013. "Inhibition of microRNA-92a Protects against Ischemia/reperfusion Injury in a Large-Animal Model." *Circulation* 128 (10): 1066–75.

Holz, A., Lautamäki, R., Sasano, T., Merrill, J., Nekolla, S.G., Lardo, A.C. and Bengel, F.M. 2009. "Expanding the Versatility of Cardiac PET/CT: Feasibility of Delayed Contrast Enhancement CT for Infarct Detection in a Porcine Model." *Journal of Nuclear Medicine : Official Publication, Society of Nuclear Medicine* 50 (2): 259–65.

Hong, X., Fan, H., Lu, R., Chan, P. and Liu, Z. 2013. "Merit of Anisodamine Combined with Opioid Δ-Receptor Activation in the Protection against Myocardial Injury during Cardiopulmonary Bypass." *BioMed Research International* 2013 (January): 212801.

Horstick, G., Bierbach, B., Abegunewardene, N., Both, S., Kuhn, S., Manefeld, D., Reinecke, H.-J. et al. 2009. "Critical Single Proximal Left Arterial Descending Coronary Artery Stenosis to Mimic Chronic Myocardial Ischemia: A New Model Induced by Minimal Invasive Technology." *Journal of Vascular Research* 46 (4): 290–98.

Hsiao, Y.-M., Mathias, C.J., Wey, S.-P., Fanwick, P.E. and Green, M.A. 2009. "Synthesis and Biodistribution of Lipophilic and Monocationic Gallium Radiopharmaceuticals Derived from N,N'-bis(3-Aminopropyl)-N,N'-Dimethylethylenediamine: Potential Agents for PET Myocardial Imaging with 68Ga." *Nuclear Medicine and Biology* 36 (1): 39–45.

Huang, Z., Ge, J., Sun, A., Wang, Y., Zhang, S., Cui, J., Qian, J. and Zou, Y. 2010. "Ligating LAD with Its Whole Length rather than Diagonal Branches as Coordinates Is More Advisable in Establishing Stable Myocardial Infarction Model of Swine." *Exp. Anim* 59: 431–39.

Hughes, G.C., Landolfo, C.K., Yin, B., DeGrado, T.R., Coleman, R.E., Landolfo, K.P. and Lowe, J.E. 2001. "Is Chronically Dysfunctional yet Viable Myocardium Distal to a Severe Coronary Stenosis Hypoperfused?" *The Annals of Thoracic Surgery* 72 (1): 163–68.

Hughes, G.C., Post, M.J., Simons, M. and Annex, B.H. 2003. "Translational Physiology: Porcine Models of Human Coronary Artery Disease: Implications for Preclinical Trials of Therapeutic Angiogenesis." *Journal of Applied Physiology (Bethesda, Md. : 1985)* 94 (5): 1689–1701.

Iida, H., Rhodes, C.G., De, S.R., Araujo, L.I., Bloomfield, P.M., Lammertsma, A.A. and Jones, T. 1992. "Use of the Left Ventricular Time-Activity Curve as a Noninvasive Input Function in Dynamic Oxygen-15-Water Positron Emission Tomography." *J.Nucl.Med.* 33: 1669–77.

Iida, H., Ruotsalainen, U., Mäki, M., Haaparnata, M., Bergman, J., Voipio-Pulkki, L.-M., Nuutila, P., Koshino, K. and Knuuti, J. 2012. "F-18 Fluorodeoxyglucose Uptake and Water-Perfusable Tissue Fraction in Assessment of Myocardial Viability." *Annals of Nuclear Medicine* 26 (8): 644–55.

Ikonen, T.S., Pätilä, T., Virtanen, K., Lommi, J., Lappalainen, K., Kankuri, E., Krogerus, L. and Harjula, A. 2007. "Ligation of Ameroid-Stenosed Coronary Artery Leads to Reproducible Myocardial Infarction--a Pilot Study in a Porcine Model." *The Journal of Surgical Research* 142 (1): 195–201.

Ishikawa, K., Ladage, D., Takewa, Y., Yaniz, E., Chen, J., Tilemann, L., Sakata, S., Badimon, J.J.,

Hajjar, R.J. and Kawase, Y. 2011. "Development of a Preclinical Model of Ischemic Cardiomyopathy in Swine." *Am.J.Physiol Heart Circ.Physiol* 301: H530–37.

Jager, N.A., Westra, J., Golestani, R., van Dam, G.M., Low, P.S., Tio, R.A., Slart, R.H.J.A., Boersma, H.H., Bijl, M. and Zeebregts, C.J. 2014. "Folate Receptor-B Imaging Using 99mTc-Folate to Explore Distribution of Polarized Macrophage Populations in Human Atherosclerotic Plaque." *Journal of Nuclear Medicine : Official Publication, Society of Nuclear Medicine* 55 (12): 1945–51.

Jiang, Y., Chang, P., Pei, Y., Li, B., Liu, Y., Zhang, Z., Yu, J., Zhu, D. and Liu, X. 2014. "Intramyocardial Injection of Hypoxia-Preconditioned Adipose-Derived Stromal Cells Treats Acute Myocardial Infarction: An in Vivo Study in Swine." *Cell and Tissue Research*, August.

Johanna Haukkala, Iina Laitinen, Pauliina Luoto, Peter Iveson, Ian Wilson, Hege Karlsen, Alan Cuthbertson et al. 2009. "68Ga-DOTA-RGD Peptide: Biodistribution and Binding into Atherosclerotic Plaques in Mice." *European Journal of Nuclear Medicine and Molecular Imaging* 36 (12): 2058–67.

Johnson, L.L., Schofield, L., Mastrofrancesco, P., Donahay, T. and Nott, L. 1998. "Technetium-99m-Nitroimadazole Uptake in a Swine Model of Demand Ischemia." *Journal of Nuclear Medicine : Official Publication, Society of Nuclear Medicine* 39 (8): 1468–75.

Johnson, L.L., Schofield, L.M., Verdesca, S.A., Sharaf, B.L., Jones, R.M., Virmani, R. and Khaw, B.A. 2000. "In Vivo Uptake of Radiolabeled Antibody to Proliferating Smooth Muscle Cells in a Swine Model of Coronary Stent Restenosis." *Journal of Nuclear Medicine : Official Publication, Society of Nuclear Medicine* 41 (9): 1535–40.

Jormalainen, M., Vento, A.E., Lukkarinen, H., Kääpä, P., Kytö, V., Lauronen, J., Paavonen, T., Suojaranta-Ylinen, R. and Petäjä, J. 2007. "Inhibition of Thrombin during Reperfusion Improves Immediate Postischemic Myocardial Function and Modulates Apoptosis in a Porcine Model of Cardiopulmonary Bypass." *Journal of Cardiothoracic and Vascular Anesthesia* 21 (2): 224–31.

Joshi, N. V, Vesey, A.T., Williams, M.C., Shah, A.S. V, Calvert, P.A., Craighead, F.H.M., Yeoh, S.E. et al. 2014. "18F-Fluoride Positron Emission Tomography for Identification of Ruptured and High-Risk Coronary Atherosclerotic Plaques: A Prospective Clinical Trial." *Lancet* 383 (9918): 705–13.

Joudinaud, T.M., Kegel, C.L., Gabster, A.A., Sanz, M.L., MacDonald, A., Propp, D., Callaghan, E., Weber, P.A., Hvass, U. and Duran, C.M.G. 2005. "An Experimental Method for the Percutaneous Induction of a Posterolateral Infarct and Functional Ischemic Mitral Regurgitation." *The Journal of Heart Valve Disease* 14 (4): 460–66.

Jugdutt, B.I., Hutchins, G.M., Bulkley, B.H. and Becker, L.C. 1979. "Myocardial Infarction in the Conscious Dog: Three-Dimensional Mapping of Infarct, Collateral Flow and Region at Risk." *Circulation* 60 (5): 1141–50.

Kamimura, R., Suzuki, S., Nozaki, S., Sakamoto, H., Maruno, H. and Kawaida, H. 1996. "Branching Patterns in Coronary Artery and Ischemic Areas Induced by Coronary Arterial Occlusion in the CLAWN Miniature Pig." *Exp.Anim* 45 (1341-1357 (Print)). Institute of Laboratory Animal Sciences, Faculty of Medicine, Kagoshima University, Japan: 149–53.

Kanlop, N., Thommasorn, S., Palee, S., Weerateerangkul, P., Suwansirikul, S., Chattipakorn, S. and Chattipakorn, N. 2011. "Granulocyte Colony-Stimulating Factor Stabilizes Cardiac Electrophysiology and Decreases Infarct Size during Cardiac Ischaemic/reperfusion in Swine." *Acta Physiologica (Oxford, England)* 202 (1): 11–20.

Kassab, G.S., Berkley, J. and Fung, Y.C. 1997. "Analysis of Pig's Coronary Arterial Blood Flow with Detailed Anatomical Data." *Annals of Biomedical Engineering* 25 (1): 204–17.

Kawamura, M., Miyagawa, S., Miki, K., Saito, A., Fukushima, S., Higuchi, T., Kawamura, T. et al. 2012. "Feasibility, Safety, and Therapeutic Efficacy of Human Induced Pluripotent Stem Cell-Derived Cardiomyocyte Sheets in a Porcine Ischemic Cardiomyopathy Model." *Circulation* 126 (11 Suppl 1): S29–37.

Kelly, J.D., Forster, A.M., Higley, B., Archer, C.M., Booker, F.S., Canning, L.R., Chiu, K.W., Edwards, B., Gill, H.K. and McPartlin, M. 1993. "Technetium-99m-Tetrofosmin as a New Radiopharmaceutical for Myocardial Perfusion Imaging." *Journal of Nuclear Medicine : Official Publication, Society of Nuclear Medicine* 34 (2): 222–27.

Kersten, J.R., Montgomery, M.W., Pagel, P.S. and Warltier, D.C. 2000. "Levosimendan, a New Positive Inotropic Drug, Decreases Myocardial Infarct Size via Activation of K(ATP) Channels." *Anesth.Analg.* 90: 5–11.

Kim, D.N., Schmee, J., Baker, J.E., Lunden, G.M., Sheehan, C.E., Lee, C.S., Eastman, A., Solis, O., Ross, J.S. and Thomas, W.A. 1993. "Dietary Fish Oil Reduces Microthrombi over Atherosclerotic Lesions in Hyperlipidemic Swine Even in the Absence of Plasma Cholesterol Reduction." *Experimental and Molecular Pathology* 59 (2): 122–35.

Kim, R.J., Wu, E., Rafael, A., Chen, E.L., Parker, M.A., Simonetti, O., Klocke, F.J., Bonow, R.O. and Judd, R.M. 2000. "The Use of Contrast-Enhanced Magnetic Resonance Imaging to Identify Reversible Myocardial Dysfunction." *The New England Journal of Medicine* 343 (20): 1445–53.

Kim, S.J., Kudej, R.K., Yatani, A., Kim, Y.K., Takagi, G., Honda, R., Colantonio, D.A. et al. 2001. "A Novel Mechanism for Myocardial Stunning Involving Impaired Ca(2+) Handling." *Circulation Research* 89 (9): 831–37.

Kim, W., Jeong, M.H., Sim, D.S., Hong, Y.J., Song, H.C., Park, J.T. and Ahn, Y.K. 2011. "A Porcine Model of Ischemic Heart Failure Produced by Intracoronary Injection of Ethyl Alcohol." *Heart and Vessels* 26 (3): 342–48.

Kiugel, M., Dijkgraaf, I., Kytö, V., Helin, S., Liljenbäck, H., Saanijoki, T., Yim, C.-B. et al. 2014. "Dimeric [(68)Ga]DOTA-RGD Peptide Targeting Avβ 3 Integrin Reveals Extracellular Matrix Alterations after Myocardial Infarction." *Molecular Imaging and Biology : MIB : The Official Publication of the Academy of Molecular Imaging*, July.

Knaapen, P., Germans, T., Knuuti, J., Paulus, W.J., Dijkmans, P.A., Allaart, C.P., Lammertsma, A.A. and Visser, F.C. 2007. "Myocardial Energetics and Efficiency: Current Status of the Noninvasive Approach." *Circulation* 115: 918–27.

Knuuti, J., Kajander, S., Mäki, M. and Ukkonen, H. 2009. "Quantification of Myocardial Blood Flow Will Reform the Detection of CAD." *Journal of Nuclear Cardiology : Official Publication of the American Society of Nuclear Cardiology* 16 (4): 497–506.

Knuuti, J., Schelbert, H.R. and Bax, J.J. 2002. "The Need for Standardisation of Cardiac FDG PET Imaging in the Evaluation of Myocardial Viability in Patients with Chronic Ischaemic Left Ventricular Dysfunction." *European Journal of Nuclear Medicine and Molecular Imaging* 29 (9): 1257–66.

Koudstaal, S., Jansen Of Lorkeers, S.J., van Slochteren, F.J., van der Spoel, T.I.G., van de Hoef, T.P., Sluijter, J.P., Siebes, M., Doevendans, P.A., Piek, J.J. and Chamuleau, S.A.J. 2013. "Assessment of Coronary Microvascular Resistance in the Chronic Infarcted Pig Heart." *Journal of Cellular and Molecular Medicine* 17 (9): 1128–35.

Kraitchman, D.L., Bluemke, D.A., Chin, B.B. and Heldman, A.W. 2000. "A Minimally Invasive Method for Creating Coronary Stenosis in a Swine Model for MRI and SPECT Imaging." *Investigative Radiology* 35 (7): 445–51.

Kraitchman, D.L., Chin, B.B., Heldman, A.W., Solaiyappan, M. and Bluemke, D.A. 2002. "MRI Detection of Myocardial Perfusion Defects due to Coronary Artery Stenosis with MS-325." *Journal of Magnetic Resonance Imaging : JMRI* 15 (2): 149–58.

Kreutz, R.P., Alloosh, M., Mansour, K., Neeb, Z., Kreutz, Y., Flockhart, D.A. and Sturek, M. 2011. "Morbid Obesity and Metabolic Syndrome in Ossabaw Miniature Swine Are Associated with Increased Platelet Reactivity." *Diabetes, Metabolic Syndrome and Obesity : Targets and Therapy* 4: 99–105.

Krombach, G.A., Kinzel, S., Mahnken, A.H., Günther, R.W. and Buecker, A. 2005. "Minimally Invasive Close-Chest Method for Creating Reperfused or Occlusive Myocardial Infarction in Swine." *Investigative Radiology* 40 (1): 14–18.

Kuster, D.W.D., Merkus, D., Kremer, A., van Ijcken, W.F.J., de Beer, V.J., Verhoeven, A.J.M. and Duncker, D.J. 2011. "Left Ventricular Remodeling in Swine after Myocardial Infarction: A Transcriptional Genomics Approach." *Basic Research in Cardiology* 106 (6): 1269–81.

Kuzuya, T., Hoshida, S., Yamashita, N., Fuji, H., Oe, H., Hori, M., Kamada, T. and Tada, M. 1993. "Delayed Effects of Sublethal Ischemia on the Acquisition of Tolerance to Ischemia." *Circulation Research* 72 (6): 1293–99.

Lai, T., Fallon, J.T., Liu, J., Mangion, J., Gillam, L., Waters, D. and Chen, C. 2000. "Reversibility and Pathohistological Basis of Left Ventricular Remodeling in Hibernating Myocardium." *Cardiovascular Pathology* 9 (6): 323–35.

Laitinen, I., Luoto, P., Någren, K., Marjamäki, P.M., Silvola, J.M.U., Hellberg, S., Laine, V.J.O., Ylä-Herttuala, S., Knuuti, J. and Roivainen, A. 2010. "Uptake of 11C-Choline in Mouse Atherosclerotic Plaques." *Journal of Nuclear Medicine : Official Publication, Society of Nuclear Medicine* 51 (5): 798–802.

Laitinen, I., Marjamäki, P., Någren, K., Laine, V.J.O., Wilson, I., Leppänen, P., Ylä-Herttuala, S., Roivainen, A. and Knuuti, J. 2009. "Uptake of Inflammatory Cell Marker [11C]PK11195 into Mouse Atherosclerotic Plaques." *European Journal of Nuclear Medicine and Molecular Imaging* 36 (1): 73–80.

Laitinen, I., Saraste, A., Weidl, E., Poethko, T., Weber, A.W., Nekolla, S.G., Leppänen, P. et al. 2009. "Evaluation of alphavbeta3 Integrin-Targeted Positron Emission Tomography Tracer 18F-Galacto-RGD for Imaging of Vascular Inflammation in

Atherosclerotic Mice." *Circulation. Cardiovascular Imaging* 2 (4): 331–38.

Lassaletta, A.D., Chu, L.M. and Sellke, F.W. 2012. "Effects of Alcohol on Pericardial Adhesion Formation in Hypercholesterolemic Swine." *The Journal of Thoracic and Cardiovascular Surgery* 143 (4): 953–59.

Laufer, E.M., Reutelingsperger, C.P.M., Narula, J. and Hofstra, L. 2008. "Annexin A5: An Imaging Biomarker of Cardiovascular Risk." *Basic Research in Cardiology* 103 (2): 95–104.

Lautamäki, R., Schuleri, K.H., Sasano, T., Javadi, M.S., Youssef, A., Merrill, J., Nekolla, S.G., Abraham, M.R., Lardo, A.C. and Bengel, F.M. 2009. "Integration of Infarct Size, Tissue Perfusion, and Metabolism by Hybrid Cardiac Positron Emission Tomography/computed Tomography: Evaluation in a Porcine Model of Myocardial Infarction." *Circulation. Cardiovascular Imaging* 2 (4): 299–305.

Li, X., Shao, D., Wang, G., Jiang, T., Wu, H., Gu, B., Cao, K., Zhang, J., Qi, L. and Chen, Y. 2014. "Effects of Different LAD-Blocked Sites on the Development of Acute Myocardial Infarction and Malignant Arrhythmia in a Swine Model." *Journal of Thoracic Disease* 6 (9): 1271–77.

Li, X., Yang, Y., Cheng, Y., Dou, K., Tian, Y. and Meng, X. 2013. "Protein Kinase A-Mediated Cardioprotection of Tongxinluo Relates to the Inhibition of Myocardial Inflammation, Apoptosis, and Edema in Reperfused Swine Hearts." *Chinese Medical Journal* 126 (8): 1469–79.

Liao, R., Nascimben, L., Friedrich, J., Gwathmey, J.K. and Ingwall, J.S. 1996. "Decreased Energy Reserve in an Animal Model of Dilated Cardiomyopathy. Relationship to Contractile Performance." *Circulation Research* 78 (5): 893–902.

Liao, S.-Y., Siu, C.-W., Liu, Y., Zhang, Y., Chan, W.-S., Wu, E.X., Wu, Y. et al. 2010. "Attenuation of Left Ventricular Adverse Remodeling with Epicardial Patching after Myocardial Infarction." *Journal of Cardiac Failure* 16 (7): 590–98.

Libby, P. 2002. "Inflammation in Atherosclerosis." *Nature* 420 (6917): 868–74.

Libby, P. 2012. "Inflammation in Atherosclerosis." *Arteriosclerosis, Thrombosis, and Vascular Biology* 32 (9): 2045–51.

Libby, P. and Theroux, P. 2005. "Pathophysiology of Coronary Artery Disease." *Circulation* 111 (25): 3481–88.

Liedtke, A.J., Renstrom, B., Nellis, S.H., Hall, J.L. and Stanley, W.C. 1995. "Mechanical and Metabolic Functions in Pig Hearts after 4 Days of Chronic Coronary Stenosis." *Journal of the American College of Cardiology* 26 (3): 815–25.

Liedtke, A.J., Renstrom, B., Nellis, S.H. and Subramanian, R. 1994. "Myocardial Function and Metabolism in Pig Hearts after Relief from Chronic Partial Coronary Stenosis." *Am J Physiol Heart Circ Physiol* 267 (4): H1312–19.

Lim, H., Fallavollita, J.A., Hard, R., Kerr, C.W. and Canty, J.M. 1999. "Profound Apoptosis-Mediated Regional Myocyte Loss and Compensatory Hypertrophy in Pigs with Hibernating Myocardium." *Circulation* 100 (23): 2380–86.

Lim, K.H.H., Halestrap, A.P., Angelini, G.D. and Suleiman, M.-S. 2005. "Propofol Is Cardioprotective in a Clinically Relevant Model of Normothermic Blood Cardioplegic Arrest and Cardiopulmonary Bypass." *Experimental Biology and Medicine* 230 (6): 413–20.

Lin, X., Lee, D. and Wu, D. 2013. "Protective Effects of NHE1 Inhibition with Sabiporide in an Experimental Model of Asphyxia-Induced Cardiac Arrest in Piglets." *Resuscitation* 84 (4): 520–25.

Lu, F., Zhao, X., Wu, J., Cui, Y., Mao, Y., Chen, K., Yuan, Y., Gong, D., Xu, Z. and Huang, S. 2013. "MSCs Transfected with Hepatocyte Growth Factor or Vascular Endothelial Growth Factor Improve Cardiac Function in the Infarcted Porcine Heart by Increasing Angiogenesis and Reducing Fibrosis." *International Journal of Cardiology* 167 (6): 2524–32.

Lukács, E., Magyari, B., Tóth, L., Petrási, Z., Repa, I., Koller, A. and Horváth, I. 2012. "Overview of Large Animal Myocardial Infarction Models (review)." *Acta Physiologica Hungarica* 99 (4): 365–81.

Maecke, H.R. and André, J.P. 2007. "68Ga-PET Radiopharmacy: A Generator-Based Alternative to 18F-Radiopharmacy." *Ernst Schering Research Foundation Workshop*, no. 62 (January): 215–42.

Mahnken, A.H., Klotz, E., Pietsch, H., Schmidt, B., Allmendinger, T., Haberland, U., Kalender, W.A. and Flohr, T. 2010. "Quantitative Whole Heart Stress Perfusion CT Imaging as Noninvasive Assessment of Hemodynamics in Coronary Artery Stenosis: Preliminary Animal Experience." *Investigative Radiology* 45 (6): 298–305.

Malmberg, M., Vähäsilta, T., Saraste, A., Kytö, V., Kiss, J., Kentala, E., Kallajoki, M. and Savunen, T. 2006. "Cardiomyocyte Apoptosis and Duration of Aortic Clamping in Pig Model of Open Heart Surgery." *European Journal of Cardio-Thoracic Surgery : Official Journal of the European Association for Cardio-Thoracic Surgery* 30 (3): 480–84.

Mateo, J., Izquierdo-Garcia, D., Badimon, J.J., Fayad, Z.A. and Fuster, V. 2014. "Noninvasive Assessment of Hypoxia in Rabbit Advanced Atherosclerosis Using ^{18}F-Fluoromisonidazole Positron Emission Tomographic Imaging." *Circulation. Cardiovascular Imaging* 7 (2): 312–20.

Matter, C.M., Wyss, M.T., Meier, P., Späth, N., von Lukowicz, T., Lohmann, C., Weber, B. et al. 2006. "18F-Choline Images Murine Atherosclerotic Plaques Ex Vivo." *Arteriosclerosis, Thrombosis, and Vascular Biology* 26 (3): 584–89.

Matyal, R., Chu, L., Mahmood, F., Robich, M.P., Wang, A., Hess, P.E., Shahul, S., Pinto, D.S., Khabbaz, K. and Sellke, F.W. 2012. "Neuropeptide Y Improves Myocardial Perfusion and Function in a Swine Model of Hypercholesterolemia and Chronic Myocardial Ischemia." *Journal of Molecular and Cellular Cardiology* 53 (6): 891–98.

Matyal, R., Sakamuri, S., Wang, A., Mahmood, E., Robich, M.P., Khabbaz, K., Hess, P.E., Sellke, F.W. and Mahmood, F. 2013. "Local Infiltration of Neuropeptide Y as a Potential Therapeutic Agent against Apoptosis and Fibrosis in a Swine Model of Hypercholesterolemia and Chronic Myocardial Ischemia." *European Journal of Pharmacology* 718 (1-3): 261–70.

McDonald, T.O., Gerrity, R.G., Jen, C., Chen, H.-J., Wark, K., Wight, T.N., Chait, A. and O'Brien, K.D. 2007. "Diabetes and Arterial Extracellular Matrix Changes in a Porcine Model of Atherosclerosis." *The Journal of Histochemistry and Cytochemistry : Official Journal of the Histochemistry Society* 55 (11): 1149–57.

McFalls, E.O., Baldwin, D., Palmer, B., Marx, D., Jaimes, D. and Ward, H.B. 1997. "Regional Glucose Uptake within Hypoperfused Swine Myocardium as Measured by Positron Emission Tomography." *The American Journal of Physiology* 272 (1 Pt 2): H343–49.

McFalls, E.O., Sluiter, W., Schoonderwoerd, K., Manintveld, O.C., Lamers, J.M.J., Bezstarosti, K., van Beusekom, H.M. et al. 2006. "Mitochondrial Adaptations within Chronically Ischemic Swine Myocardium." *Journal of Molecular and Cellular Cardiology* 41 (6): 980–88.

McMurray, J.J. V and Pfeffer, M.A. 2005. "Heart Failure." *Lancet* 365 (9474): 1877–89.

Metzsch, C., Liao, Q., Steen, S. and Algotsson, L. 2006. "Myocardial Glycerol Release, Arrhythmias and Hemodynamic Instability during Regional Ischemia-Reperfusion in an Open Chest Pig Model." *Acta Anaesthesiologica Scandinavica* 50 (1): 99–107.

Meyer, M., Bell, S.P., Chen, Z., Nyotowidjojo, I., Lachapelle, R.R., Christian, T.F., Gibson, P.C., Keating, F.F., Dauerman, H.L. and LeWinter, M.M. 2013. "High Dose Intracoronary N-Acetylcysteine in a Porcine Model of ST-Elevation Myocardial Infarction." *Journal of Thrombosis and Thrombolysis* 36 (4): 433–41.

Mihaylov, D., van Luyn, M.J. and Rakhorst, G. 2000. "Development of an Animal Model of Selective Coronary Atherosclerosis." *Coronary Artery Disease* 11 (2): 145–49.

Mills, I., Fallon, J.T., Wrenn, D., Sasken, H., Gray, W., Bier, J., Levine, D., Berman, S., Gilson, M. and Gewirtz, H. 1994. "Adaptive Responses of Coronary Circulation and Myocardium to Chronic Reduction in Perfusion Pressure and Flow." *The American Journal of Physiology* 266 (2 Pt 2): H447–57.

Mohler, E.R., Sarov-Blat, L., Shi, Y., Hamamdzic, D., Zalewski, A., Macphee, C., Llano, R. et al. 2008. "Site-Specific Atherogenic Gene Expression Correlates with Subsequent Variable Lesion Development in Coronary and Peripheral Vasculature." *Arteriosclerosis, Thrombosis, and Vascular Biology* 28 (5): 850–55.

Munz, M.R., Faria, M.A., Monteiro, J.R., Aguas, A.P. and Amorim, M.J. 2011. "Surgical Porcine Myocardial Infarction Model through Permanent Coronary Occlusion." *Comparative Medicine* 61 (5): 445–52.

Murry, C.E., Jennings, R.B. and Reimer, K.A. 1986. "Preconditioning with Ischemia: A Delay of Lethal Cell Injury in Ischemic Myocardium." *Circulation* 74 (5): 1124–36.

Nahrendorf, M., Keliher, E., Panizzi, P., Zhang, H., Hembrador, S., Figueiredo, J.-L., Aikawa, E., Kelly, K., Libby, P. and Weissleder, R. 2009. "18F-4V for PET-CT Imaging of VCAM-1 Expression in Atherosclerosis." *JACC. Cardiovascular Imaging* 2 (10): 1213–22.

Nakamura, I., Hasegawa, K., Wada, Y., Hirase, T., Node, K. and Watanabe, Y. 2013. "Detection of Early Stage Atherosclerotic Plaques Using PET and CT Fusion Imaging Targeting P-Selectin in Low Density Lipoprotein Receptor-Deficient Mice." *Biochemical and Biophysical Research Communications* 433 (1): 47–51.

Napoli, C., D'Armiento, F.P., Mancini, F.P., Postiglione, A., Witztum, J.L., Palumbo, G. and Palinski, W. 1997. "Fatty Streak Formation Occurs in Human Fetal Aortas and Is Greatly Enhanced by Maternal Hypercholesterolemia. Intimal Accumulation of Low Density Lipoprotein and Its Oxidation Precede Monocyte Recruitment into Early Atherosclerotic

Lesions." *The Journal of Clinical Investigation* 100 (11): 2680–90.

Neeb, Z.P., Edwards, J.M., Alloosh, M., Long, X., Mokelke, E.A. and Sturek, M. 2010. "Metabolic Syndrome and Coronary Artery Disease in Ossabaw Compared with Yucatan Swine." *Comparative Medicine* 60 (4): 300–315.

Näslund, U., Häggmark, S., Johansson, G., Marklund, S.L. and Reiz, S. 1992. "A Closed-Chest Myocardial Occlusion-Reperfusion Model in the Pig: Techniques, Morbidity and Mortality." *European Heart Journal* 13 (9): 1282–89.

Näslund, U., Häggmark, S., Johansson, G., Pennert, K., Reiz, S. and Marklund, S.L. 1992. "Effects of Reperfusion and Superoxide Dismutase on Myocardial Infarct Size in a Closed Chest Pig Model." *Cardiovascular Research* 26 (2): 170–78.

Ogura, Y., Ouchi, N., Ohashi, K., Shibata, R., Kataoka, Y., Kambara, T., Kito, T. et al. 2012. "Therapeutic Impact of Follistatin-like 1 on Myocardial Ischemic Injury in Preclinical Models." *Circulation* 126 (14): 1728–38.

Ohtsuka, S., Ishikawa, K., Suzuki, S., Yamaguchi, I., Masuda, N., Wada, K. and Uchid, W. 2003. "A Porcine Model of Ischemic Heart Failure Produced by Chronic Placement of a Tube in a Coronary Artery." *European Journal of Heart Failure* 5 (5): 591–98.

Olson, A.K., Bouchard, B., Ning, X.-H., Isern, N., Rosiers, C. Des and Portman, M.A. 2012. "Triiodothyronine Increases Myocardial Function and Pyruvate Entry into the Citric Acid Cycle after Reperfusion in a Model of Infant Cardiopulmonary Bypass." *American Journal of Physiology. Heart and Circulatory Physiology* 302 (5): H1086–93.

Osipov, R.M., Robich, M.P., Feng, J., Liu, Y., Clements, R.T., Glazer, H.P., Sodha, N.R., Szabo, C., Bianchi, C. and Sellke, F.W. 2009. "Effect of Hydrogen Sulfide in a Porcine Model of Myocardial Ischemia-Reperfusion: Comparison of Different Administration Regimens and Characterization of the Cellular Mechanisms of Protection." *Journal of Cardiovascular Pharmacology* 54 (4): 287–97.

Oyamada, S., Bianchi, C., Takai, S., Robich, M.P., Clements, R.T., Chu, L. and Sellke, F.W. 2010. "Impact of Acute Myocardial Ischemia Reperfusion on the Tissue and Blood-Borne Renin-Angiotensin System." *Basic Research in Cardiology* 105 (4): 513–22.

Paeng, J.C., Lee, Y.-S., Lee, J.S., Jeong, J.M., Kim, K.-B., Chung, J.-K. and Lee, D.S. 2013. "Feasibility and Kinetic Characteristics of (68)Ga-NOTA-RGD PET for in Vivo Atherosclerosis Imaging." *Annals of Nuclear Medicine* 27 (9): 847–54.

Papp, Z., Édes, I., Fruhwald, S., De Hert, S.G., Salmenperä, M., Leppikangas, H., Mebazaa, A. et al. 2012. "Levosimendan: Molecular Mechanisms and Clinical Implications: Consensus of Experts on the Mechanisms of Action of Levosimendan." *International Journal of Cardiology* 159 (2): 82–87.

Pavo, N., Zimmermann, M., Pils, D., Mildner, M., Petrási, Z., Petneházy, Ö., Fuzik, J. et al. 2014. "Long-Acting Beneficial Effect of Percutaneously Intramyocardially Delivered Secretome of Apoptotic Peripheral Blood Cells on Porcine Chronic Ischemic Left Ventricular Dysfunction." *Biomaterials* 35 (11): 3541–50.

Pennell, D.J., Sechtem, U.P., Higgins, C.B., Manning, W.J., Pohost, G.M., Rademakers, F.E., van Rossum, A.C., Shaw, L.J. and Yucel, E.K. 2004. "Clinical Indications for Cardiovascular Magnetic Resonance (CMR): Consensus Panel Report." *European Heart Journal* 25 (21): 1940–65.

Pérez de Prado, A., Cuellas-Ramón, C., Regueiro-Purriños, M., Gonzalo-Orden, J.M., Pérez-Martínez, C., Altónaga, J.R., García-Iglesias, M.J., Orden-Recio, M.A., García-Marín, J.F. and Fernández-Vázquez, F. 2009. "Closed-Chest Experimental Porcine Model of Acute Myocardial Infarction-Reperfusion." *Journal of Pharmacological and Toxicological Methods* 60 (3): 301–6.

Peukert, D., Laule, M., Kaufels, N., Schnorr, J., Taupitz, M., Hamm, B. and Dewey, M. 2009. "A Minimally Invasive Method for Induction of Myocardial Infarction in an Animal Model Using Tungsten Spirals." *The International Journal of Cardiovascular Imaging* 25 (5): 529–35.

Pleger, S.T., Shan, C., Ksienzyk, J., Bekeredjian, R., Boekstegers, P., Hinkel, R., Schinkel, S. et al. 2011. "Cardiac AAV9-S100A1 Gene Therapy Rescues Post-Ischemic Heart Failure in a Preclinical Large Animal Model." *Science Translational Medicine* 3 (92): 92ra64.

Poulsen, R.H., Bøtker, H.E. and Rehling, M. 2011. "Postreperfusion Myocardial Technetium-99m-Sestamibi Defect Corresponds to Area at Risk: Experimental Results from an Ischemia-Reperfusion Porcine Model." *Nuclear Medicine and Biology* 38 (6): 819–25.

Prescimone, T., Lionetti, V., Cabiati, M., Caselli, C., Aquaro, G.D., Matteucci, M., Del Ry, S. and Giannessi, D. 2013. "Apoptotic Transcriptional Profile Remains Activated in Late Remodeled Left Ventricle after Myocardial Infarction in Swine Infarcted Hearts with Preserved Ejection Fraction."

Pharmacological Research : The Official Journal of the Italian Pharmacological Society 70 (1): 41–49.

Prescott, M.F., Hasler-Rapacz, J., von Linden-Reed, J. and Rapacz, J. 1995. "Familial Hypercholesterolemia Associated with Coronary Atherosclerosis in Swine Bearing Different Alleles for Apolipoprotein B." *Annals of the New York Academy of Sciences* 748: 283–92; discussion 292–93.

Prescott, M.F., McBride, C.H., Hasler-Rapacz, J., Von Linden, J. and Rapacz, J. 1991. "Development of Complex Atherosclerotic Lesions in Pigs with Inherited Hyper-LDL Cholesterolemia Bearing Mutant Alleles for Apolipoprotein B." *The American Journal of Pathology* 139 (1): 139–47.

Przyklenk, K., Vivaldi, M.T., Schoen, F.J., Malcolm, J., Arnold, O. and Kloner, R.A. 1986. "Salvage of Ischaemic Myocardium by Reperfusion: Importance of Collateral Blood Flow and Myocardial Oxygen Demand during Occlusion." *Cardiovascular Research* 20 (6): 403–14.

Pueyo Palazón, C., Alfón, J., Gaffney, P., Berrozpe, M., Royo, T. and Badimon, L. 1998. "Effects of Reducing LDL and Increasing HDL with Gemfibrozil in Experimental Coronary Lesion Development and Thrombotic Risk." *Atherosclerosis* 136 (2): 333–45.

Pätilä, T., Ikonen, T., Kankuri, E., Ahonen, A., Krogerus, L., Lauerma, K. and Harjula, A. 2009. "Spontaneous Recovery of Myocardial Function after Ligation of Ameroid-Stenosed Coronary Artery." *Scandinavian Cardiovascular Journal : SCJ* 43 (6): 408–16.

Qu, X., Fang, W., Ye, J., Koh, A.S., Xu, Y., Guan, S., Li, R. and Shen, Y. 2012. "Acute and Chronic Myocardial Infarction in a Pig Model: Utility of Multi-Slice Cardiac Computed Tomography in Assessing Myocardial Viability and Infarct Parameters." *European Journal of Radiology* 81 (4): e431–37.

Reffelmann, T., Sensebat, O., Birnbaum, Y., Stroemer, E., Hanrath, P., Uretsky, B.F. and Schwarz, E.R. 2004. "A Novel Minimal-Invasive Model of Chronic Myocardial Infarction in Swine." *Coronary Artery Disease* 15 (1): 7–12.

Reimer, K.A. and Jennings, R.B. 1979. "The 'Wavefront Phenomenon' of Myocardial Ischemic Cell Death. II. Transmural Progression of Necrosis within the Framework of Ischemic Bed Size (myocardium at Risk) and Collateral Flow." *Laboratory Investigation; a Journal of Technical Methods and Pathology* 40 (6): 633–44.

Reimer, K.A., Lowe, J.E., Rasmussen, M.M. and Jennings, R.B. 1977. "The Wavefront Phenomenon of Ischemic Cell Death. 1. Myocardial Infarct Size vs Duration of Coronary Occlusion in Dogs." *Circulation* 56 (5): 786–94.

Robich, M.P., Osipov, R.M., Chu, L.M., Han, Y., Feng, J., Nezafat, R., Clements, R.T., Manning, W.J. and Sellke, F.W. 2011. "Resveratrol Modifies Risk Factors for Coronary Artery Disease in Swine with Metabolic Syndrome and Myocardial Ischemia." *European Journal of Pharmacology* 664 (1-3): 45–53.

Rodrigo, G.C. and Samani, N.J. 2008. "Ischemic Preconditioning of the Whole Heart Confers Protection on Subsequently Isolated Ventricular Myocytes." *American Journal of Physiology. Heart and Circulatory Physiology* 294 (1): H524–31.

Rogers, I.S., Nasir, K., Figueroa, A.L., Cury, R.C., Hoffmann, U., Vermylen, D.A., Brady, T.J. and Tawakol, A. 2010. "Feasibility of FDG Imaging of the Coronary Arteries: Comparison between Acute Coronary Syndrome and Stable Angina." *JACC. Cardiovasc.Imaging* 3: 388–97.

Rominger, A., Saam, T., Vogl, E., Ubleis, C., la Fougère, C., Förster, S., Haug, A. et al. 2010. "In Vivo Imaging of Macrophage Activity in the Coronary Arteries Using 68Ga-DOTATATE PET/CT: Correlation with Coronary Calcium Burden and Risk Factors." *Journal of Nuclear Medicine : Official Publication, Society of Nuclear Medicine* 51 (2): 193–97.

Roth, D.M., Maruoka, Y., Rogers, J., White, F.C., Longhurst, J.C. and Bloor, C.M. 1987. "Development of Coronary Collateral Circulation in Left Circumflex Ameroid-Occluded Swine Myocardium." *The American Journal of Physiology* 253 (5 Pt 2): H1279–88.

Rud Andersen, H., M ng, M., Thorwest, M. and Falk, E. 1996. "Remodeling Rather Than Neointimal Formation Explains Luminal Narrowing After Deep Vessel Wall Injury : Insights From a Porcine Coronary (Re)stenosis Model." *Circulation* 93 (9): 1716–24.

Rudd, J.H., Warburton, E.A., Fryer, T.D., Jones, H.A., Clark, J.C., Antoun, N., Johnstrom, P. et al. 2002. "Imaging Atherosclerotic Plaque Inflammation with [18F]-Fluorodeoxyglucose Positron Emission Tomography." *Circulation* 105: 2708–11.

Ruifrok, A.C. and Johnston, D.A. 2001. "Quantification of Histochemical Staining by Color Deconvolution." *Anal.Quant.Cytol.Histol.* 23: 291–99.

Saeed, M., Hetts, S.W., Do, L., Sullivan, S.M. and Wilson, M.W. 2013. "MRI Quantification of Left Ventricular Function in Microinfarct versus Large Infarct in Swine Model." *The International Journal of Cardiovascular Imaging* 29 (1): 159–68.

Sahul, Z.H., Mukherjee, R., Song, J., McAteer, J., Stroud, R.E., Dione, D.P., Staib, L. et al. 2011. "Targeted Imaging of the Spatial and Temporal Variation of Matrix Metalloproteinase Activity in a Porcine Model of Postinfarct Remodeling: Relationship to Myocardial Dysfunction." *Circulation. Cardiovascular Imaging* 4 (4): 381–91.

Sakaguchi, G., Sakakibara, Y., Tambara, K., Lu, F., Premaratne, G., Nishimura, K. and Komeda, M. 2003. "A Pig Model of Chronic Heart Failure by Intracoronary Embolization with Gelatin Sponge." *The Annals of Thoracic Surgery* 75 (6): 1942–47.

Sala-Mercado, J.A., Wider, J., Undyala, V.V.R., Jahania, S., Yoo, W., Mentzer, R.M., Gottlieb, R.A. and Przyklenk, K. 2010. "Profound Cardioprotection with Chloramphenicol Succinate in the Swine Model of Myocardial Ischemia-Reperfusion Injury." *Circulation* 122 (11 Suppl): S179–84.

Salminen, P.-R., Jonassen, A.K., Aarnes, E.-K., Moen, C.A., Stangeland, L., Eliassen, F., Kongsvik, R., Matre, K., Haaverstad, R. and Grong, K. 2011. "Antiapoptotic Intervention in Repeated Blood Cardioplegia: A Porcine Study of Myocardial Function." *The Annals of Thoracic Surgery* 91 (3): 784–91.

Sanz, J., Moreno, P.R. and Fuster, V. 2013. "The Year in Atherothrombosis." *Journal of the American College of Cardiology* 62 (13): 1131–43.

Saraste, A., Kajander, S., Han, C., Nesterov, S. V and Knuuti, J. 2012. "PET: Is Myocardial Flow Quantification a Clinical Reality?" *Journal of Nuclear Cardiology : Official Publication of the American Society of Nuclear Cardiology* 19 (5): 1044–59.

Sassen, L.M., den Boer, M.O., Rensen, R.J., Saxena, P.R. and Verdouw, P.D. 1988. "Bisoprolol Improves Perfusion of Ischaemic Myocardium in Anaesthetized Pigs." *British Journal of Pharmacology* 95 (2): 361–70.

Schelbert, H.R., Wisenberg, G., Phelps, M.E., Gould, K.L., Henze, E., Hoffman, E.J., Gomes, A. and Kuhl, D.E. 1982. "Noninvasive Assessment of Coronary Stenoses by Myocardial Imaging during Pharmacologic Coronary Vasodilation. VI. Detection of Coronary Artery Disease in Human Beings with Intravenous N-13 Ammonia and Positron Computed Tomography." *The American Journal of Cardiology* 49 (5): 1197–1207.

Schneider, C., Jaquet, K., Geidel, S., Malisius, R., Boczor, S., Rau, T., Zienkiewicz, T., Hennig, D., Kuck, K.-H. and Krause, K. 2010. "Regional Diastolic and Systolic Function by Strain Rate Imaging for the Detection of Intramural Viability during Dobutamine Stress Echocardiography in a Porcine Model of Myocardial Infarction." *Echocardiography* 27 (5): 552–62.

Scholtz, L., Sarkin, A. and Lockhat, Z. 2014. "Current Clinical Applications of Cardiovascular Magnetic Resonance Imaging." *Cardiovascular Journal of Africa* 25 (4): 185–90.

Schuleri, K.H., Boyle, A.J., Centola, M., Amado, L.C., Evers, R., Zimmet, J.M., Evers, K.S. et al. 2008. "The Adult Göttingen Minipig as a Model for Chronic Heart Failure after Myocardial Infarction: Focus on Cardiovascular Imaging and Regenerative Therapies." *Comparative Medicine* 58 (6): 568–79.

Schwartz, R.S., Huber, K.C., Murphy, J.G., Edwards, W.D., Camrud, A.R., Vlietstra, R.E. and Holmes, D.R. 1992. "Restenosis and the Proportional Neointimal Response to Coronary Artery Injury: Results in a Porcine Model." *Journal of the American College of Cardiology* 19 (2): 267–74.

Schwartz, R.S., Murphy, J.G., Edwards, W.D., Camrud, A.R., Vliestra, R.E. and Holmes, D.R. 1990. "Restenosis after Balloon Angioplasty. A Practical Proliferative Model in Porcine Coronary Arteries." *Circulation* 82 (6): 2190–2200.

Seol, S.-H. and Lindner, J.R. 2014. "A Primer on the Methods and Applications for Contrast Echocardiography in Clinical Imaging." *Journal of Cardiovascular Ultrasound* 22 (3): 101–10.

Sheriff, A., Schindler, R., Vogt, B., Abdel-Aty, H., Unger, J.K., Bock, C., Gebauer, F. et al. 2014. "Selective Apheresis of C-Reactive Protein: A New Therapeutic Option in Myocardial Infarction?" *Journal of Clinical Apheresis* 30(1):15-21.

Shimokawa, H., Tomoike, H., Nabeyama, S., Yamamoto, H., Ishii, Y., Tanaka, K. and Nakamura, M. 1985. "Coronary Artery Spasm Induced in Miniature Swine: Angiographic Evidence and Relation to Coronary Atherosclerosis." *American Heart Journal* 110 (2): 300–310.

Shimokawa, H. and Vanhoutte, P.M. 1988. "Dietary Cod-Liver Oil Improves Endothelium-Dependent Responses in Hypercholesterolemic and Atherosclerotic Porcine Coronary Arteries." *Circulation* 78 (6): 1421–30.

Shinohara, G., Morita, K., Nagahori, R., Koh, Y., Kinouchi, K., Abe, T. and Hashimoto, K. 2011. "Ischemic Postconditioning Promotes Left Ventricular Functional Recovery after Cardioplegic Arrest in an in Vivo Piglet Model of Global Ischemia Reperfusion Injury on Cardiopulmonary Bypass." *The Journal of Thoracic and Cardiovascular Surgery* 142 (4): 926–32.

Shudo, Y., Miyagawa, S., Fukushima, S., Saito, A., Shimizu, T., Okano, T. and Sawa, Y. 2011. "Novel

Regenerative Therapy Using Cell-Sheet Covered with Omentum Flap Delivers a Huge Number of Cells in a Porcine Myocardial Infarction Model." *The Journal of Thoracic and Cardiovascular Surgery* 142 (5): 1188–96.

Shuros, A.C., Salo, R.W., Florea, V.G., Pastore, J., Kuskowski, M.A., Chandrashekhar, Y. and Anand, I.S. 2007. "Ventricular Preexcitation Modulates Strain and Attenuates Cardiac Remodeling in a Swine Model of Myocardial Infarction." *Circulation* 116 (10): 1162–69.

Silva, G. V, Fernandes, M.R., Madonna, R., Clubb, F., Oliveira, E., Jimenez-Quevedo, P., Branco, R. et al. 2009. "Comparative Healing Response after Sirolimus- and Paclitaxel-Eluting Stent Implantation in a Pig Model of Restenosis." *Catheterization and Cardiovascular Interventions : Official Journal of the Society for Cardiac Angiography & Interventions* 73 (6): 801–8.

Silvola, J.M.U., Saraste, A., Forsback, S., Laine, V.J.O., Saukko, P., Heinonen, S.E., Ylä-Herttuala, S., Roivainen, A. and Knuuti, J. 2011. "Detection of Hypoxia by [18F]EF5 in Atherosclerotic Plaques in Mice." *Arteriosclerosis, Thrombosis, and Vascular Biology* 31 (5): 1011–15.

Skyschally, A., Walter, B., Schultz Hansen, R. and Heusch, G. 2013. "The Antiarrhythmic Dipeptide ZP1609 (danegaptide) When given at Reperfusion Reduces Myocardial Infarct Size in Pigs." *Naunyn-Schmiedeberg's Archives of Pharmacology* 386 (5): 383–91.

Skålén, K., Gustafsson, M., Rydberg, E.K., Hultén, L.M., Wiklund, O., Innerarity, T.L. and Borén, J. 2002. "Subendothelial Retention of Atherogenic Lipoproteins in Early Atherosclerosis." *Nature* 417 (6890): 750–54.

So, A., Hsieh, J., Li, J.-Y., Hadway, J., Kong, H.-F. and Lee, T.-Y. 2012. "Quantitative Myocardial Perfusion Measurement Using CT Perfusion: A Validation Study in a Porcine Model of Reperfused Acute Myocardial Infarction." *The International Journal of Cardiovascular Imaging* 28 (5): 1237–48.

Sodha, N.R., Clements, R.T., Feng, J., Liu, Y., Bianchi, C., Horvath, E.M., Szabo, C., Stahl, G.L. and Sellke, F.W. 2009. "Hydrogen Sulfide Therapy Attenuates the Inflammatory Response in a Porcine Model of Myocardial Ischemia/reperfusion Injury." *The Journal of Thoracic and Cardiovascular Surgery* 138 (4): 977–84.

Sorop, O., Merkus, D., de Beer, V.J., Houweling, B., Pistea, A., McFalls, E.O., Boomsma, F. et al. 2008. "Functional and Structural Adaptations of Coronary Microvessels Distal to a Chronic Coronary Artery Stenosis." *Circulation Research* 102 (7): 795–803.

St. Louis, J.D., Hughes, G.C., Kypson, A.P., DeGrado, T.R., Donovan, C.L., Coleman, R.E., Yin, B., Steenbergen, C., Landolfo, K.P. and Lowe, J.E. 2000. "An Experimental Model of Chronic Myocardial Hibernation." *The Annals of Thoracic Surgery* 69 (5): 1351–57.

Stanley, W.C. 2001. "Cardiac Energetics during Ischaemia and the Rationale for Metabolic Interventions." *Coronary Artery Disease* 12 Suppl 1: S3–7.

Stanley, W.C. 2004. "Myocardial Energy Metabolism during Ischemia and the Mechanisms of Metabolic Therapies." *Journal of Cardiovascular Pharmacology and Therapeutics* 9 Suppl 1 (September): S31–45.

Stary, H.C. 2000. "Lipid and Macrophage Accumulations in Arteries of Children and the Development of Atherosclerosis." *The American Journal of Clinical Nutrition* 72 (5 Suppl): 1297S – 1306S.

Swindle, M.M., Makin, A., Herron, A.J., Clubb, F.J. and Frazier, K.S. 2012. "Swine as Models in Biomedical Research and Toxicology Testing." *Veterinary Pathology* 49 (2): 344–56.

Swynghedauw, B. 1999. "Molecular Mechanisms of Myocardial Remodeling." *Physiol Rev.* 79: 215–62.

Szilárd, M., Mesotten, L., Maes, A., Liu, X., Nuyts, J., Bormans, G., De Groot, T. et al. 2000. "A Nonsurgical Porcine Model of Left Ventricular Dysfunction. Validation of Myocardial Viability Using Dobutamine Stress Echocardiography and Positron Emission Tomography." *International Journal of Cardiovascular Interventions* 3 (2): 111–20.

Tahara, N., Mukherjee, J., de Haas, H.J., Petrov, A.D., Tawakol, A., Haider, N., Tahara, A. et al. 2014. "2-Deoxy-2-[18F]fluoro-D-Mannose Positron Emission Tomography Imaging in Atherosclerosis." *Nature Medicine* 20 (2): 215–19.

Tanaka, Y., Genet, M., Lee, L.C., Martin, A.J., Sievers, R., Gerstenfeld, E.P. and Chuan Lee, L. 2014. "Utility of High-Resolution Electroanatomic Mapping of the Left Ventricle Using a Multispline Basket Catheter in a Swine Model of Chronic Myocardial Infarction." *Heart Rhythm : The Official Journal of the Heart Rhythm Society*, August.

Tarkin, J.M., Joshi, F.R. and Rudd, J.H.F. 2014. "PET Imaging of Inflammation in Atherosclerosis." *Nature Reviews. Cardiology* 11 (8): 443–57.

Tellez, A., Krueger, C.G., Seifert, P., Winsor-Hines, D., Piedrahita, C., Cheng, Y., Milewski, K. et al. 2010. "Coronary Bare Metal Stent Implantation in Homozygous LDL Receptor Deficient Swine

Induces a Neointimal Formation Pattern Similar to Humans." *Atherosclerosis* 213 (2): 518–24.

Tellez, A., Schuster, D.S., Alviar, C., López-Berenstein, G., Sanguino, A., Ballantyne, C., Perrard, X.-Y.D. et al. 2011. "Intramural Coronary Lipid Injection Induces Atheromatous Lesions Expressing Proinflammatory Chemokines: Implications for the Development of a Porcine Model of Atherosclerosis." *Cardiovascular Revascularization Medicine : Including Molecular Interventions* 12 (5): 304–11.

Teramoto, N., Koshino, K., Yokoyama, I., Miyagawa, S., Zeniya, T., Hirano, Y., Fukuda, H. et al. 2011. "Experimental Pig Model of Old Myocardial Infarction with Long Survival Leading to Chronic Left Ventricular Dysfunction and Remodeling as Evaluated by PET." *J.Nucl.Med.* 52: 761–68.

Thim, T., Hagensen, M.K., Drouet, L., Bal Dit Sollier, C., Bonneau, M., Granada, J.F., Nielsen, L.B., Paaske, W.P., Bøtker, H.E. and Falk, E. 2010. "Familial Hypercholesterolaemic Downsized Pig with Human-like Coronary Atherosclerosis: A Model for Preclinical Studies." *EuroIntervention : Journal of EuroPCR in Collaboration with the Working Group on Interventional Cardiology of the European Society of Cardiology* 6 (2): 261–68.

Thim, T., Hagensen, M.K., Wallace-Bradley, D., Granada, J.F., Kaluza, G.L., Drouet, L., Paaske, W.P., Bøtker, H.E. and Falk, E. 2010. "Unreliable Assessment of Necrotic Core by Virtual Histology Intravascular Ultrasound in Porcine Coronary Artery Disease." *Circulation. Cardiovascular Imaging* 3 (4): 384–91.

Thomas, S.A., Fallavollita, J.A., Lee, T.-C., Feng, J. and Canty, J.M. 1999. "Absence of Troponin I Degradation or Altered Sarcoplasmic Reticulum Uptake Protein Expression After Reversible Ischemia in Swine." *Circulation Research* 85 (5): 446–56.

Thorpe, P.E., Hunter, W.J., Dovgan, P.S. and Agrawal, D.K. 1996. "A Noninjury, Diet-Induced Swine Model of Atherosclerosis for Cardiovascular-Interventional Research." *Angiology* 47 (9): 849–58.

Tillisch, J., Brunken, R., Marshall, R., Schwaiger, M., Mandelkern, M., Phelps, M. and Schelbert, H. 1986. "Reversibility of Cardiac Wall-Motion Abnormalities Predicted by Positron Tomography." *New England Journal of Medicine* 314 (14): 884–88.

Torrado, M., Iglesias, R., Centeno, A., López, E. and Mikhailov, A.T. 2011. "Targeted Gene-Silencing Reveals the Functional Significance of Myocardin Signaling in the Failing Heart." *PloS One* 6 (10): e26392.

Turk, J.R., Henderson, K.K., Vanvickle, G.D., Watkins, J. and Laughlin, M.H. 2005. "Arterial Endothelial Function in a Porcine Model of Early Stage Atherosclerotic Vascular Disease." *International Journal of Experimental Pathology* 86 (5): 335–45.

Tuunanen, H. and Knuuti, J. 2011. "Metabolic Remodelling in Human Heart Failure." *Cardiovascular Research* 90 (2): 251–57.

Tuzun, E., Oliveira, E., Narin, C., Khalil, H., Jimenez-Quevedo, P., Perin, E. and Silva, G. 2010. "Correlation of Ischemic Area and Coronary Flow with Ameroid Size in a Porcine Model." *The Journal of Surgical Research* 164 (1): 38–42.

Ukkonen, H., Saraste, M., Akkila, J., Knuuti, J., Karanko, M., Iida, H., Lehikoinen, P., Nagren, K., Lehtonen, L. and Voipio-Pulkki, L.M. 2000. "Myocardial Efficiency during Levosimendan Infusion in Congestive Heart Failure." *Clin. Pharmacol.Ther.* 68: 522–31.

Ukkonen, H., Tops, L., Saraste, A., Naum, A., Koistinen, J., Bax, J. and Knuuti, J. 2009. "The Effect of Right Ventricular Pacing on Myocardial Oxidative Metabolism and Efficiency: Relation with Left Ventricular Dyssynchrony." *Eur.J.Nucl.Med. Mol.Imaging* 36: 2042–48.

Waksman, R., Fournadjiev, J., Baffour, R., Pakala, R., Hellinga, D., Leborgne, L., Yazdi, H. et al. 2004. "Transepicardial Autologous Bone Marrow-Derived Mononuclear Cell Therapy in a Porcine Model of Chronically Infarcted Myocardium." *Cardiovascular Radiation Medicine* 5 (3): 125–31.

Van den Hoff, J., Burchert, W., Borner, A.R., Fricke, H., Kuhnel, G., Meyer, G.J., Otto, D., Weckesser, E., Wolpers, H.G. and Knapp, W.H. 2001. "[1-(11) C]Acetate as a Quantitative Perfusion Tracer in Myocardial PET." *J.Nucl.Med.* 42: 1174–82.

Van der Pals, J., Koul, S., Andersson, P., Götberg, M., Ubachs, J.F.A., Kanski, M., Arheden, H., Olivecrona, G.K., Larsson, B. and Erlinge, D. 2010. "Treatment with the C5a Receptor Antagonist ADC-1004 Reduces Myocardial Infarction in a Porcine Ischemia-Reperfusion Model." *BMC Cardiovascular Disorders* 10: 45.

Van Hout, G.P.J., de Jong, R., Vrijenhoek, J.E.P., Timmers, L., Duckers, H.J. and Hoefer, I.E. 2013. "Admittance-Based Pressure-Volume Loop Measurements in a Porcine Model of Chronic Myocardial Infarction." *Experimental Physiology* 98 (11): 1565–75.

Vanoverschelde, J.L., Wijns, W., Depré, C., Essamri, B., Heyndrickx, G.R., Borgers, M., Bol, A. and Melin, J.A. 1993. "Mechanisms of Chronic Regional Postischemic Dysfunction in Humans.

New Insights from the Study of Noninfarcted Collateral-Dependent Myocardium." *Circulation* 87 (5): 1513–23.

Varga-Szemes, A., Simor, T., Lenkey, Z., van der Geest, R.J., Kirschner, R., Toth, L., Brott, B.C., Elgavish, A. and Elgavish, G.A. 2014. "Infarct Density Distribution by MRI in the Porcine Model of Acute and Chronic Myocardial Infarction as a Potential Method Transferable to the Clinic." *The International Journal of Cardiovascular Imaging* 30 (5): 937–48.

Watanabe, I., Johnson, T.A., Buchanan, J., Engle, C.L. and Gettes, L.S. 1987. "Effect of Graded Coronary Flow Reduction on Ionic, Electrical, and Mechanical Indexes of Ischemia in the Pig." *Circulation* 76 (5): 1127–34.

Weaver, M.E., Pantely, G.A., Bristow, J.D. and Ladley, H.D. 1986. "A Quantitative Study of the Anatomy and Distribution of Coronary Arteries in Swine in Comparison with Other Animals and Man." *Cardiovascular Research* 20 (12): 907–17.

Weiss, S.M. and Saint, D.A. 2010. "The Persistent Sodium Current Blocker Riluzole Is Antiarrhythmic and Anti-Ischaemic in a Pig Model of Acute Myocardial Infarction." *PloS One* 5 (11): e14103.

Wheeler, D.G., Joseph, M.E., Mahamud, S.D., Aurand, W.L., Mohler, P.J., Pompili, V.J., Dwyer, K.M. et al. 2012. "Transgenic Swine: Expression of Human CD39 Protects against Myocardial Injury." *Journal of Molecular and Cellular Cardiology* 52 (5): 958–61.

Wiggers, H., Klebe, T., Heickendorff, L., Høst, N.B., Danielsen, C.C., Baandrup, U. and Andersen, H.R. 1997. "Ischemia and Reperfusion of the Porcine Myocardium: Effect on Collagen." *Journal of Molecular and Cellular Cardiology* 29 (1): 289–99.

Vilahur, G., Casani, L., Peña, E., Juan-Babot, O., Mendieta, G., Crespo, J. and Badimon, L. 2014. "HMG-CoA Reductase Inhibition Prior Reperfusion Improves Reparative Fibrosis Post-Myocardial Infarction in a Preclinical Experimental Model." *International Journal of Cardiology* 175 (3): 528–38.

Wilensky, R.L., Shi, Y., Mohler, E.R., Hamamdzic, D., Burgert, M.E., Li, J., Postle, A. et al. 2008. "Inhibition of Lipoprotein-Associated Phospholipase A2 Reduces Complex Coronary Atherosclerotic Plaque Development." *Nature Medicine* 14 (10): 1059–66.

Virmani, R., Kolodgie, F.D., Burke, A.P., Farb, A. and Schwartz, S.M. 2000. "Lessons from Sudden Coronary Death: A Comprehensive Morphological Classification Scheme for Atherosclerotic Lesions." *Arteriosclerosis, Thrombosis, and Vascular Biology* 20 (5): 1262–75.

Wojakowski, W., Tendera, M., Cybulski, W., Zuba-Surma, E.K., Szade, K., Florczyk, U., Kozakowska, M. et al. 2012. "Effects of Intracoronary Delivery of Allogenic Bone Marrow-Derived Stem Cells Expressing Heme Oxygenase-1 on Myocardial Reperfusion Injury." *Thrombosis and Haemostasis* 108 (3): 464–75.

Wolpers, H.G., Buck, A., Nguyen, N., Marcowitz, P.A., Armstrong, W.F., Starling, M.R., Hicks, R., Mangner, T.J. and Schwaiger, M. 1994. "An Approach to Ventricular Efficiency by Use of Carbon 11-Labeled Acetate and Positron Emission Tomography." *Journal of Nuclear Cardiology : Official Publication of the American Society of Nuclear Cardiology* 1 (3): 262–69.

Wolpers, H.G., Burchert, W., van den Hoff, J., Weinhardt, R., Meyer, G.J. and Lichtlen, P.R. 1997. "Assessment of Myocardial Viability by Use of 11C-Acetate and Positron Emission Tomography. Threshold Criteria of Reversible Dysfunction." *Circulation* 95 (0009-7322 (Print)). Department of Internal Medicine, Hannover Medical School, Germany: 1417–24.

Von Degenfeld, G., Raake, P., Kupatt, C., Lebherz, C., Hinkel, R., Gildehaus, F.J., Münzing, W. et al. 2003. "Selective Pressure-Regulated Retroinfusion of Fibroblast Growth Factor-2 into the Coronary Vein Enhances Regional Myocardial Blood Flow and Function in Pigs with Chronic Myocardial Ischemia." *Journal of the American College of Cardiology* 42 (6): 1120–28.

Worthley, S.G., Helft, G., Fuster, V., Fayad, Z.A., Fallon, J.T., Osende, J.I., Roqué, M. et al. 2000. "High Resolution Ex Vivo Magnetic Resonance Imaging of in Situ Coronary and Aortic Atherosclerotic Plaque in a Porcine Model." *Atherosclerosis* 150 (2): 321–29.

Worthley, S.G., Helft, G., Fuster, V., Fayad, Z.A., Rodriguez, O.J., Zaman, A.G., Fallon, J.T. and Badimon, J.J. 2000. "Noninvasive In Vivo Magnetic Resonance Imaging of Experimental Coronary Artery Lesions in a Porcine Model." *Circulation* 101 (25): 2956–61.

Wu, M., Bogaert, J., D'hooge, J., Sipido, K., Maes, F., Dymarkowski, S., Rademakers, F.E. and Claus, P. 2010. "Closed-Chest Animal Model of Chronic Coronary Artery Stenosis. Assessment with Magnetic Resonance Imaging." *The International Journal of Cardiovascular Imaging* 26 (3): 299–308.

Wu, M., D'hooge, J., Ganame, J., Ferferieva, V., Sipido, K.R., Maes, F., Dymarkowski, S., Bogaert, J., Rademakers, F.E. and Claus, P. 2011. "Non-

Invasive Characterization of the Area-at-Risk Using Magnetic Resonance Imaging in Chronic Ischaemia." *Cardiovascular Research* 89 (1): 166–74.

Wykrzykowska, J., Lehman, S., Williams, G., Parker, J.A., Palmer, M.R., Varkey, S., Kolodny, G. and Laham, R. 2009. "Imaging of Inflamed and Vulnerable Plaque in Coronary Arteries with 18F-FDG PET/CT in Patients with Suppression of Myocardial Uptake Using a Low-Carbohydrate, High-Fat Preparation." *J.Nucl.Med.* 50: 563–68.

Vähäsilta, T., Saraste, A., Kytö, V., Malmberg, M., Kiss, J., Kentala, E., Kallajoki, M. and Savunen, T. 2005. "Cardiomyocyte Apoptosis after Antegrade and Retrograde Cardioplegia." *The Annals of Thoracic Surgery* 80 (6): 2229–34.

Yan, Z. and Hansson, G.K. 2007. "Innate Immunity, Macrophage Activation, and Atherosclerosis." *Immunological Reviews* 219: 187–203.

Yang, K., Xiang, P., Zhang, C., Zou, L., Wu, X., Gao, Y., Kang, Z., He, K., Liu, J. and Peng, C. 2011. "Magnetic Resonance Evaluation of Transplanted Mesenchymal Stem Cells after Myocardial Infarction in Swine." *The Canadian Journal of Cardiology* 27 (6): 818–25.

Zhang, J., Wilke, N., Wang, Y., Zhang, Y., Wang, C., Eijgelshoven, M.H., Cho, Y.K. et al. 1996. "Functional and Bioenergetic Consequences of Postinfarction Left Ventricular Remodeling in a New Porcine Model. MRI and 31 P-MRS Study." *Circulation* 94: 1089–1100.

Zhang, L., Zalewski, A., Liu, Y., Mazurek, T., Cowan, S., Martin, J.L., Hofmann, S.M., Vlassara, H. and Shi, Y. 2003. "Diabetes-Induced Oxidative Stress and Low-Grade Inflammation in Porcine Coronary Arteries." *Circulation* 108 (4): 472–78.

Zhu, X.-Y., Zhang, Z.-L., Li, P., Liang, W.-Y., Feng, X.-R. and Liu, M.-L. 2013. "Shenyuan, an Extract of American Ginseng and Corydalis Tuber Formula, Attenuates Cardiomyocyte Apoptosis via Inhibition of Endoplasmic Reticulum Stress and Oxidative Stress in a Porcine Model of Acute Myocardial Infarction." *Journal of Ethnopharmacology* 150 (2): 672–81.